Time-of-Flight Imaging & Single-Photon Imaging

lidar, non-line-of-sight imaging, ultrafast imaging

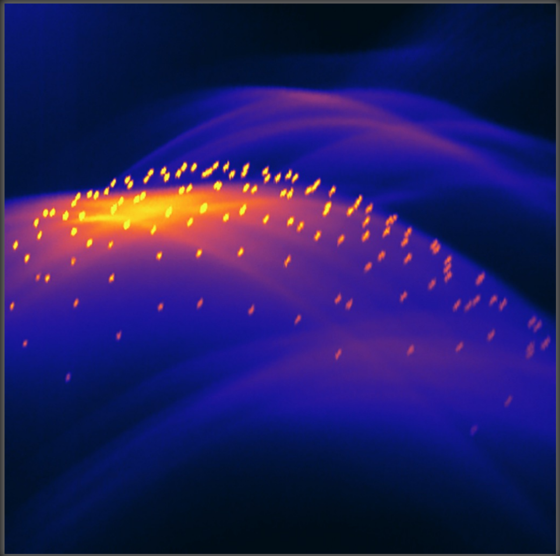

CSC2529

David Lindell

University of Toronto

cs.toronto.edu/~lindell/teaching/2529

*slides adapted from Matt O'Toole, Gordon Wetzstein, Yannis Gkioulekas

Poster Session

- Thursday Dec 7th 2-4pm
    - Bahen Atrium
    - you MUST attend in person or make alternative arrangments with me (only in extenuating circumstances)
- You are responsible for making sure that your poster is printed on time!
    - use the “same-day” or ”next-day” ordering option from https://utposter.com/
    - use the offer code on Quercus (“pages”) so you don’t have to pay
    - Pick up poster from 339 Bloor St W
    - bring it to the poster session and put it up before poster session begin
- You have from November 18 until December 6 (the day before the poster session) to print your poster using this service.

Poster Session

- feedback on proposals out by end of today
    - we will message you on Piazza

- Check Quercus->Assignments->Final Project for rubric for the poster session, code, report

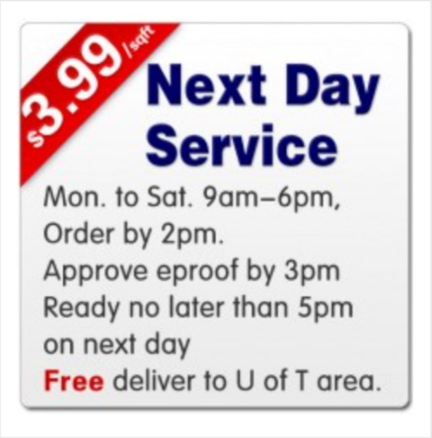

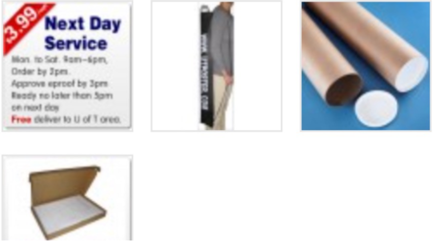

Product Code: Next day service

Price: $3.99

Available Options

* **Shorter Side (24-60 inch):**
24

* **Longer Side (36-200 inch):**
36

* **Materials:**
High Quality Glossy Photo Paper

Tube (Mandatory for Paper Poster Shipping):
☐ Yes (+$3.99)

How Many Letter Size Handout Copies (Optional):
--- Please Select ---

* **Pick Up /Shipping Options:**
Pick Up @ store Mon-Sat 9am-6pm. Exclude Long Weekend Sat & Mon

Use the offer code on Quercus

Machine learning for determining protein structure and dynamics from cryo-EM images

Ellen Zhong
Assistant Professor, Princeton University

Wednesday Nov 22, 3-4 PM
DGP Seminar Room (Bahen 5187)

5 bonus points if you attend and upload selfie to the Quercus assignment

Co-Designing Optics and Algorithms for High-Dimensional Visual Computing

Vishwanath Saragadam
Incoming Assistant Professor,
UC Riverside

Monday Nov 27, 2-4 PM (lecture 10)

Next Generation Black-Hole Imaging

Aviad Levis
Incoming Assistant Professor,
University of Toronto

Monday Dec 4, 2-4 PM (lecture 11)

transient imaging (a.k.a. femtophotography)

Raskar et al. [2011]

overview

- Time-resolved imaging
- Single-photon avalanche diodes (SPADs)
- Single-photon lidar
- Non-line-of-sight imaging
- passive ultra-wideband sensing

echolocation

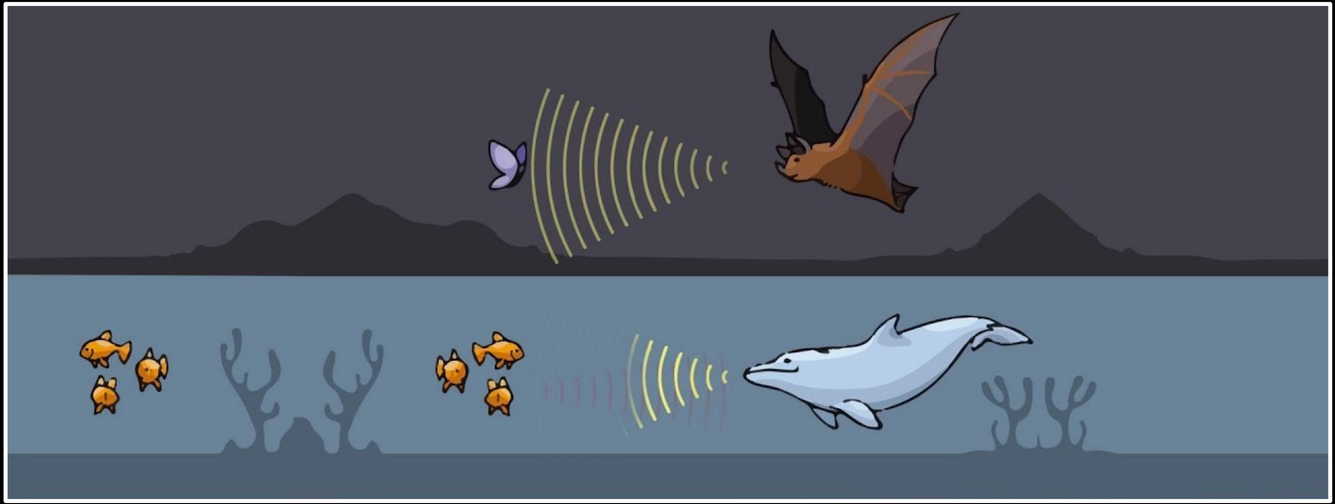

speed of sound in air: 343 meters / sec
in water: 1480 meters / sec

Light takes 1.255 seconds to travel from the earth to the moon

speed of light in a vacuum: **299,792,458** meters / sec

(Light travels approximation **1 MILLION** times faster than sound!)

transient imaging

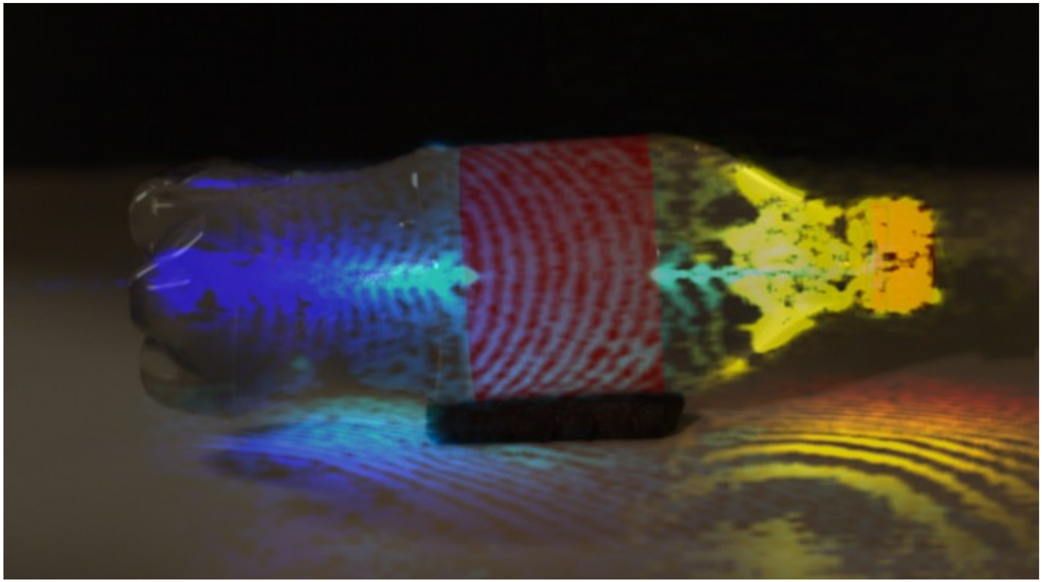

speed of light in a vacuum: **299,792,458** meters / sec

(Light travels approximation **1 MILLION** times faster than sound!)

direct and **indirect** time-of-flight sensors
for transient imaging

Velodyne VLS-128

Direct time-of-flight sensor


Microsoft Kinect v2

Indirect time-of-flight sensor

direct and indirect time-of-flight sensing

Velodyne VLS-128

Direct time-of-flight sensor


Microsoft Kinect v2

Indirect time-of-flight sensor

direct and indirect time-of-flight sensing

Velodyne VLS-128

Direct time-of-flight sensor

direct time-of-flight principle

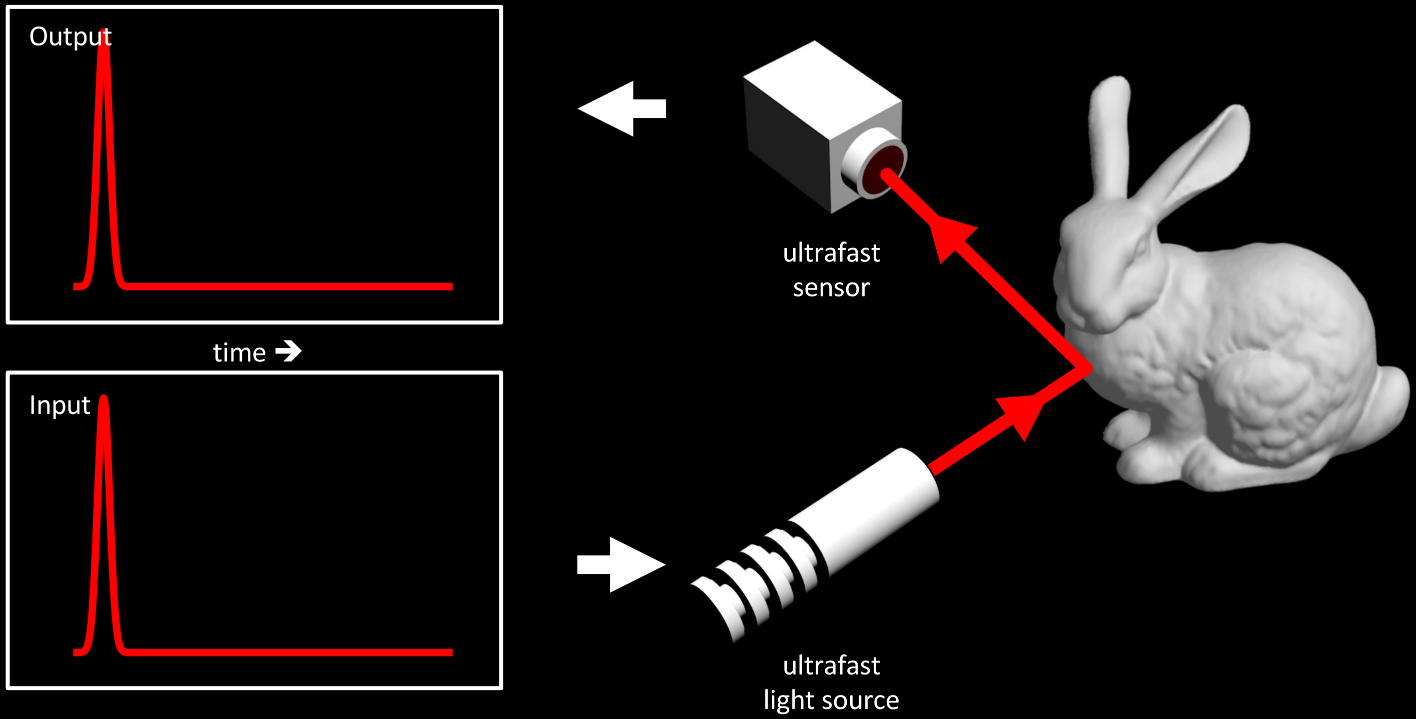

direct time-of-flight principle

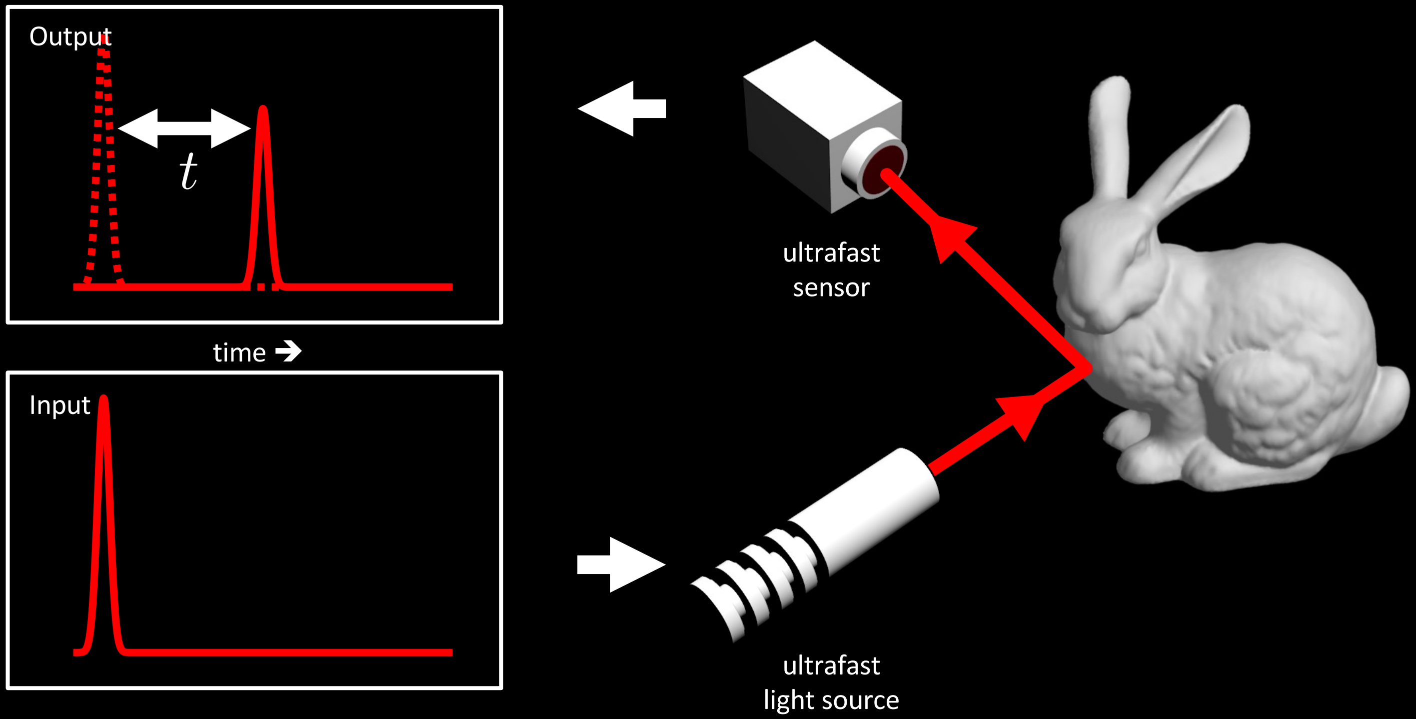

direct time-of-flight principle

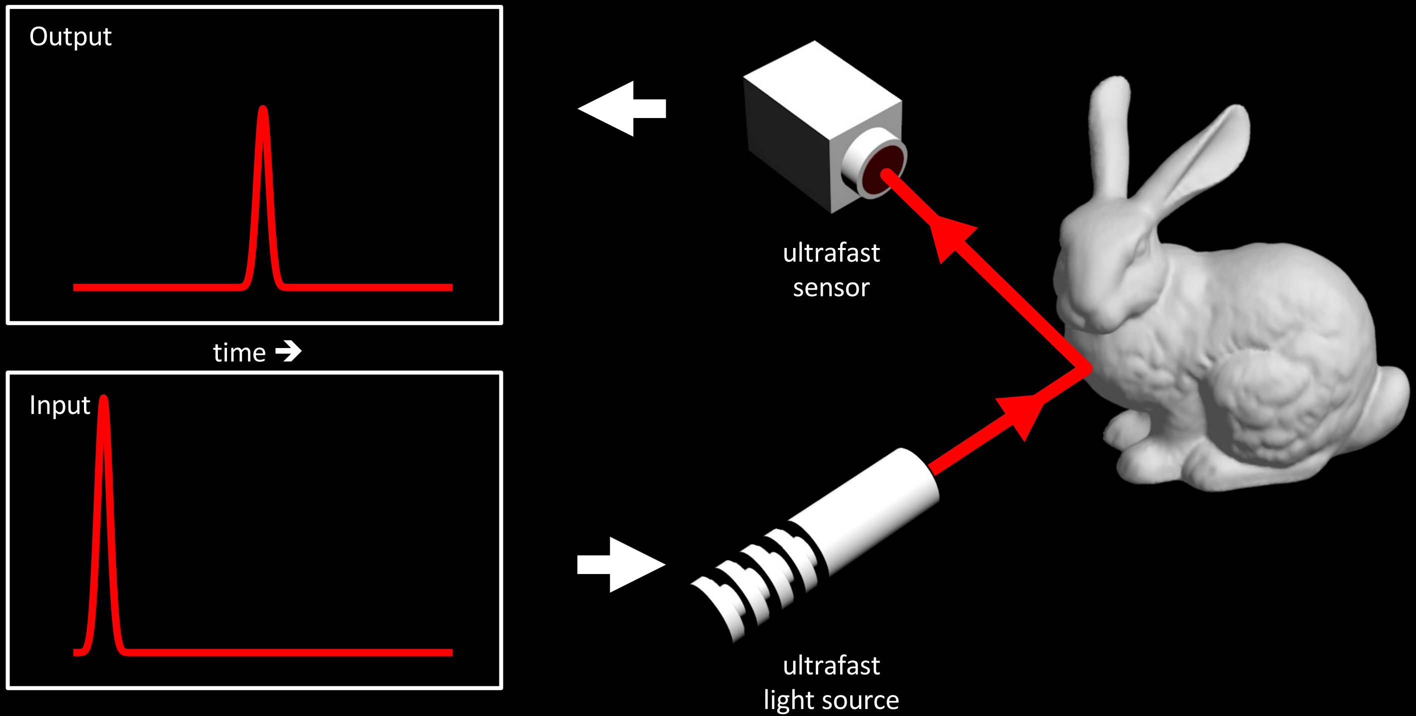

direct time-of-flight principle

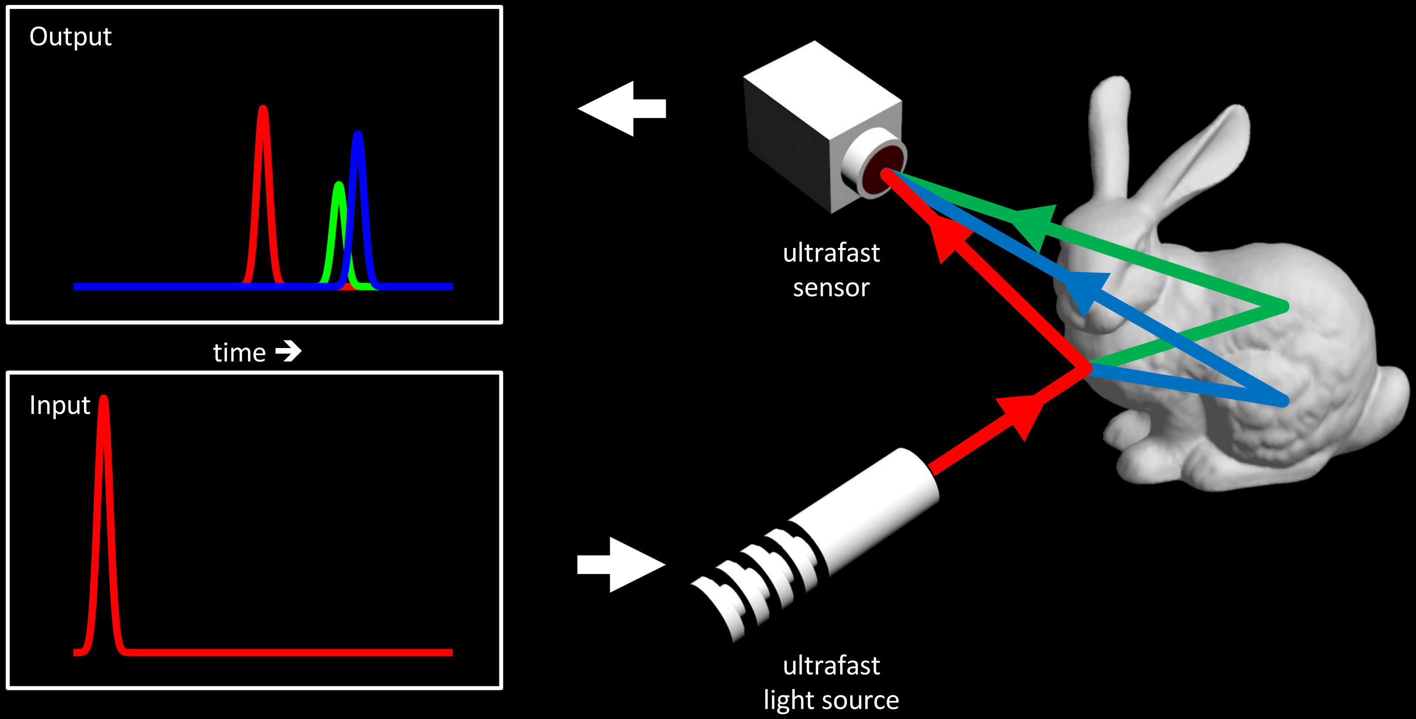

direct time-of-flight principle

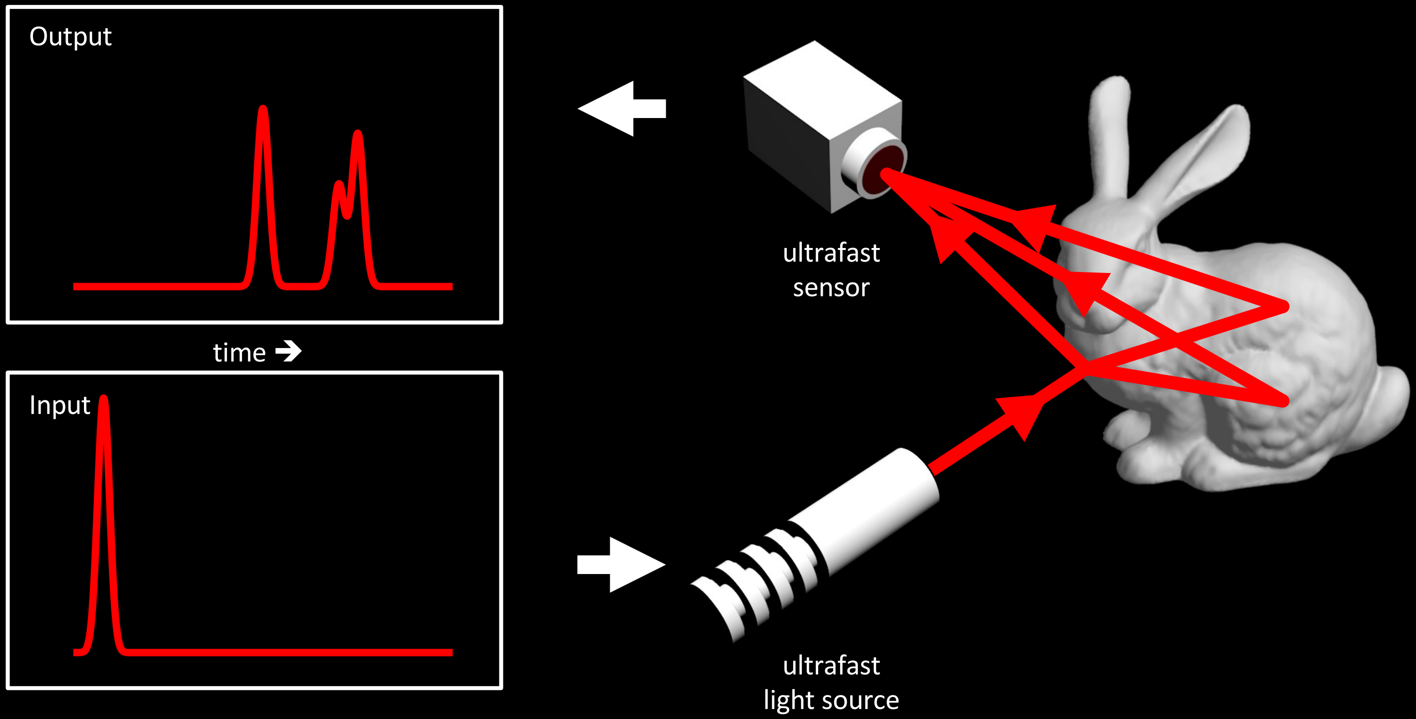

direct time-of-flight principle

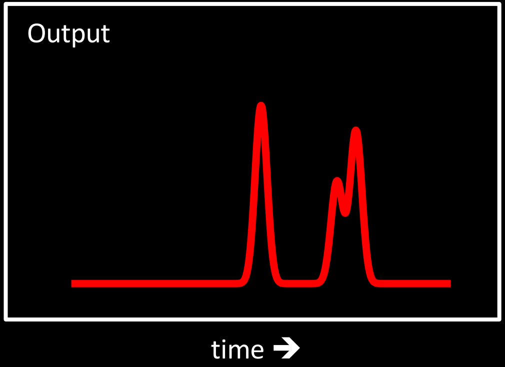

transient measurement

direct and indirect time-of-flight sensing

Velodyne VLS-128

Microsoft Kinect v2

Direct time-of-flight sensor

Indirect time-of-flight sensor

direct and indirect time-of-flight sensing

Microsoft Kinect v2

Indirect time-of-flight sensor

indirect time-of-flight principle

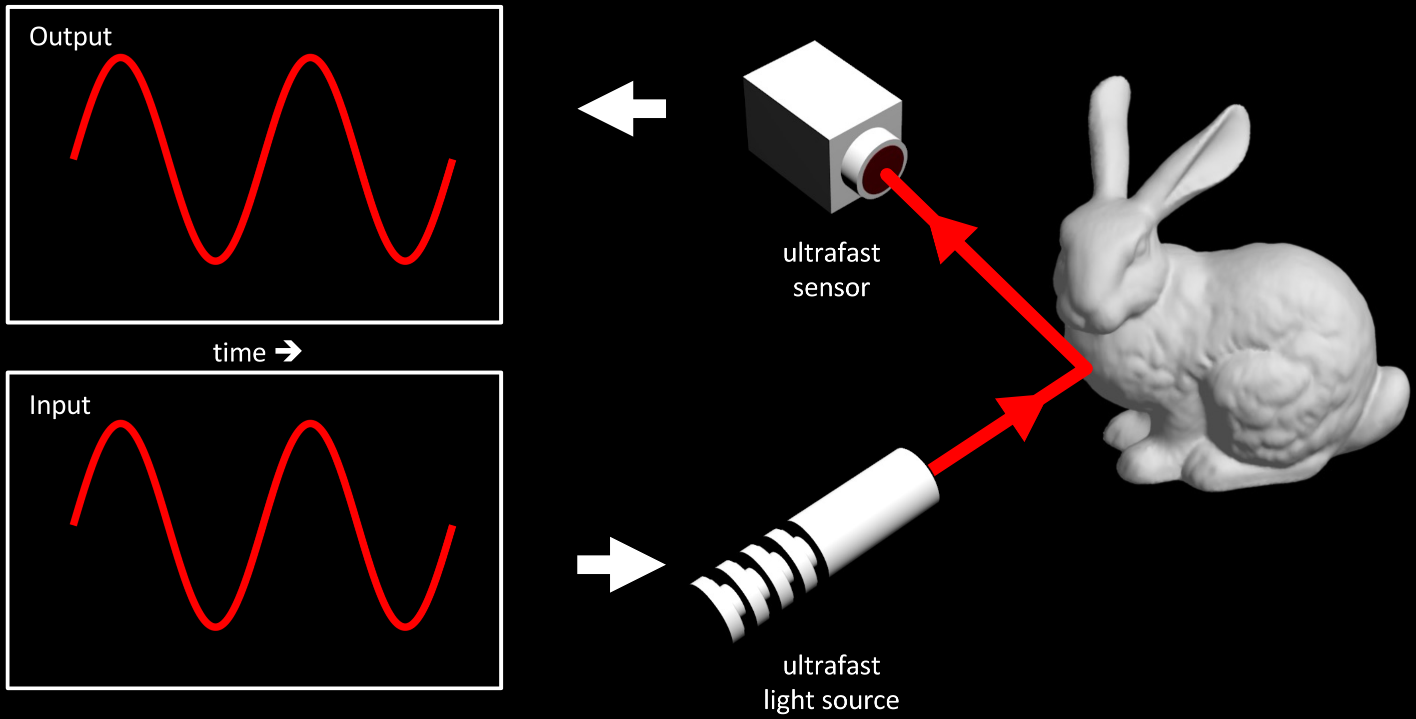

indirect time-of-flight principle

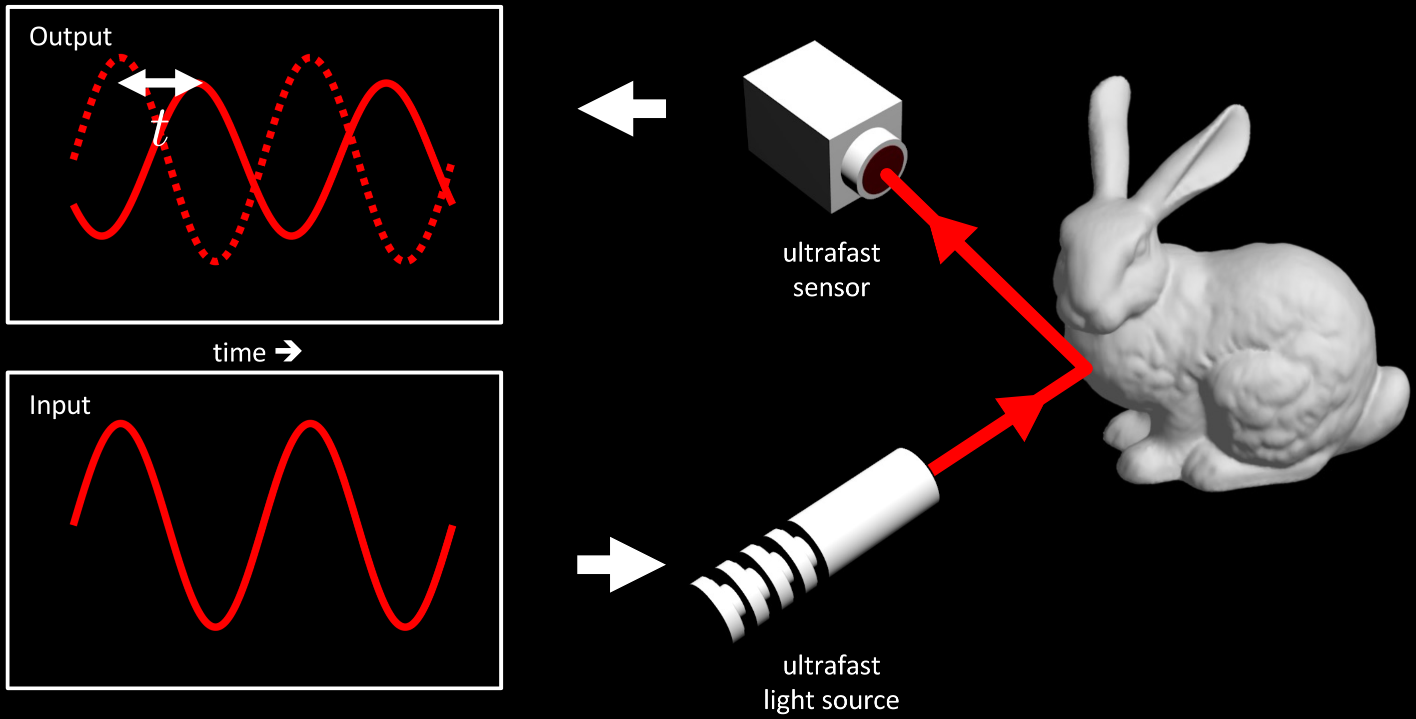

indirect time-of-flight principle

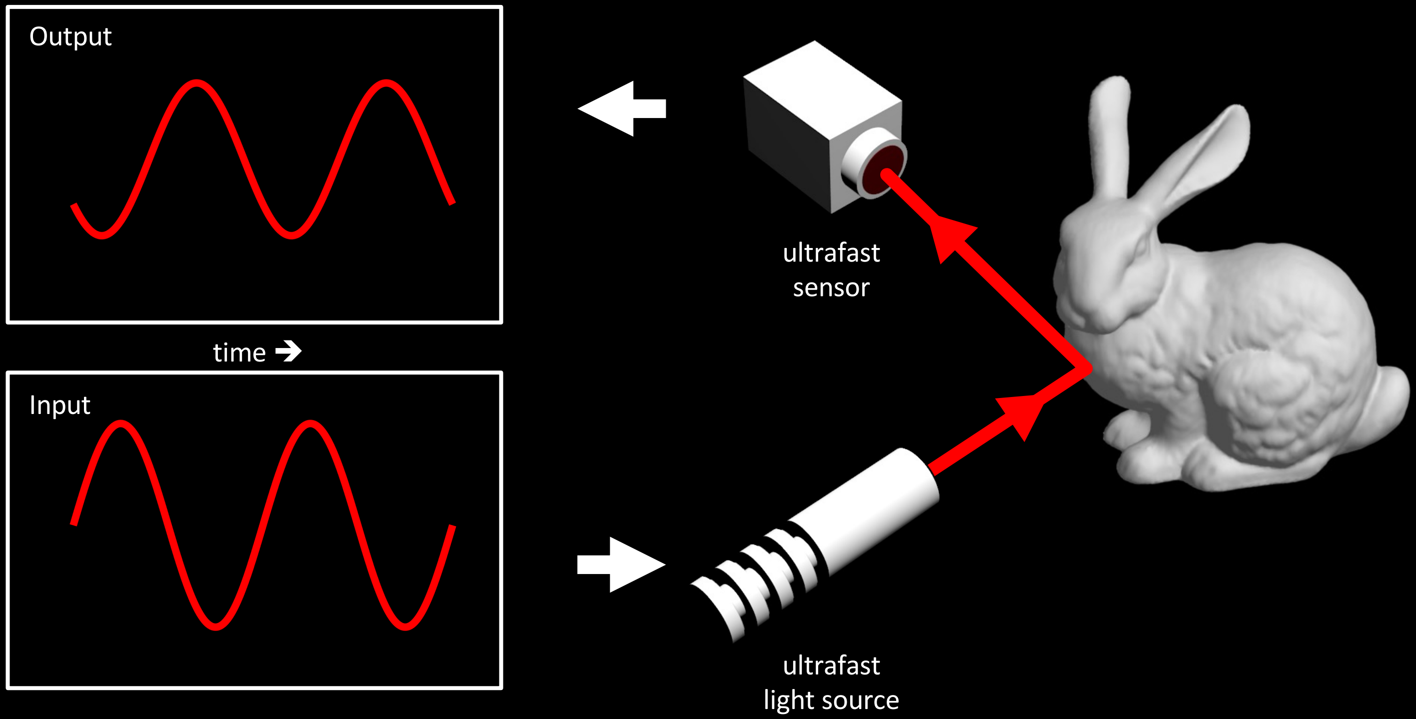

indirect time-of-flight principle

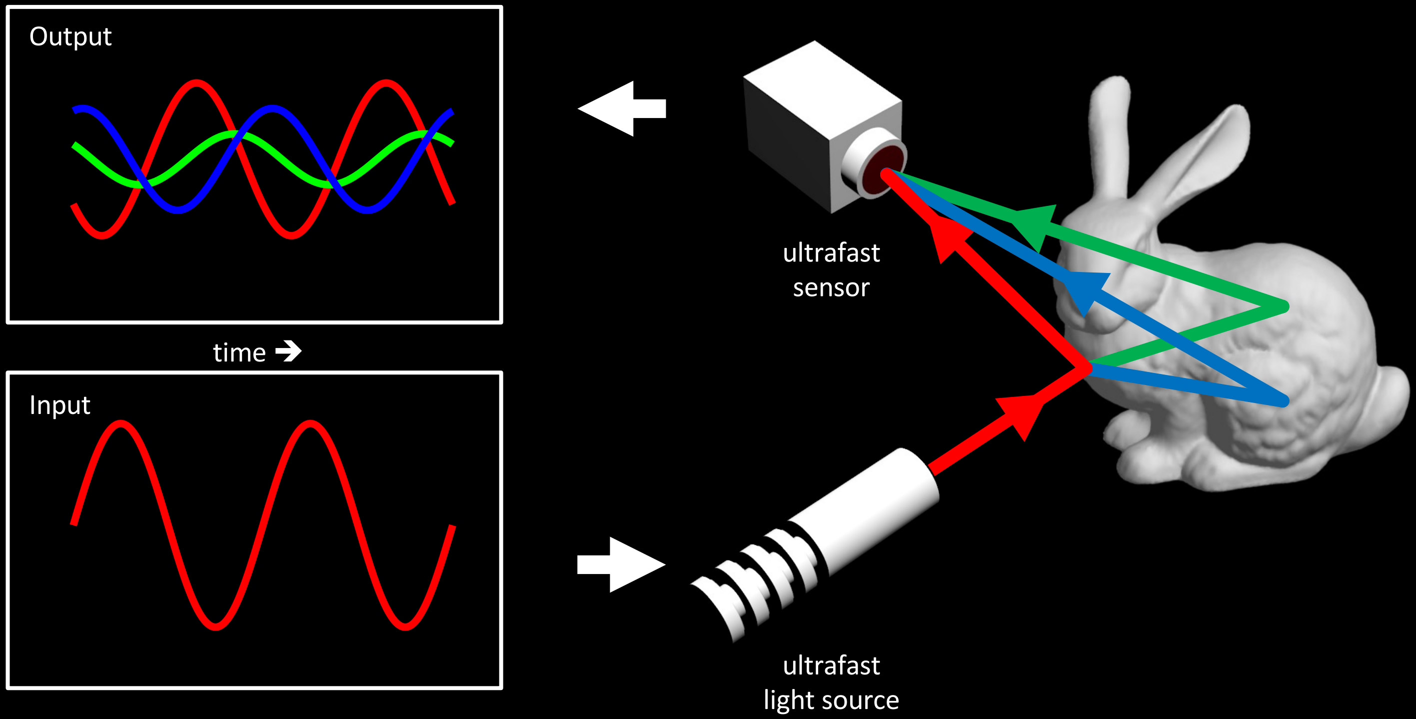

indirect time-of-flight principle

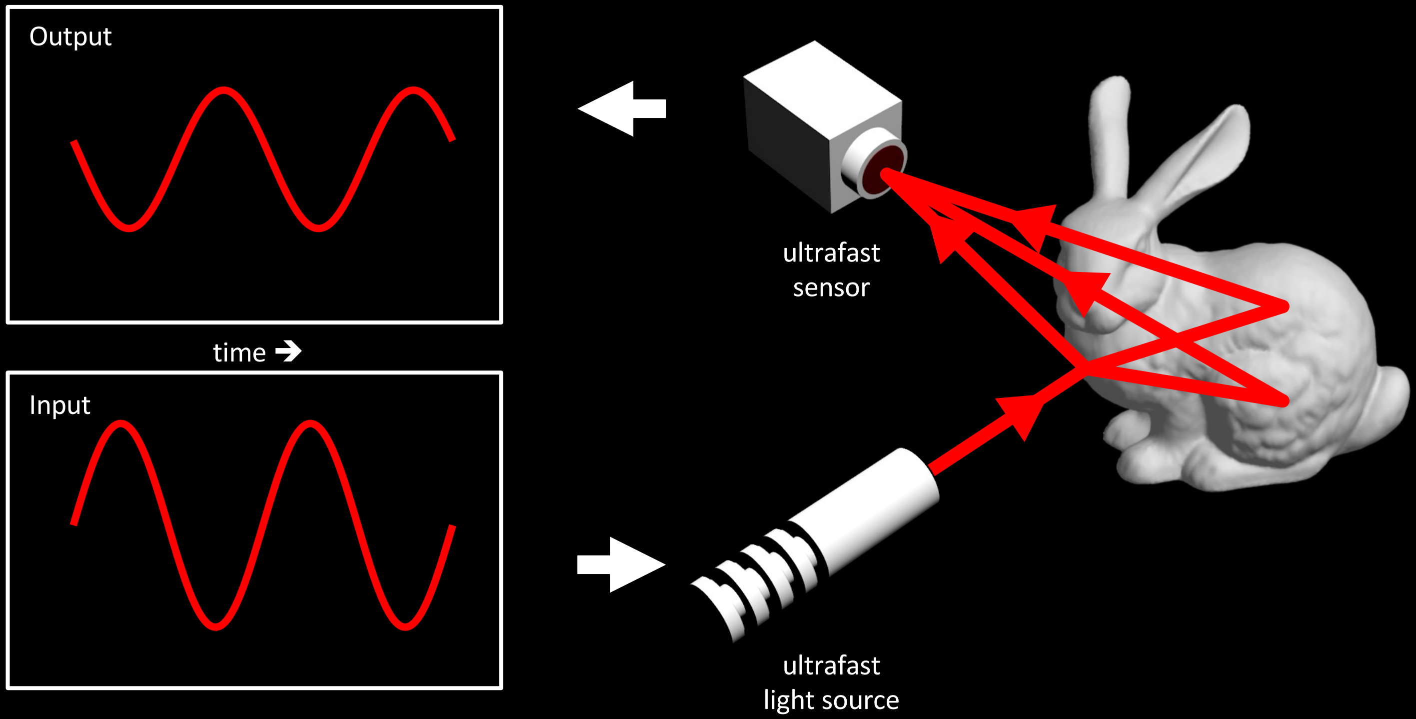

indirect time-of-flight principle

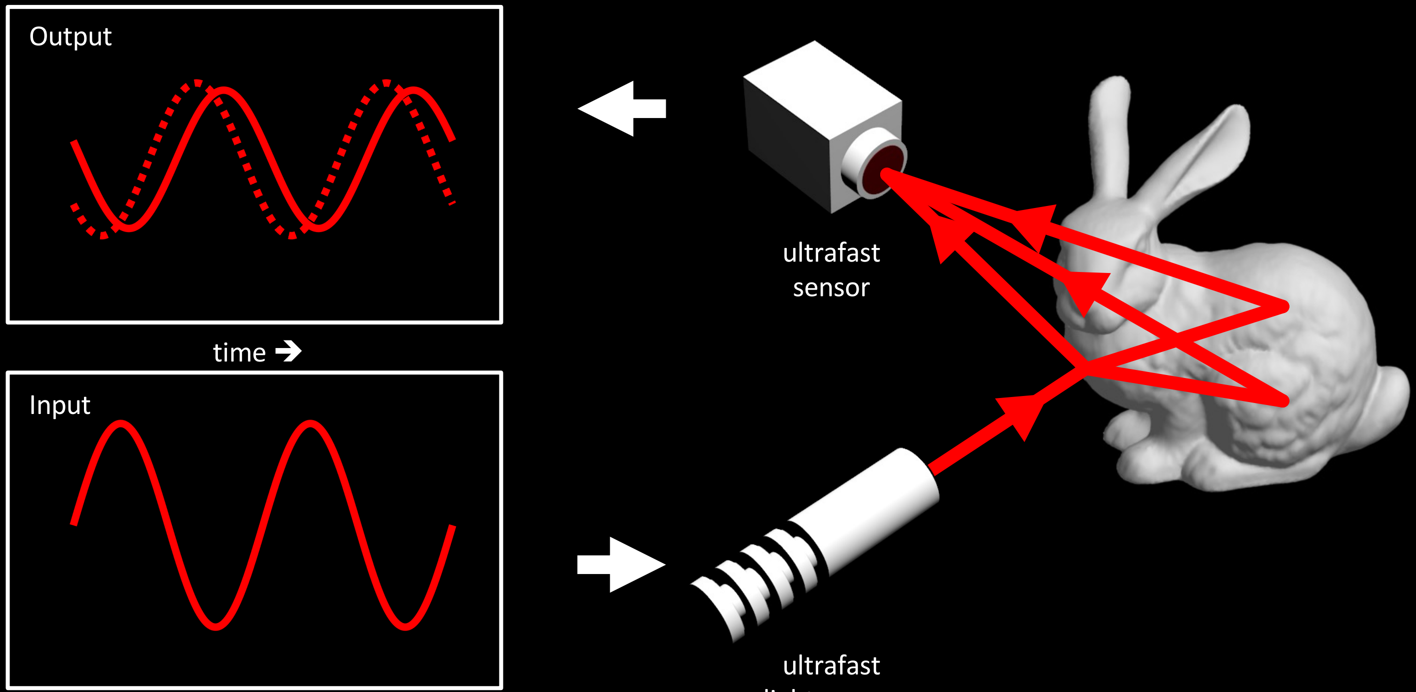

indirect time-of-flight principle

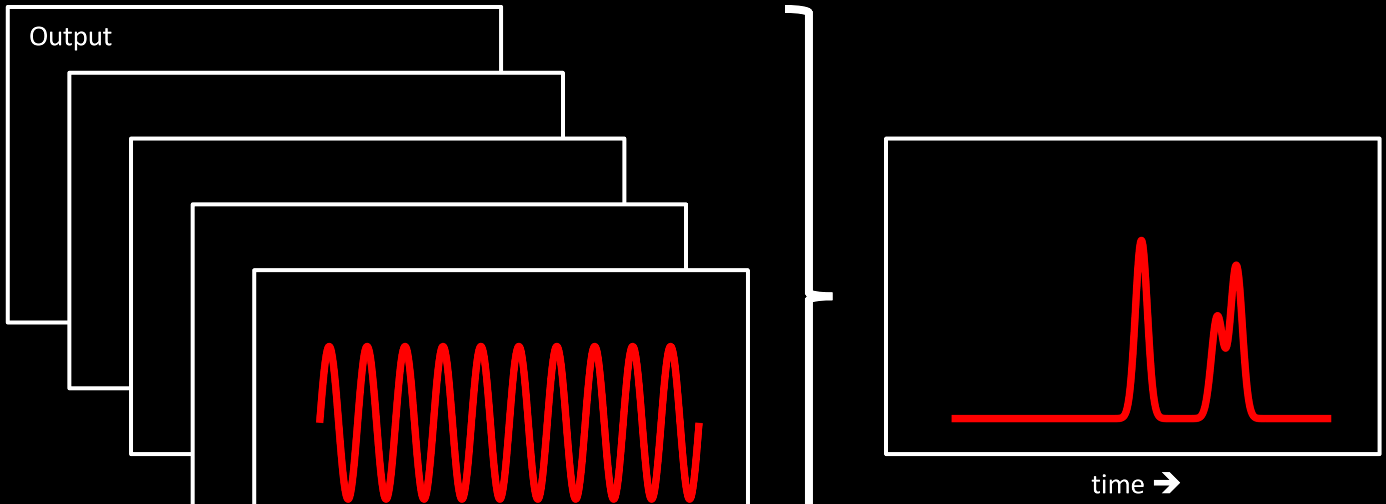

transient measurement

transient sensing technologies

	optical coherence tomography	streak camera	single-photon avalanche diodes	time-of-flight cameras	avalanche photodiode
temporal resolution	1 femtosecond (10^{-15} secs)	1 picosecond (10^{-12} secs)	100 picosecond (10^{-10} secs)	1 nanosecond (10^{-9} secs)	10 nanoseconds (10^{-8} secs)
frame rate	quadrillion fps	trillion fps	10 billion fps	billion fps	100 million fps
distance travelled	1 micron (10^{-6} meters)	1 millimeter (10^{-3} meters)	10 centimeters (10^{-1} meters)	1 meter (10^{0} meters)	10 meters (10^{1} meters)

transient sensing technologies

	optical coherence tomography	streak camera	single-photon avalanche diodes	time-of-flight cameras	avalanche photodiode
temporal resolution	1 femtosecond (10^{-15} secs)	1 picosecond (10^{-12} secs)	100 picosecond (10^{-10} secs)	1 nanosecond (10^{-9} secs)	10 nanoseconds (10^{-8} secs)
frame rate	quadrillion fps	trillion fps	10 billion fps	billion fps	100 million fps
distance travelled	1 micron (10^{-6} meters)	1 millimeter (10^{-3} meters)	10 centimeters (10^{-1} meters)	1 meter (10^{0} meters)	10 meters (10^{1} meters)

transient sensing technologies

	optical coherence tomography	streak camera	single-photon	time-of-flight	avalanche
temporal resolution	1 femtosecond (10^{-15} secs)	1 picosecond (10^{-12} secs)			
frame rate	quadrillion fps	trillion fps			
distance travelled	1 micron (10^{-6} meters)	1 millimeter (10^{-3} meters)	10 centimeters (10^{-1} meters)	1 meter (10^{0} meters)	10 meters (10^{1} meters)

Velten et al. [2012]

transient sensing technologies

Micro Photon Devices

	optical coherence tomography	streak camera	single-photon avalanche diodes	time-of-flight cameras	avalanche photodiode
temporal resolution			100 picosecond (10^{-10} secs)	1 nanosecond (10^{-9} secs)	10 nanoseconds (10^{-8} secs)
frame rate			10 billion fps	billion fps	100 million fps
distance travelled	1 micron (10^{-6} meters)	1 millimeter (10^{-3} meters)	10 centimeters (10^{-1} meters)	1 meter (10^{0} meters)	10 meters (10^{1} meters)

transient sensing technologies

	optical coherence tomography	streak camera	single-photon	time-of-flight	avalanche photodiode
temporal resolution	1 femtosecond (10^{-15} secs)	1 picosecond (10^{-12} secs)			10 nanoseconds (10^{-8} secs)
frame rate	quadrillion fps	trillion fps			100 million fps
distance travelled	1 micron (10^{-6} meters)	1 millimeter (10^{-3} meters)	10 centimeters (10^{-1} meters)	1 meter (10^{0} meters)	10 meters (10^{1} meters)

Velodyne VLS-128

transient sensing technologies

	optical coherence tomography	streak camera	single-photon avalanche diodes	time-of-flight cameras	avalanche photodiode
temporal resolution	1 femtosecond (10^{-15} secs)	1 picosecond (10^{-12} secs)	100 picosecond (10^{-10} secs)	1 nanosecond (10^{-9} secs)	10 nanoseconds (10^{-8} secs)
frame rate	quadrillion fps	trillion fps	10 billion fps	billion fps	100 million fps
distance travelled	1 micron (10^{-6} meters)	1 millimeter (10^{-3} meters)	10 centimeters (10^{-1} meters)	1 meter (10^{0} meters)	10 meters (10^{1} meters)

transient sensing technologies

	optical coherence tomography	streak camera	single-photon	time-of-flight	avalanche photodiode
temporal resolution	1 femtosecond (10^{-15} secs)				0 nanoseconds (10^{-8} secs)
frame rate	quadrillion fps				100 million fps
distance travelled	1 micron (10^{-6} meters)	1 millimeter (10^{-3} meters)	10 centimeters (10^{-1} meters)	1 meter (10^{0} meters)	10 meters (10^{1} meters)

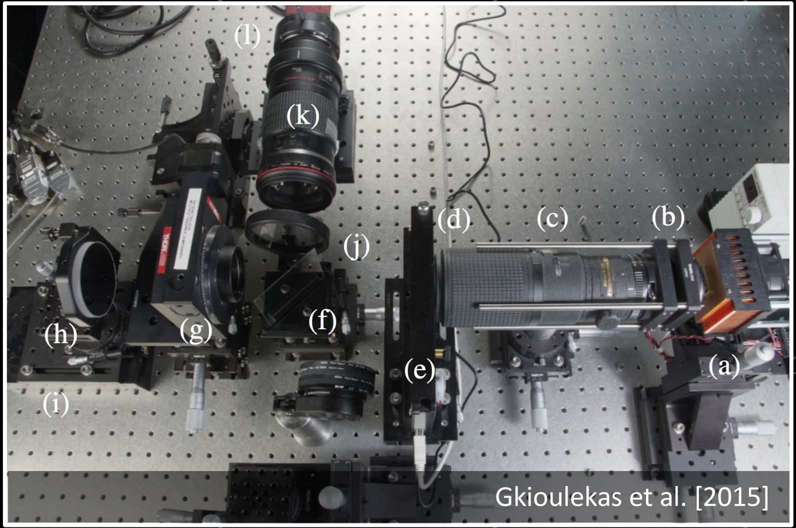

Gkioulekas et al. [2015]

transient sensing technologies

	optical coherence tomography	streak camera	single-photon avalanche diodes	**time-of-flight cameras**	avalanche photodiode
temporal resolution				1 nanosecond (10^{-9} secs)	10 nanoseconds (10^{-8} secs)
frame rate				billion fps	100 million fps
distance travelled	1 micron (10^{-6} meters)	1 millimeter (10^{-3} meters)	10 centimeters (10^{-1} meters)	1 meter (10^{0} meters)	10 meters (10^{1} meters)

Heide et al. [2013]

spectrum of transient sensing technologies

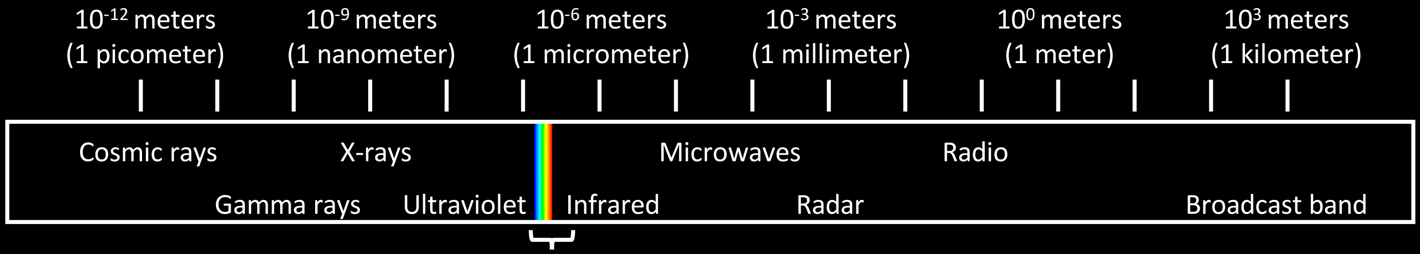

- **optical coherence tomography**
- **streak camera**
- **single-photon avalanche diodes**
- **time-of-flight cameras**
- **avalanche photodiode**

spectrum of transient sensing technologies

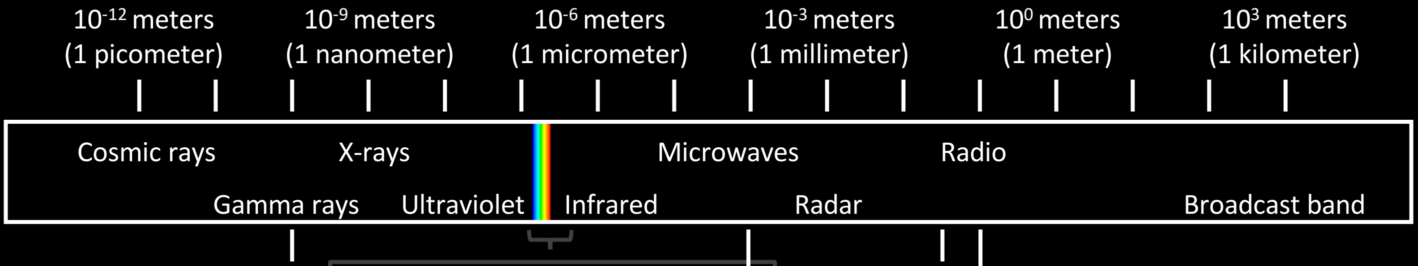

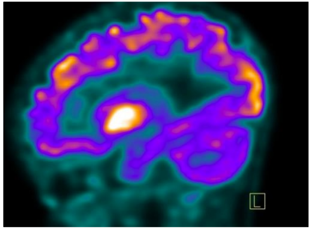

Positron Emission Tomography (PET) Scan

- optical coherence tomography
- streak camera
- single-photon avalanche diodes
- time-of-flight cameras
- avalanche photodiode

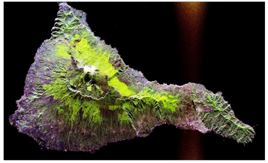

Synthetic Aperture Radar (SAR)

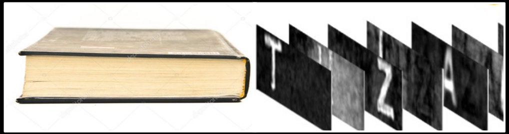

Terahertz Time-gated Imaging [Redo-Sanchez et al., 2015]

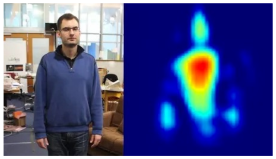

Seeing through Walls [Adib et al., 2015]

spectrum of transient sensing technologies

10^{-12} meters (1 picometer)

10^{-9} meters (1 nanometer)

10^{-6} meters (1 micrometer)

10^{-3} meters (1 millimeter)

10^{0} meters (1 meter)

10^{3} meters (1 kilometer)

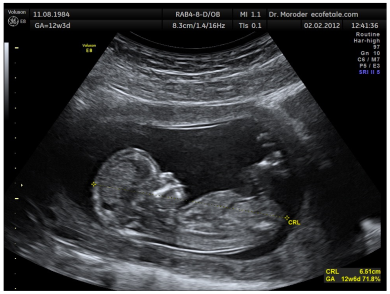

Ultrasound Imaging

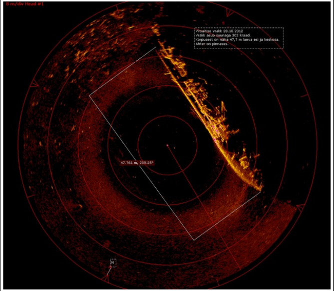

SONAR
(Sound Navigation and Ranging)

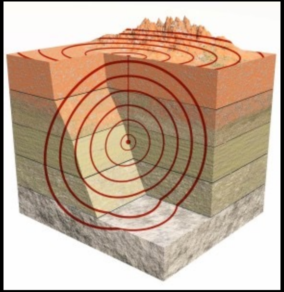

Seismic Imaging

overview

- Time-resolved imaging
- Single-photon avalanche diodes (SPADs)
- Single-photon lidar
- Non-line-of-sight imaging
- passive ultra-wideband sensing

picosecond laser

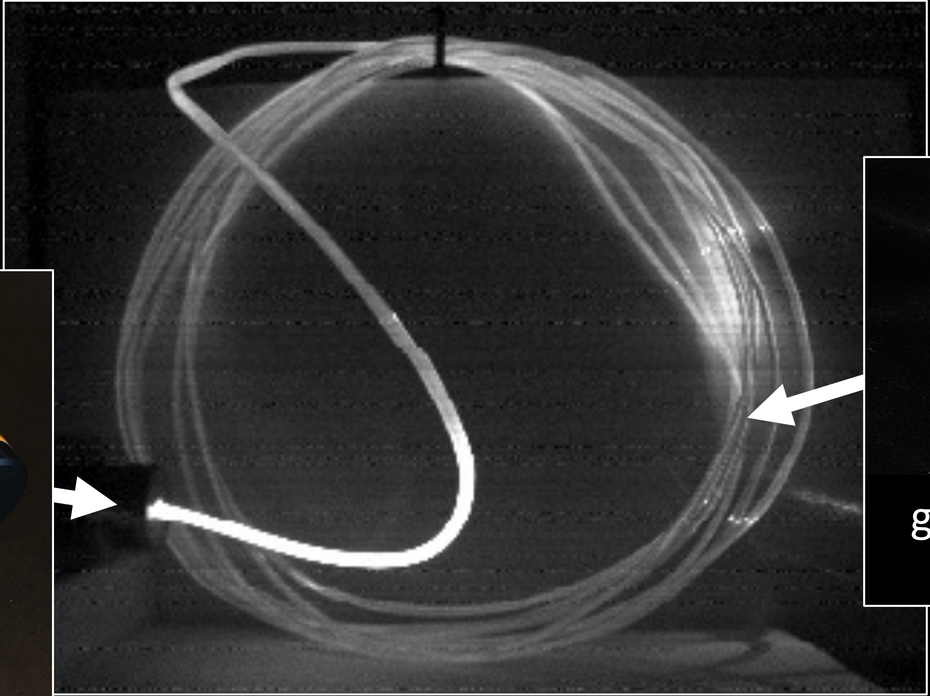

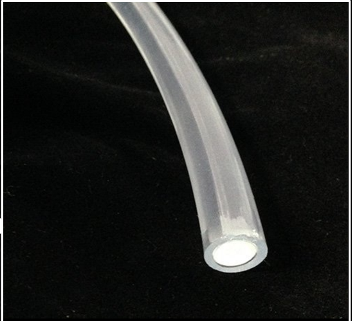

glowing fiber optic cable

regular image

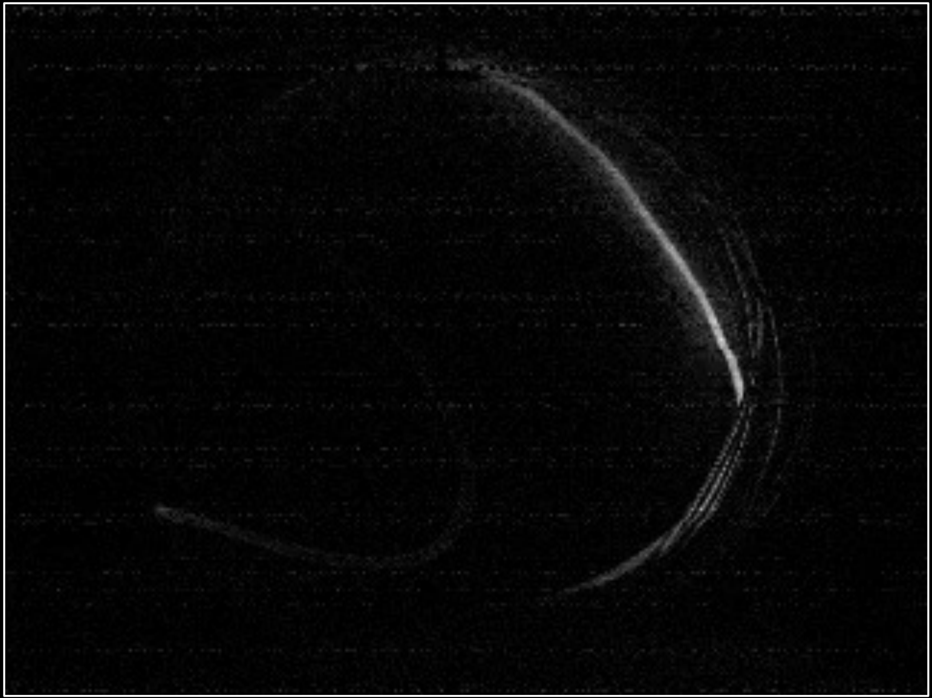

transient image

Applications

Autonomous Navigation
Image by Wikimedia Commons

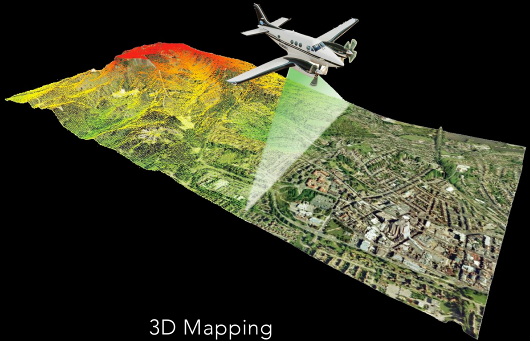

3D Mapping
Image by LIDAR-America

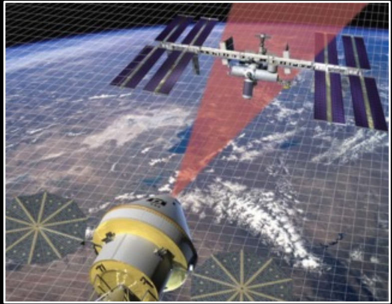

Space Station Docking
Image by NASA

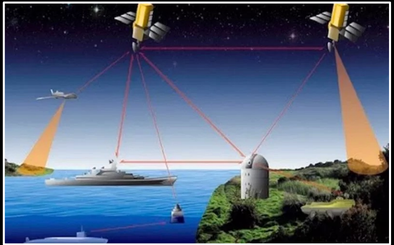

Optical Communications
Image by Siasat Daily

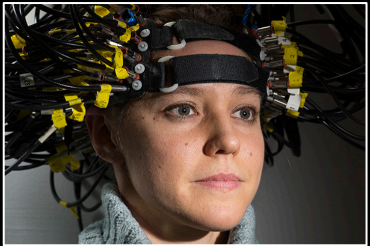

Biomedical Imaging
Image by Washington University

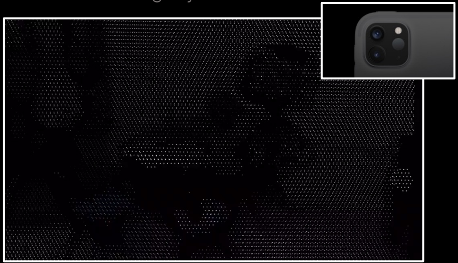

Consumer Electronics (2020 iPad Pro)
Video by Tim Fields

Appl

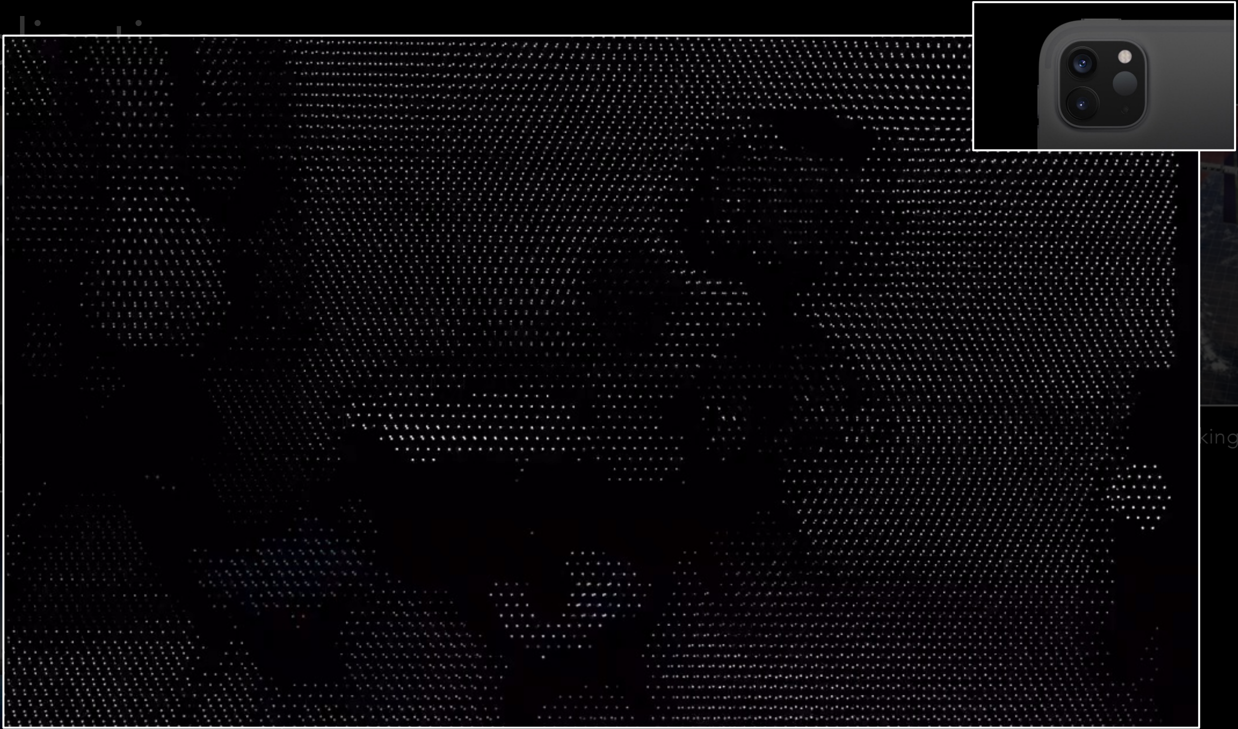

Au
Ima

king

Optical Communications
Image by Siasat Daily

Biomedical Imaging
Image by Washington University

Consumer Electronics (2020 iPad Pro)
Video by Tim Fields

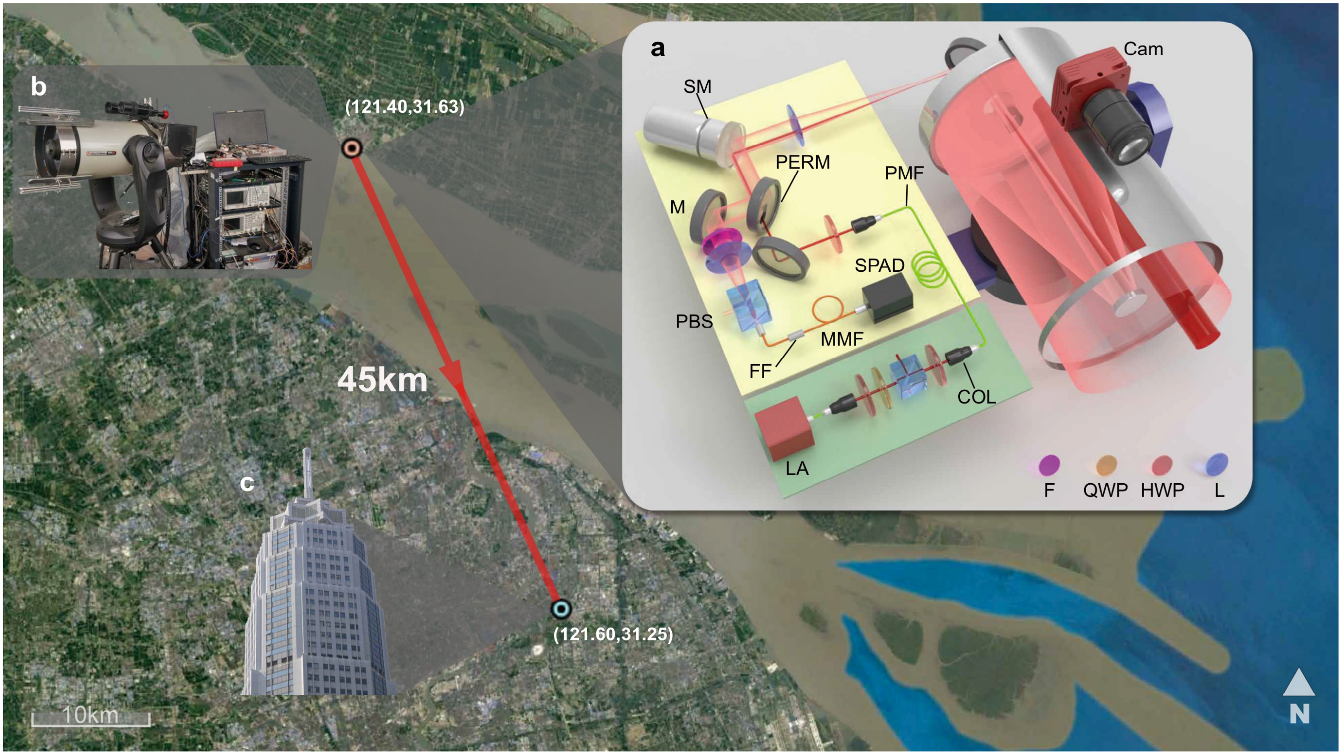

a
Cam
SM
PERM
PMF
M
SPAD
PBS
MMF
FF
COL
LA
F
QWP
HWP
L
b
(121.40,31.63)
45km
c
(121.60,31.25)
10km
N

International Laser Ranging Service (ILRS)

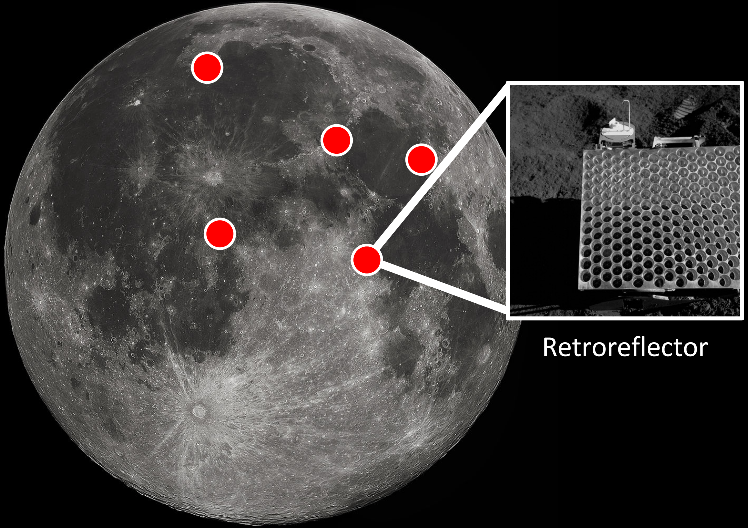

Lunar Laser Ranging (LLR)

- Location of Lunar Retroreflector

single-photon avalanche diode (SPAD)

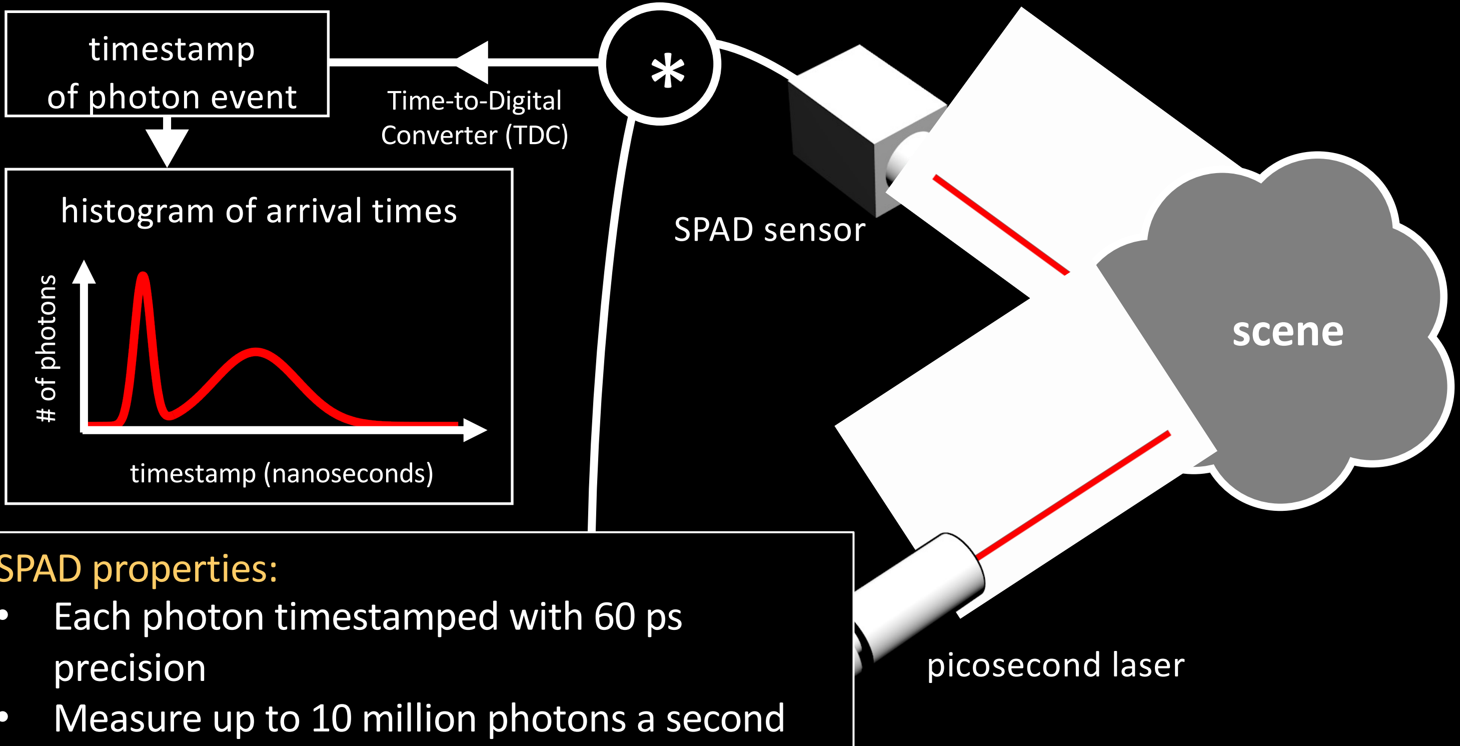

SPAD properties:

- Each photon timestamped with 60 ps precision
- Measure up to 10 million photons a second

linear array of SPADs

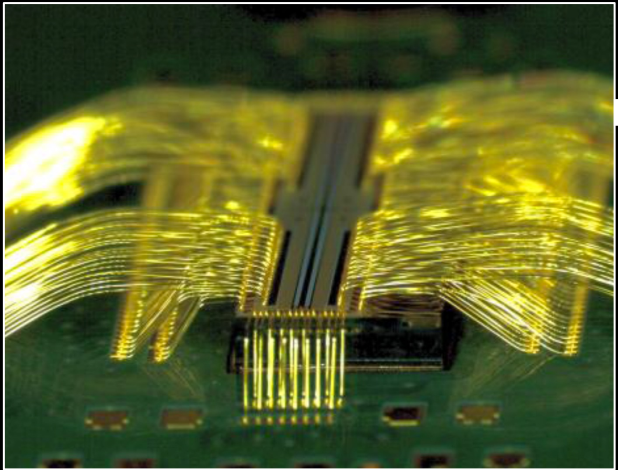

LinoSPAD from FastTree 3D

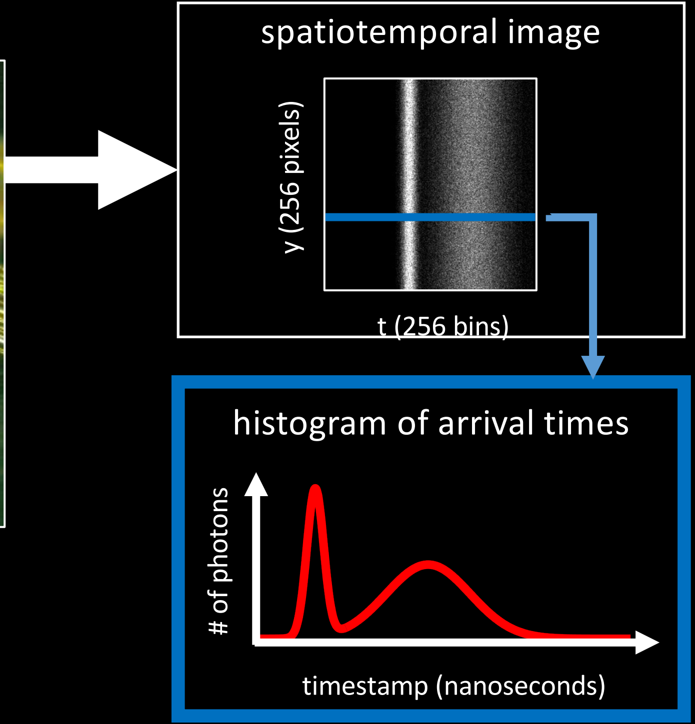

scanning procedure

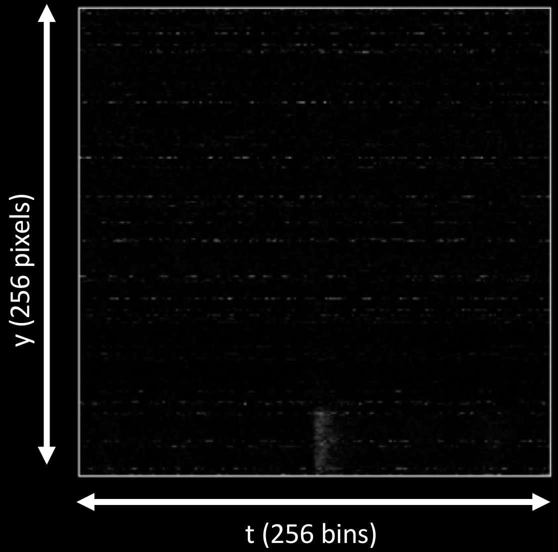

SPAD output

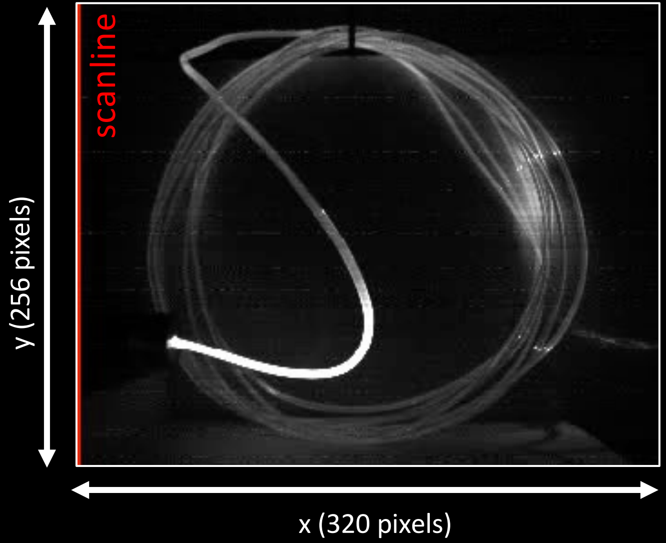

regular image

scanning procedure

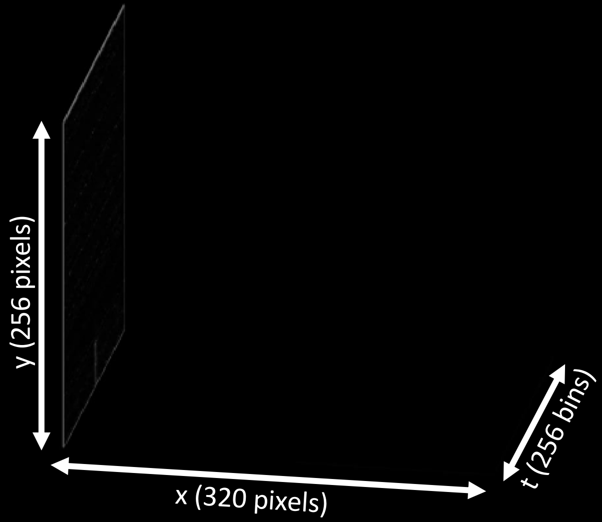

transient image

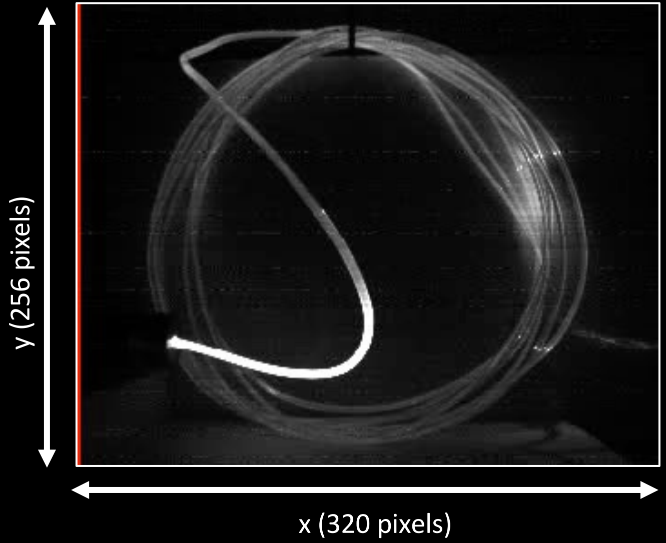

regular image

scanning procedure

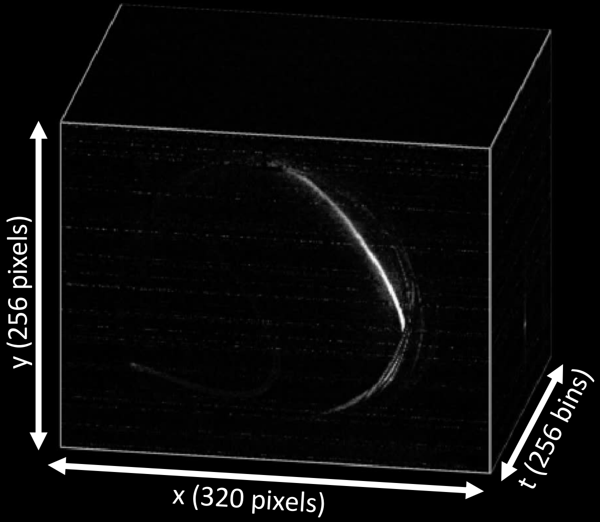

transient image

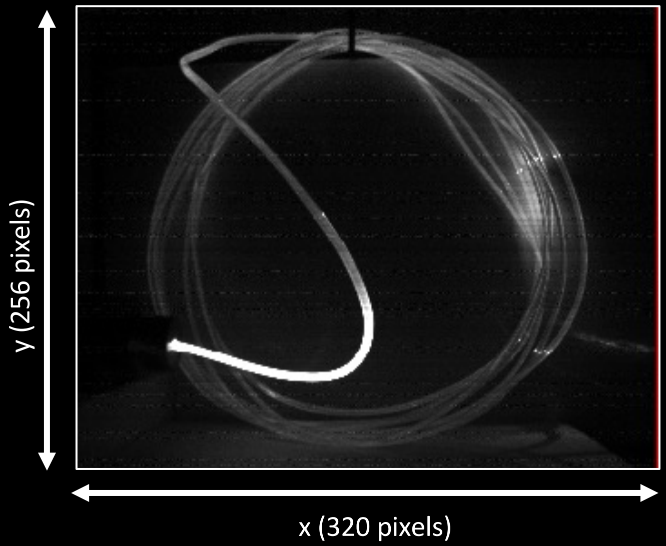

regular image

overview

- Time-resolved imaging
- Single-photon avalanche diodes (SPADs)
- Single-photon lidar
- Non-line-of-sight imaging
- passive ultra-wideband sensing

LiDAR

LiDAR

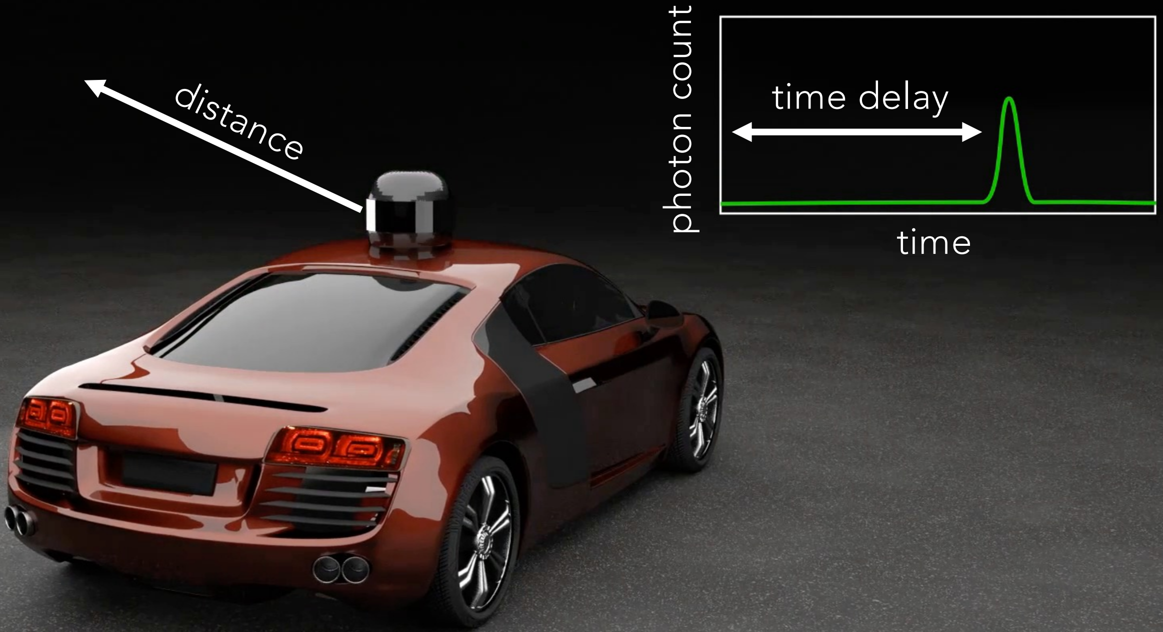

LiDAR

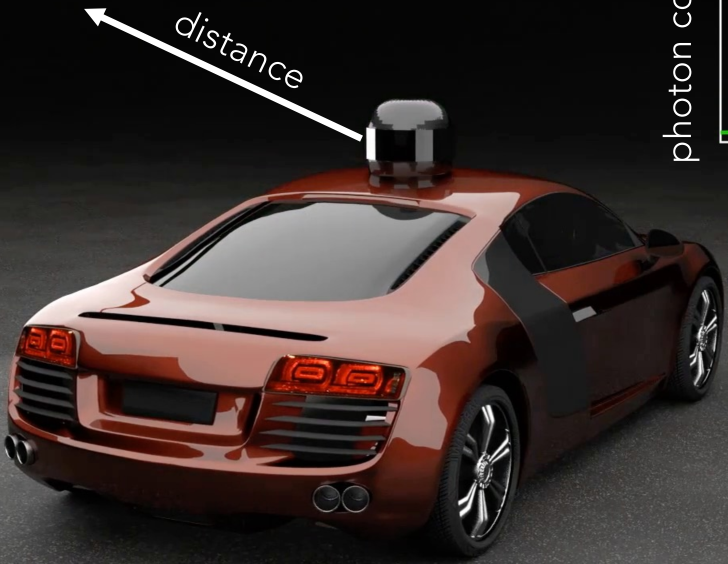

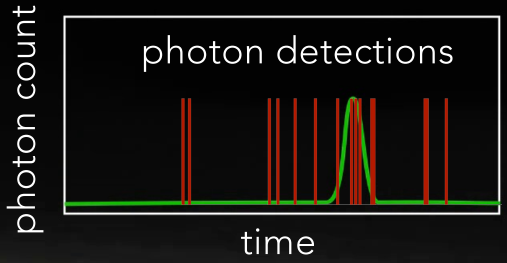

LiDAR

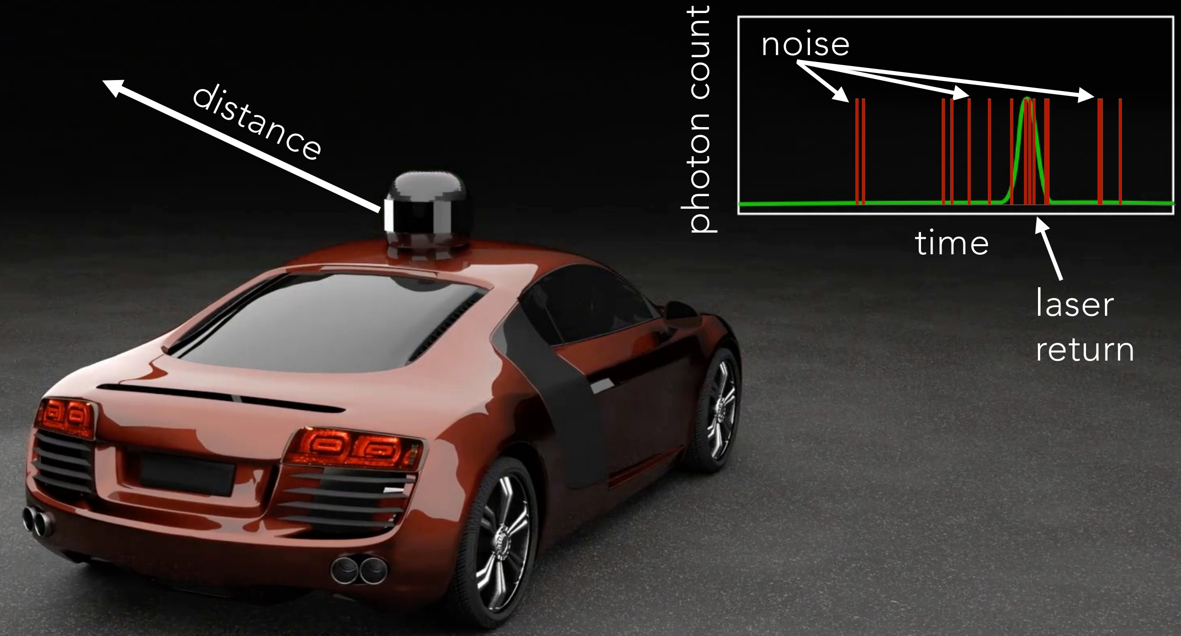

LiDAR

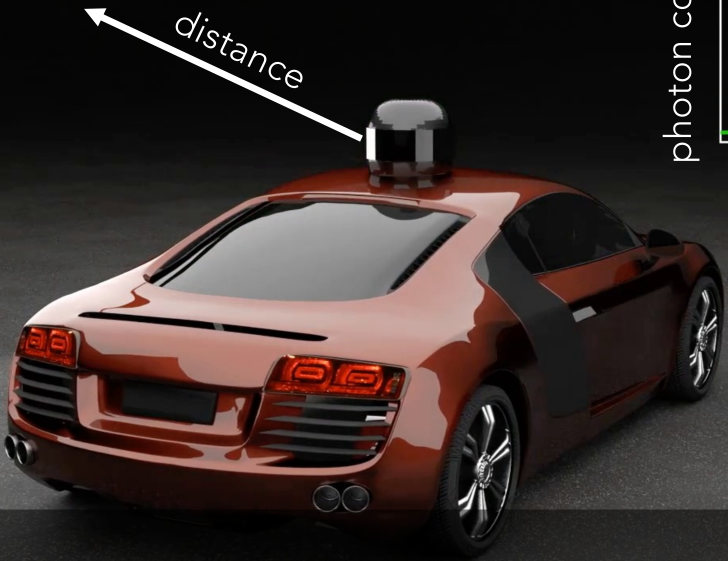

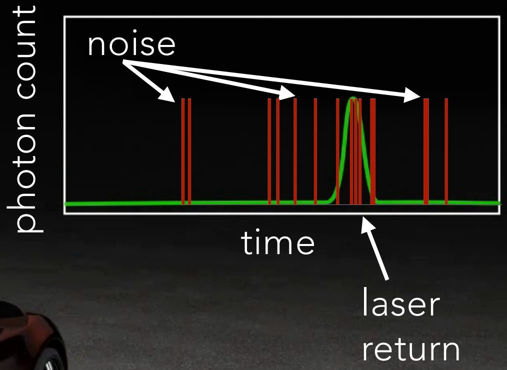

Challenges

1. Light efficiency / photon sensitivity (determines range)
2. High-speed time stamping (determines accuracy)
3. Computational algorithms (determines range and accuracy)

Challenges

1. Light efficiency / photon sensitivity (determines range)

- intensity of returned light falls off with $1/d^2$, i.e. very quickly!
- emit as much light as possible - ***fundamentally limited by eye safety*** (in most applications)
- detect as much light as possible, ideally individual photons

Challenges

2. High-speed time stamping (determines accuracy)

- speed of light is ~300,000,000 m/s
- 1 m = 3.3 ns; 1 cm = 33 ps; 1 mm = 3.3 ps
- need picosecond-accurate time-stamping → usually high-end electronics, but also done with ASICs, FPGAs

Challenges

3. Computational algorithms (determines range and accuracy)

   - robust depth estimation from single photon per pixel!

Kirmani et al. “First-photon Imaging”, Science 2014

conventional method first-photon imaging

(Single-photon) Avalanche Photodiodes

Linear mode (i.e., avalanche photodiode or ***APD***):

acts like a conventional photodiode with extremely high gain or amplification

time resolution >300 ps – 10 ns

Geiger mode (i.e., single-photon avalanche photodiode ***SPAD***):

500x more sensitive, i.e. single-photon sensitive

time resolution ~50 ps

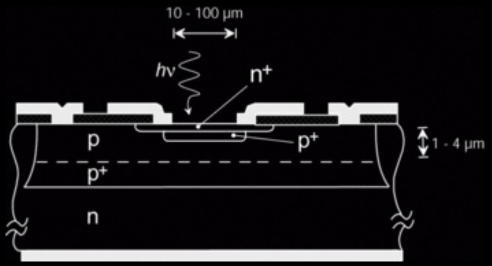

Semiconductor devices

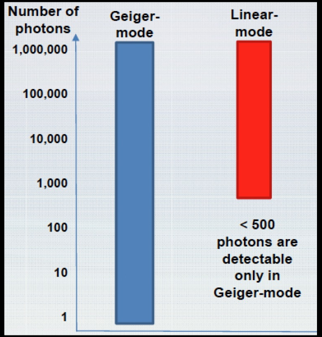

image by Princeton Lightwave

Single-Photon Avalanche Diodes

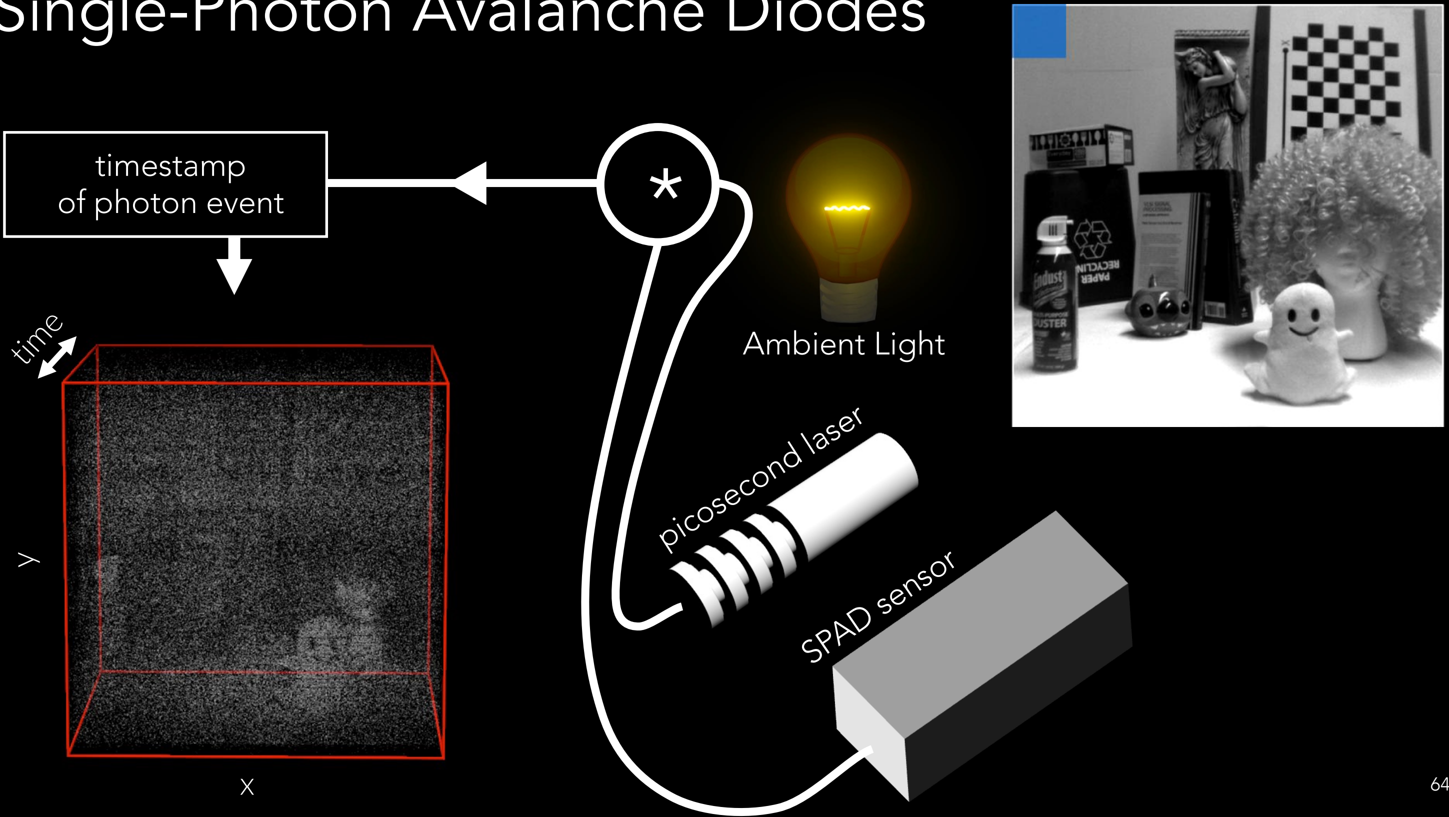

Measurements

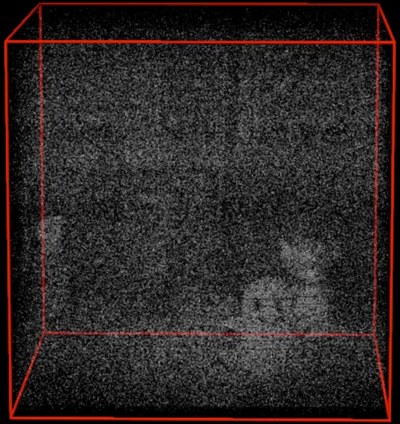

SPAD measurements
(256 x 256 x 1536)

Intensity image
(1024 x 1024)

Noisy <1 photon per pix., low spatial resolution

clean, high spatial resolution

How to fuse information from both?

Lindell et al., SIGGRAPH 2018

CNN Architecture for Depth Estimation

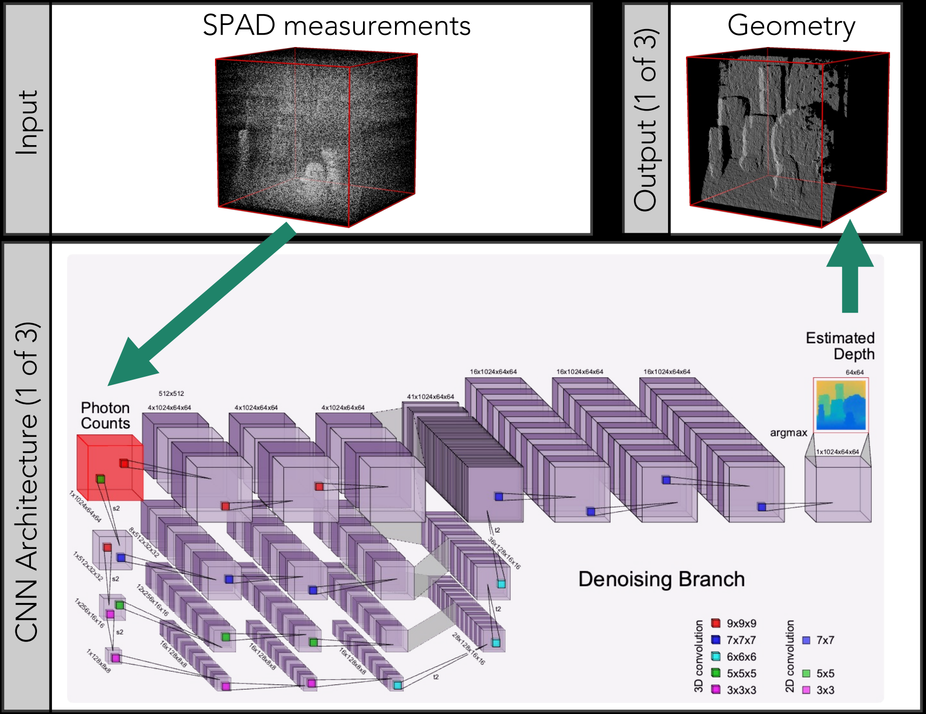

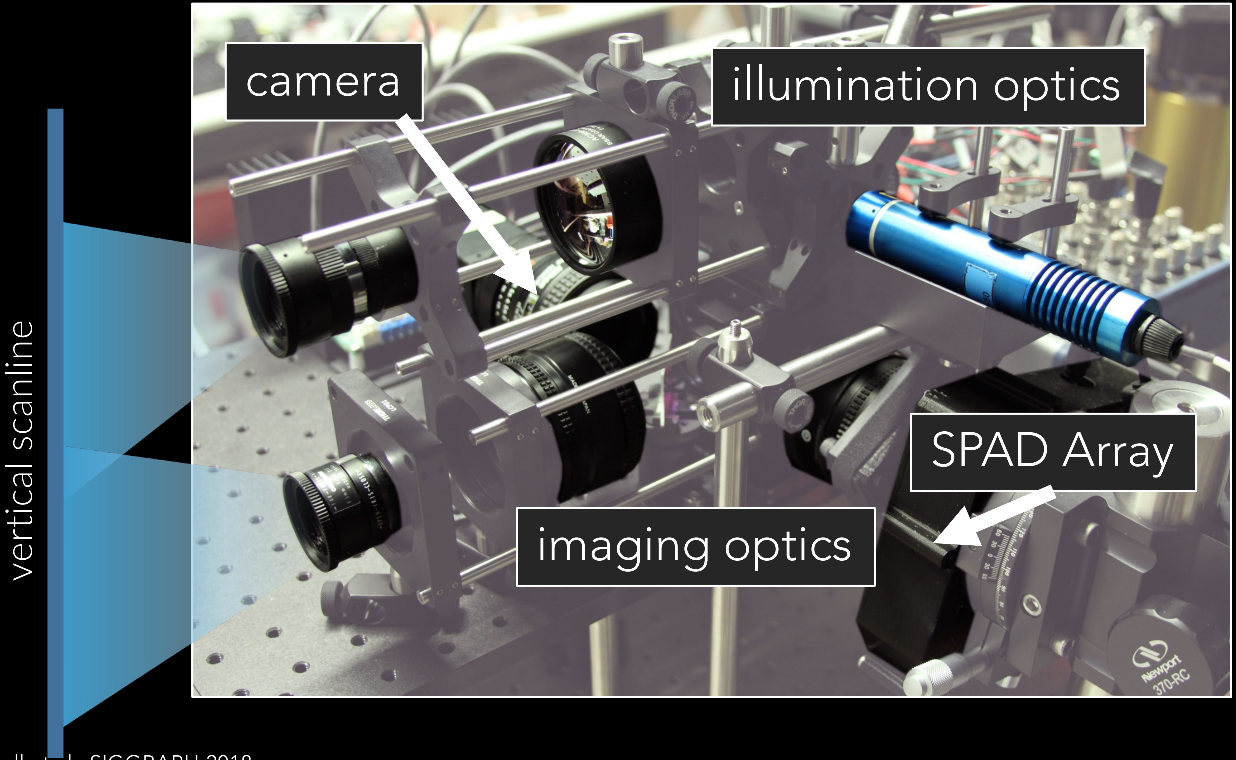

Lindell et al., SIGGRAPH 2018

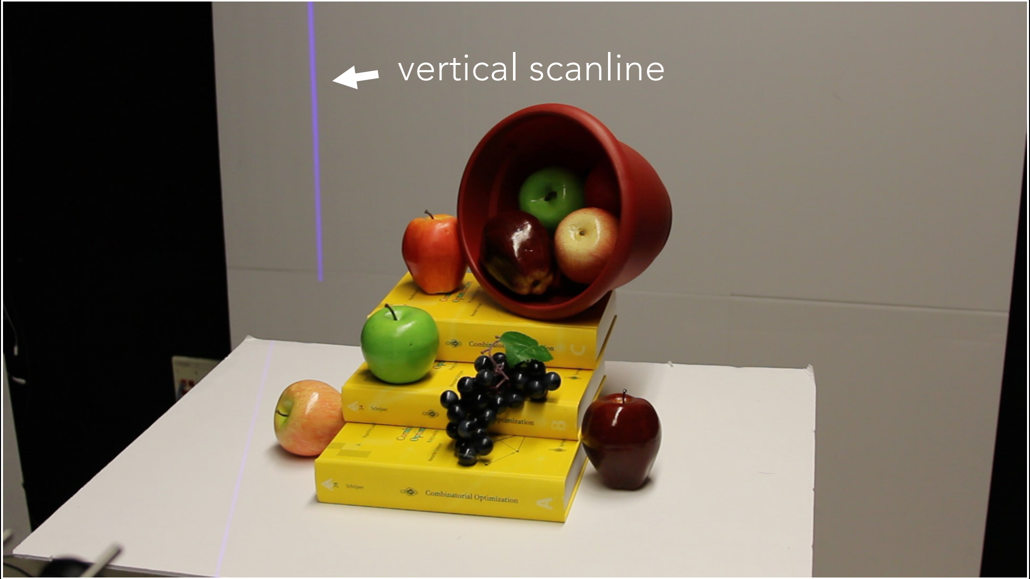

scan rate: 20 Hz

lights on

(note: laser illumination is too weak to observe visually while scanning under ambient light)

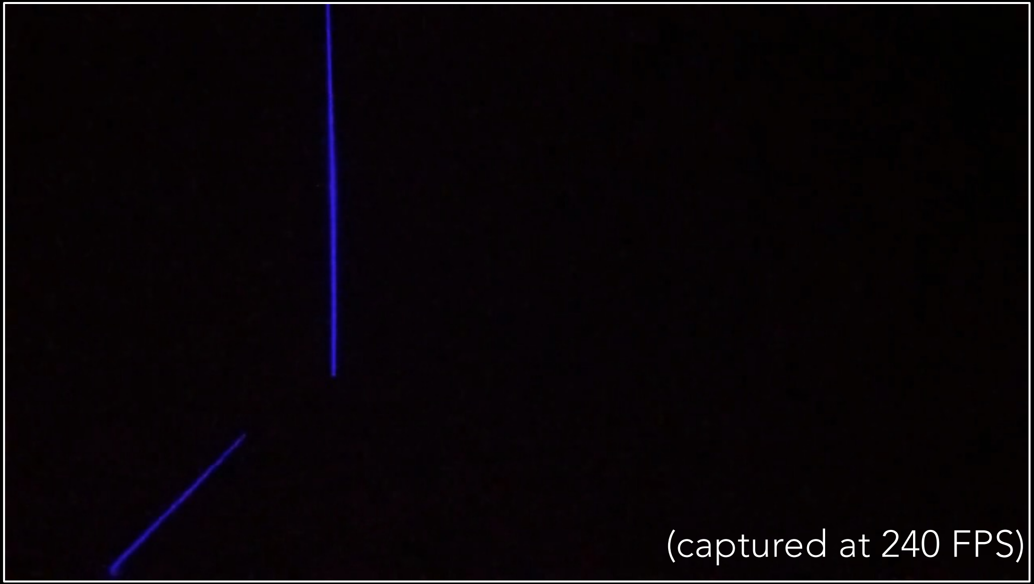

scan rate: 20 Hz

lights off

Lindell et al., SIGGRAPH 2018

Intensity image

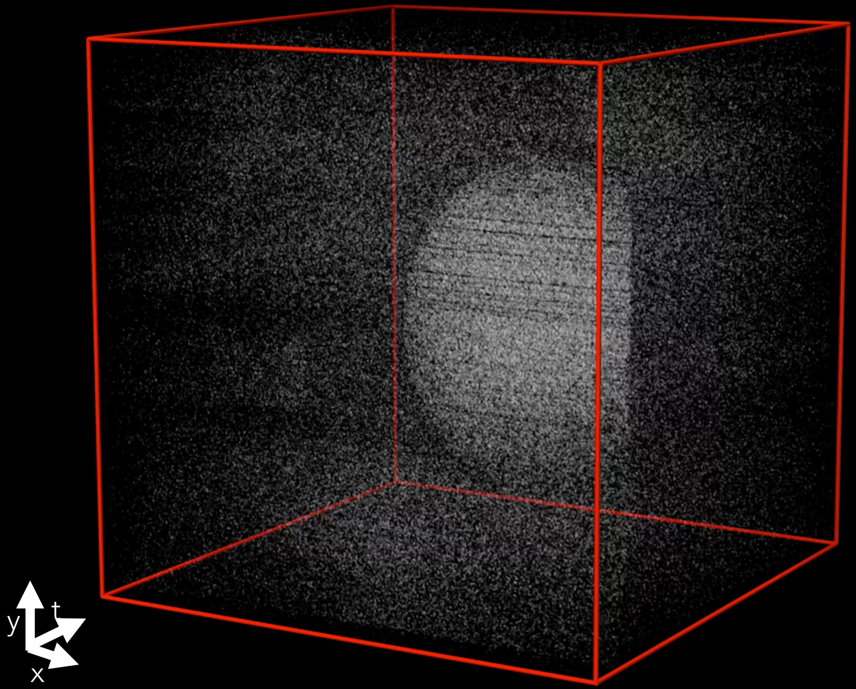

SPAD measurements (20 Hz)

Average per spatial position
0.64 Signal Detections
0.87 Background Detections

Lindell et al., SIGGRAPH 2018

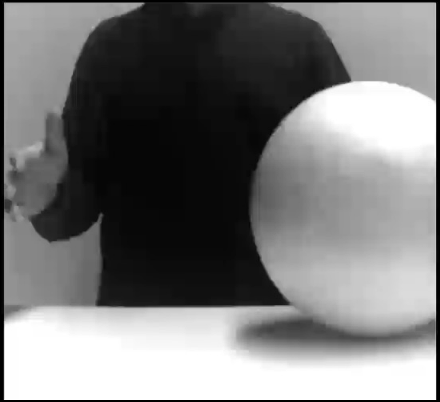

Intensity image

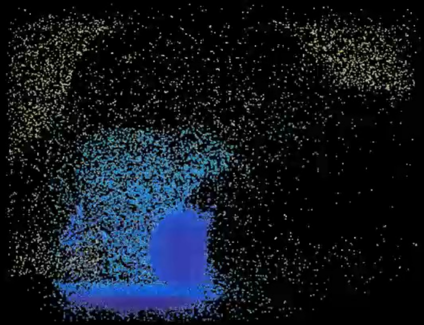

Log-matched filter

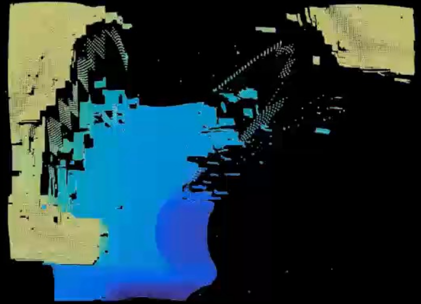

[Rapp and Goyal 2017]

CASPI: collaborative photon processing for active single-photon imaging

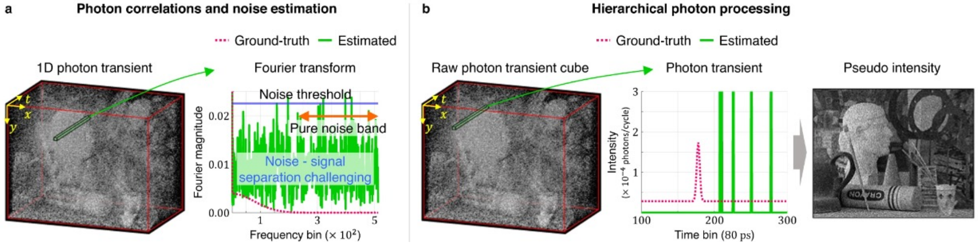

CASPI: collaborative photon processing for active single-photon imaging

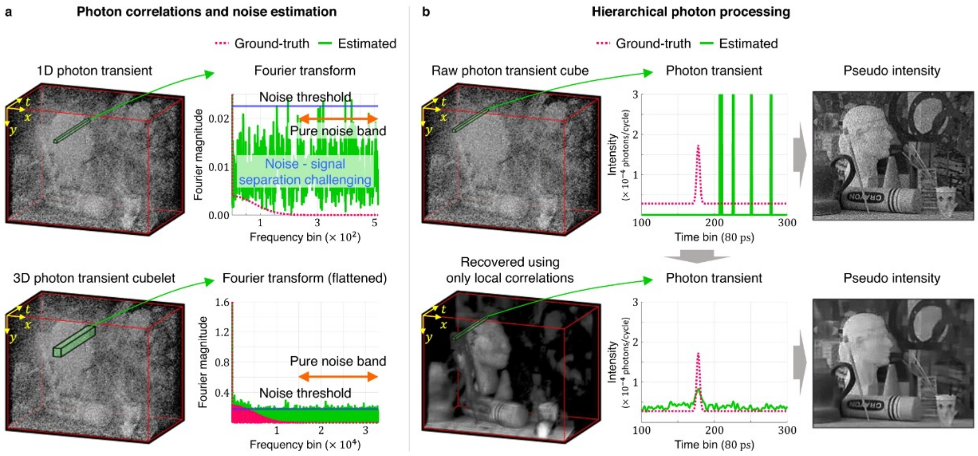

CASPI: collaborative photon processing for active single-photon imaging

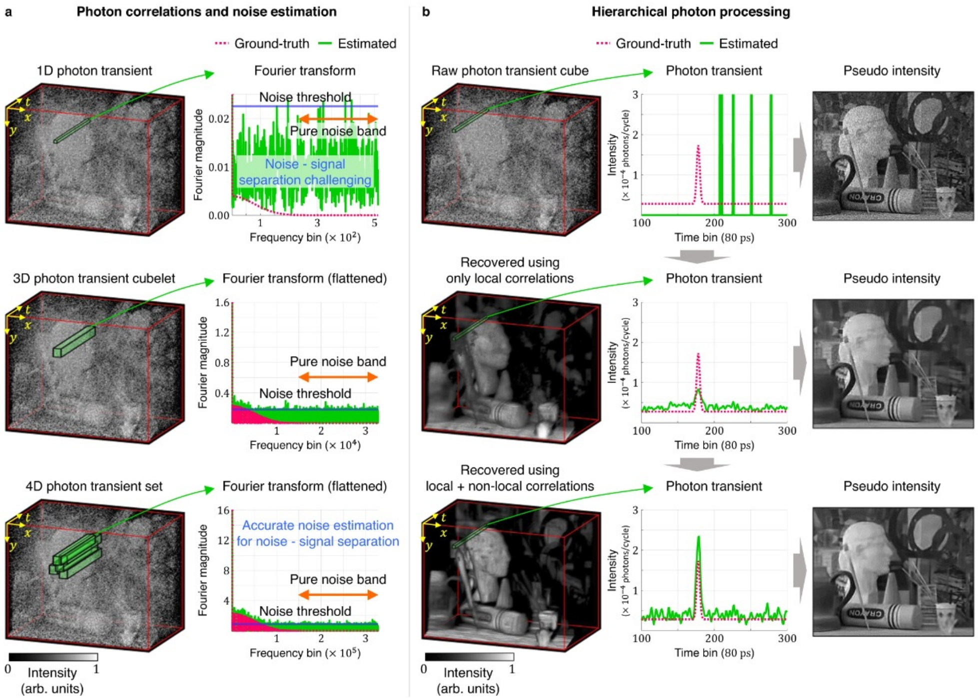

CASPI: collaborative photon processing for active single-photon imaging

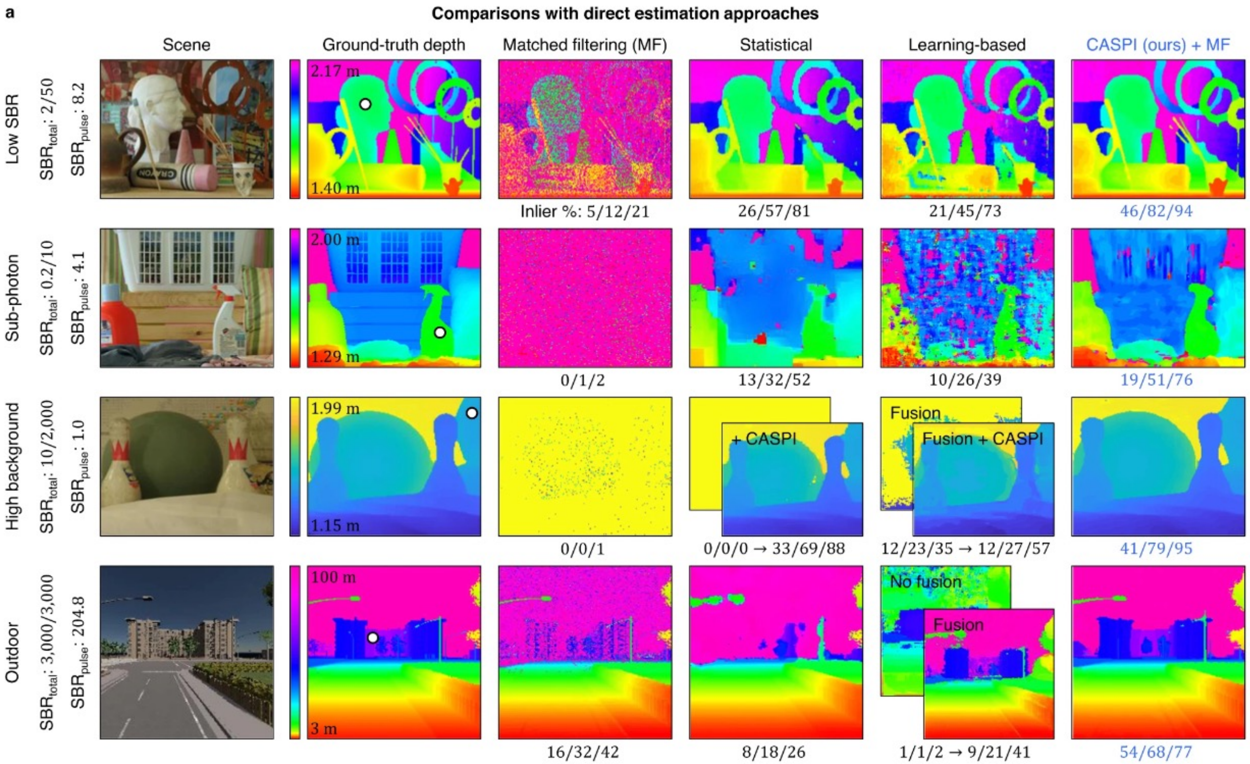

CASPI: collaborative photon processing for active single-photon imaging

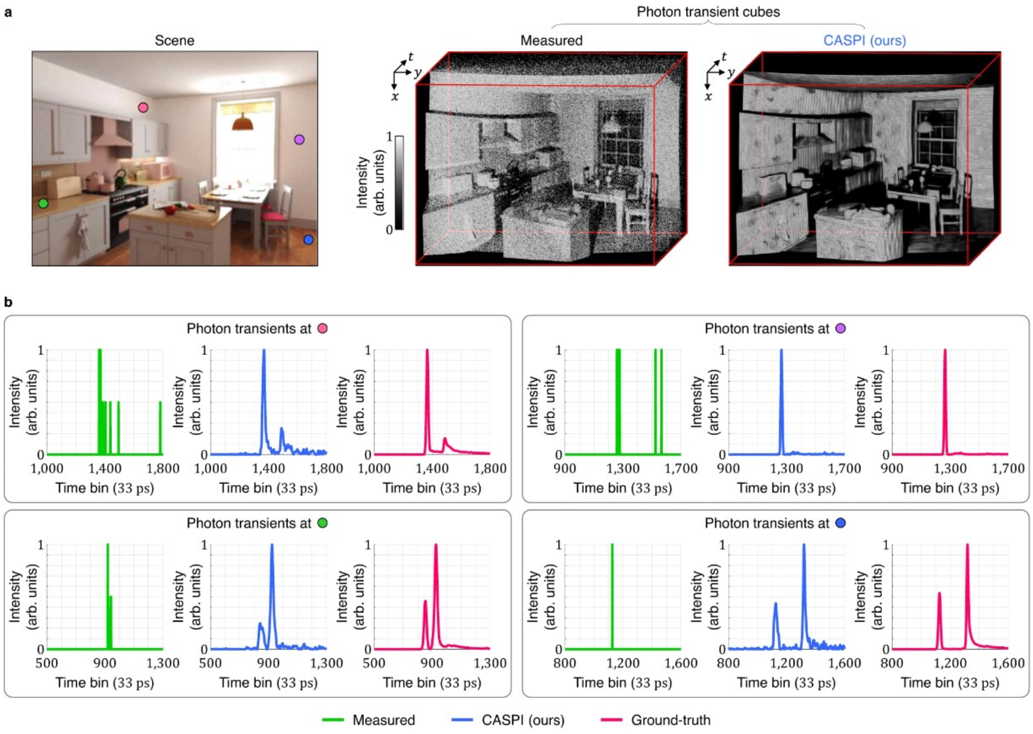

overview

- Time-resolved imaging
- Single-photon avalanche diodes (SPADs)
- Single-photon lidar
- Non-line-of-sight imaging (part 1)
- passive ultra-wideband sensing

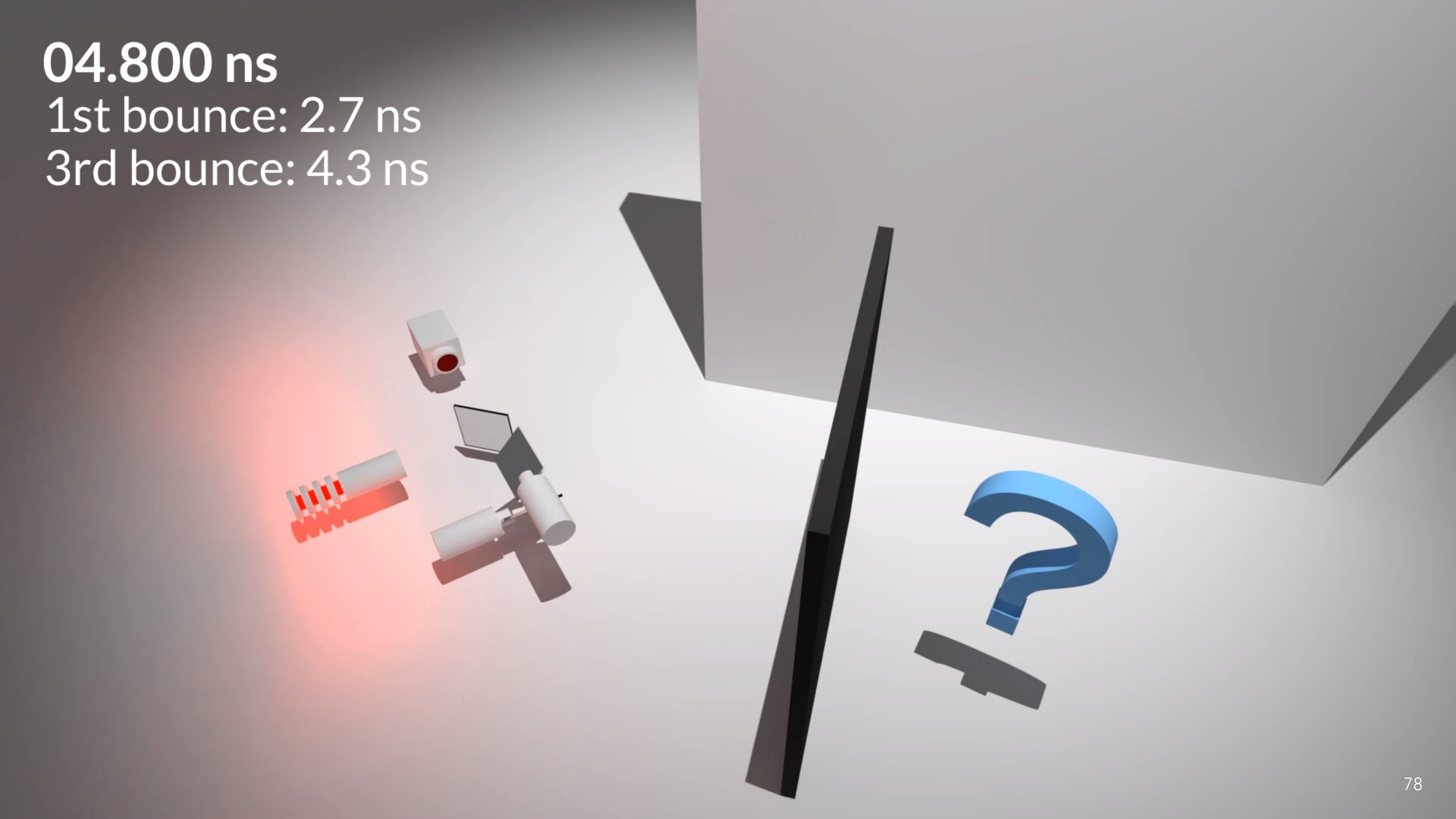
04.800 ns
1st bounce: 2.7 ns
3rd bounce: 4.3 ns

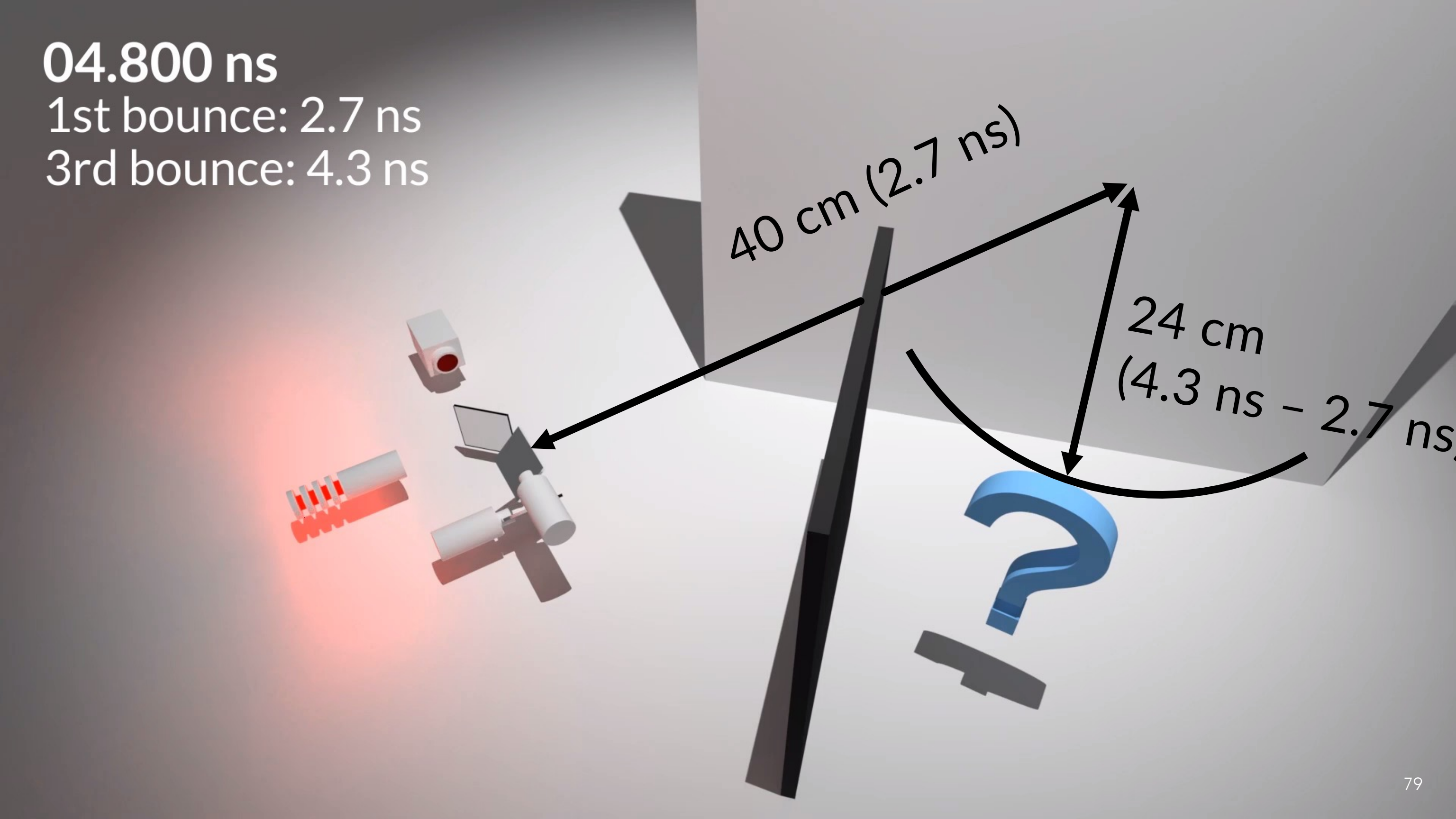
04.800 ns
1st bounce: 2.7 ns
3rd bounce: 4.3 ns
40 cm (2.7 ns)
24 cm
(4.3 ns – 2.7 ns)

RAW histogram (10 FPS)

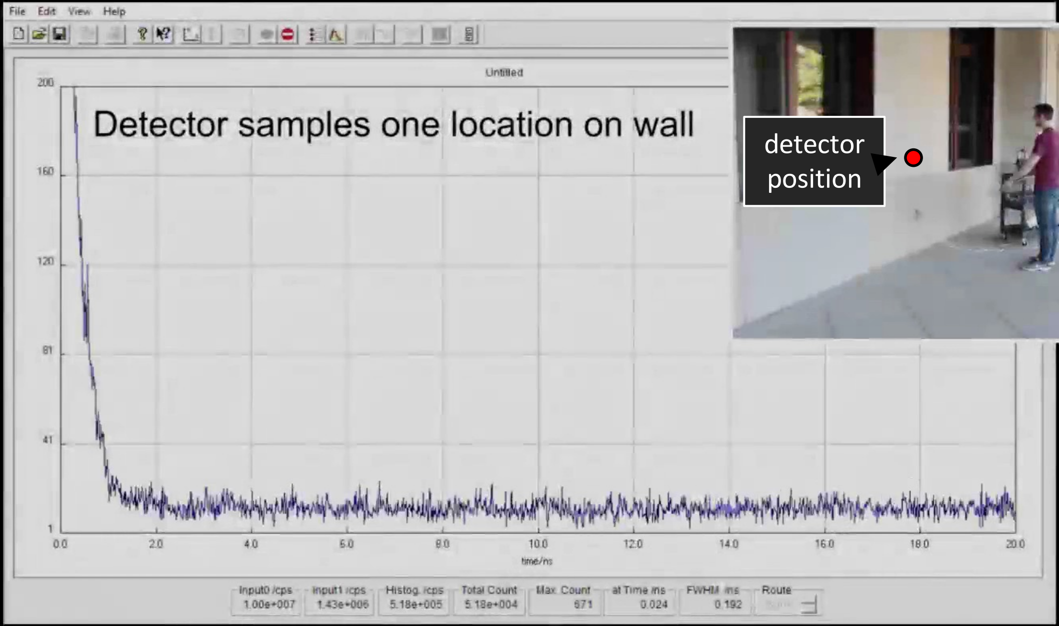

object

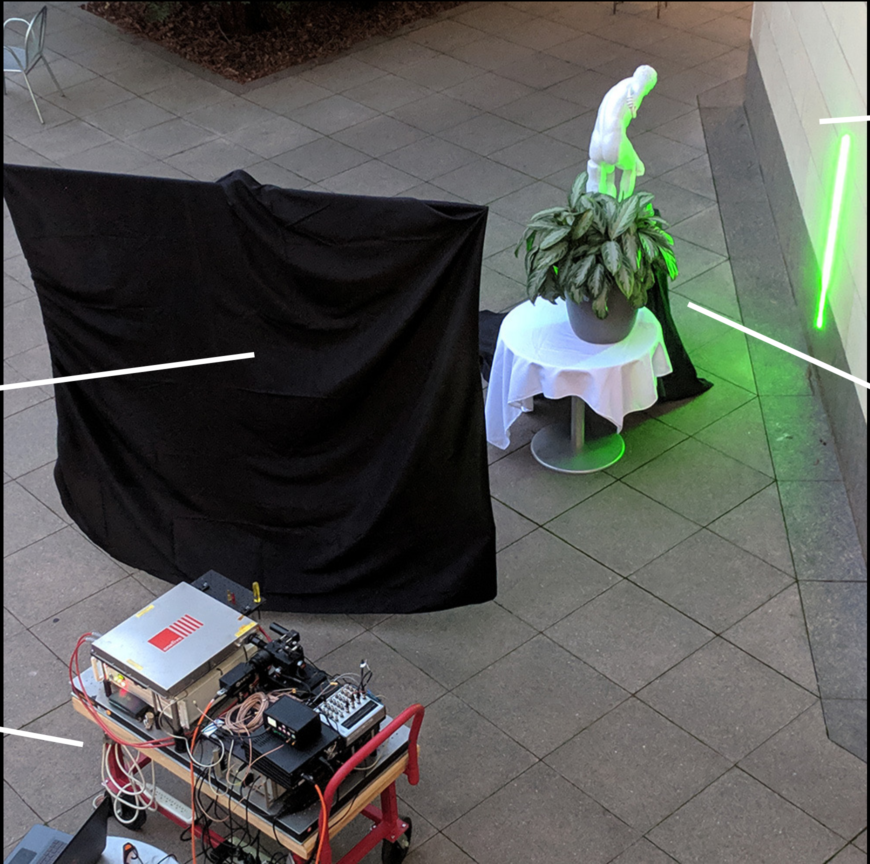

wall

occluder

hidden scene

NLOS imaging system


scanning mirrors
laser
detector
PICOSECOND DELAYER
INPUT
MPD
NIM OUT
TTL OUT


resolution: 128 x 128
area: 2 m × 2 m

scene photo

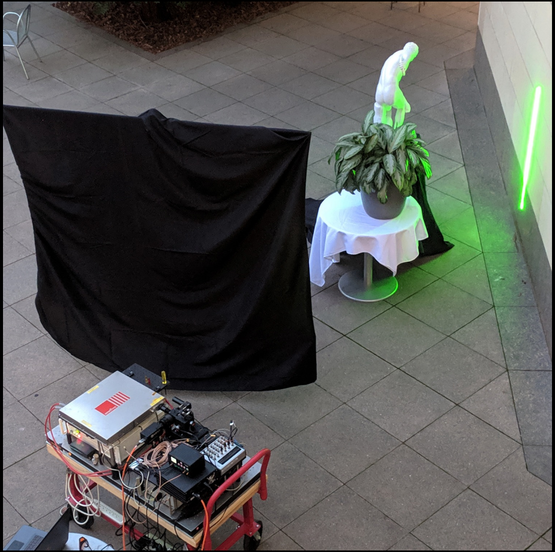

measurements

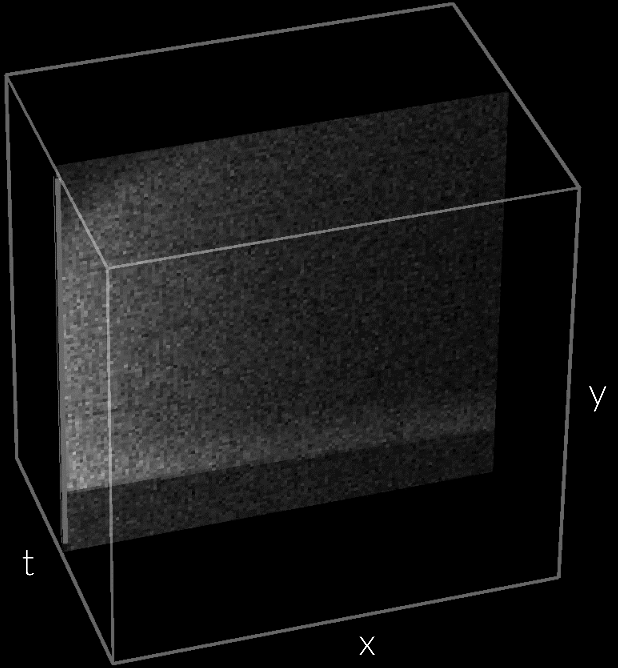

Lindell et al., SIGGRAPH 2019

scene photo

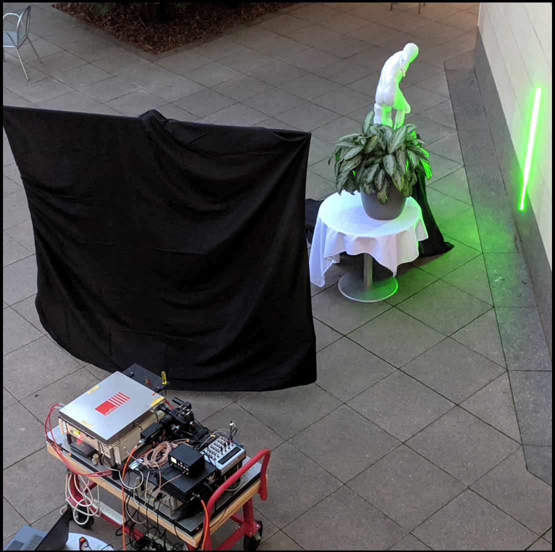

reconstruction

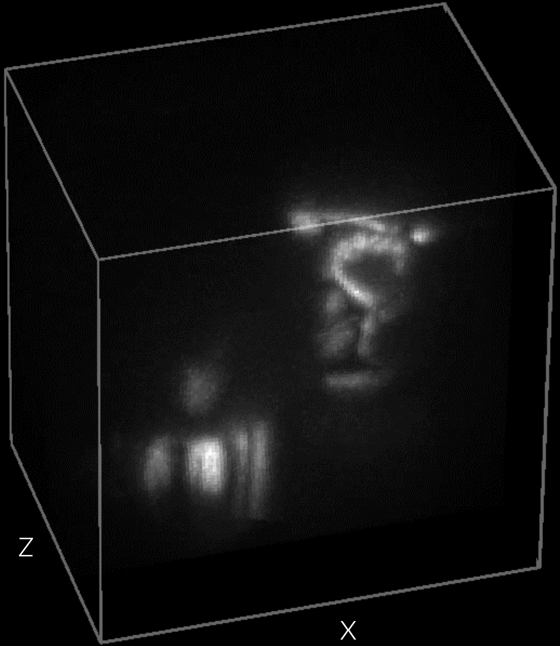

Lindell et al., SIGGRAPH 2019

Dimensions: 2 m x 2 m x 1.5 m

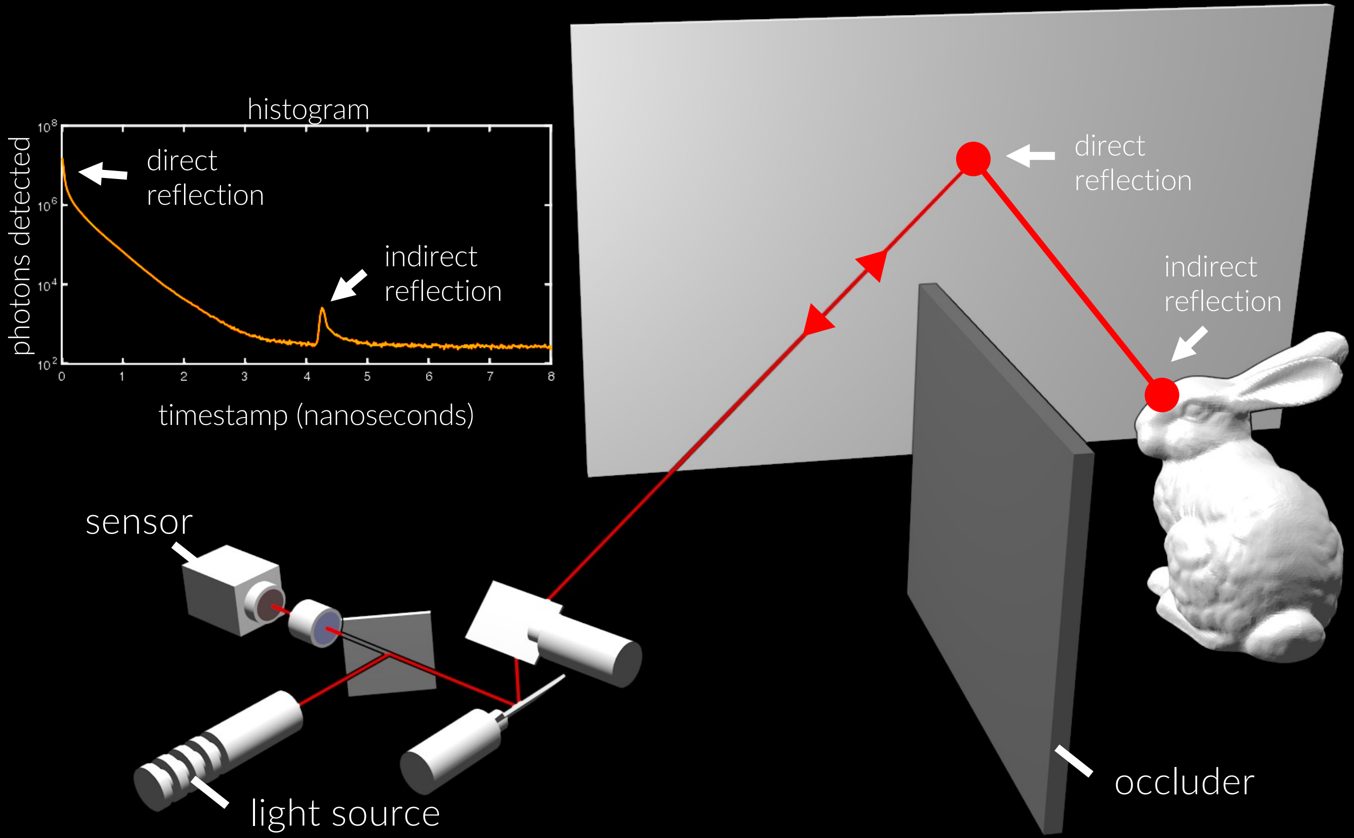
histogram
photons detected
10^8
10^6
10^4
10^2
0
1
2
3
4
5
6
7
8
timestamp (nanoseconds)
direct
reflection
indirect
reflection
direct
reflection
indirect
reflection
sensor
light source
occluder

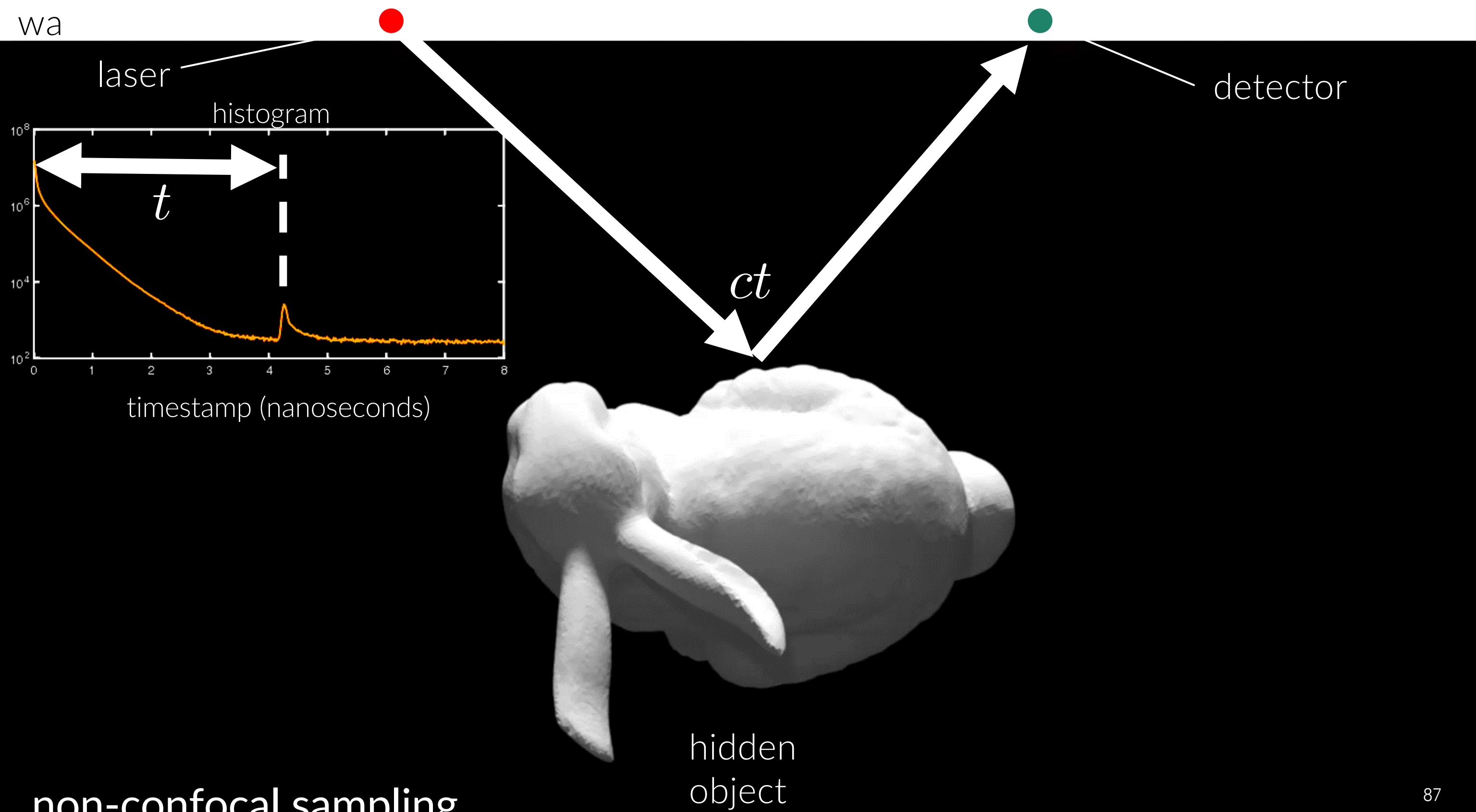

non-confocal sampling

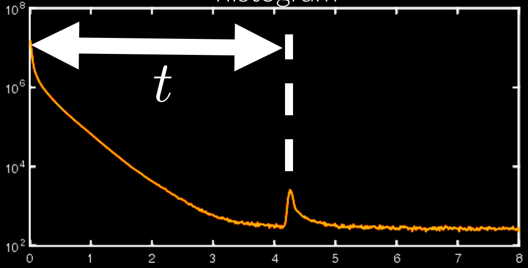

ct

laser and detector focus on this point

hidden object

APJarvis [CC BY-SA 4.0]

lasers and detectors illuminate and image same points

confocal sampling

wa

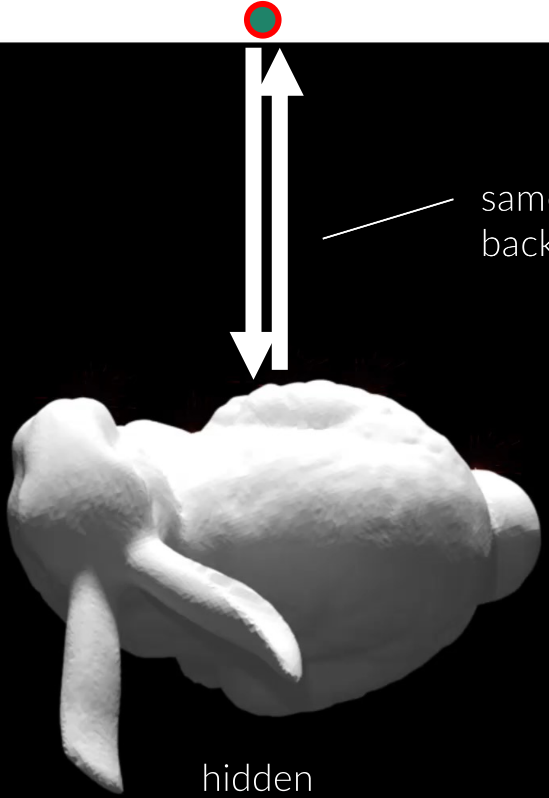

same path to the object and back

hidden object

confocal sampling

wa

- simplified NLOS mathematical model
- enables efficient NLOS reconstruction

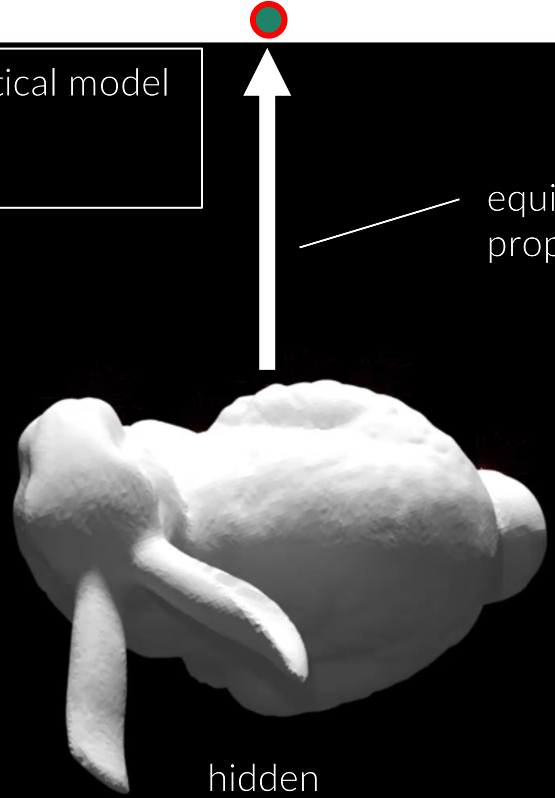

equivalent to one-way propagation at half-speed

hidden object

confocal sampling

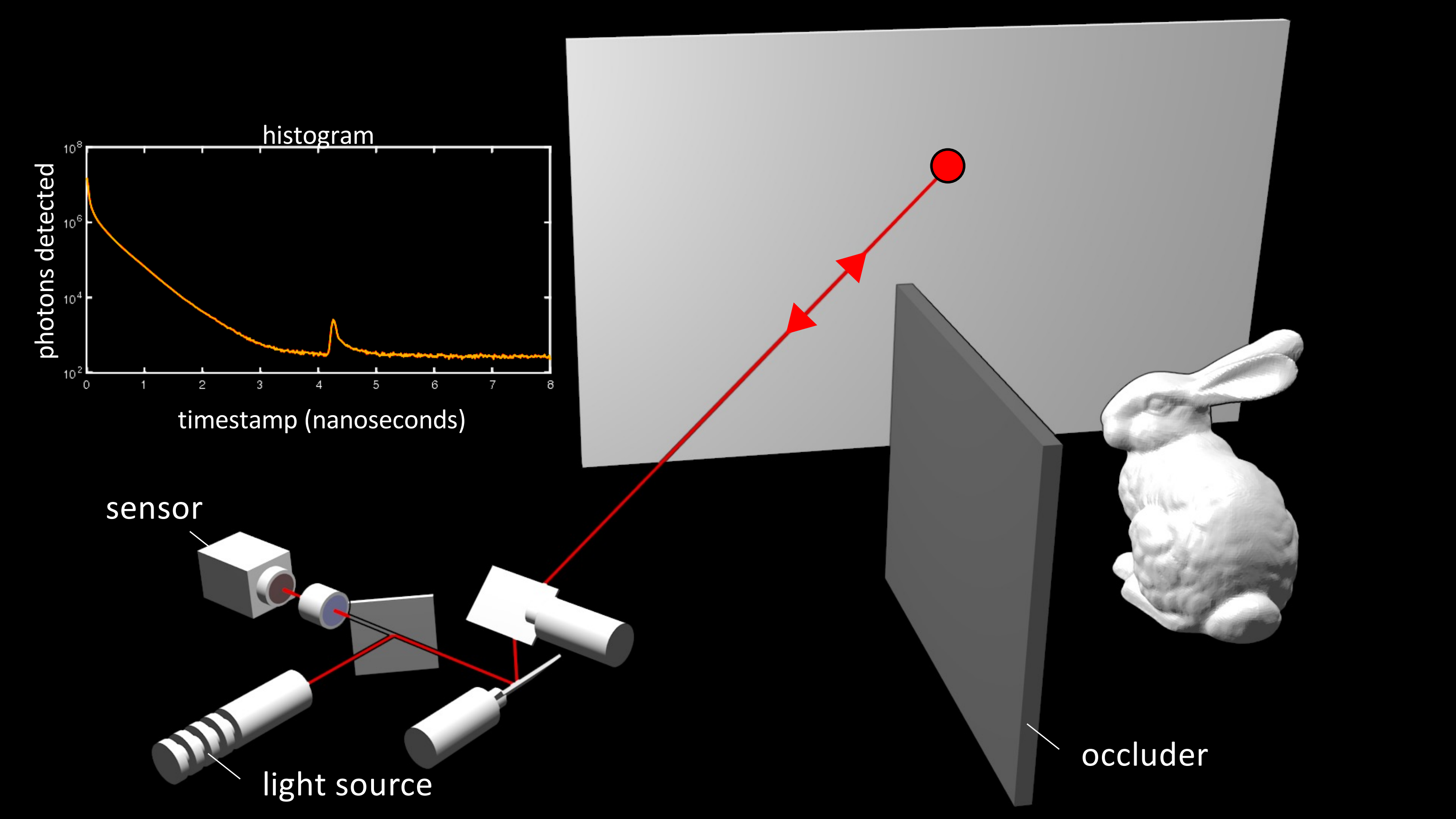

histogram
photons detected
timestamp (nanoseconds)
sensor
light source
occluder

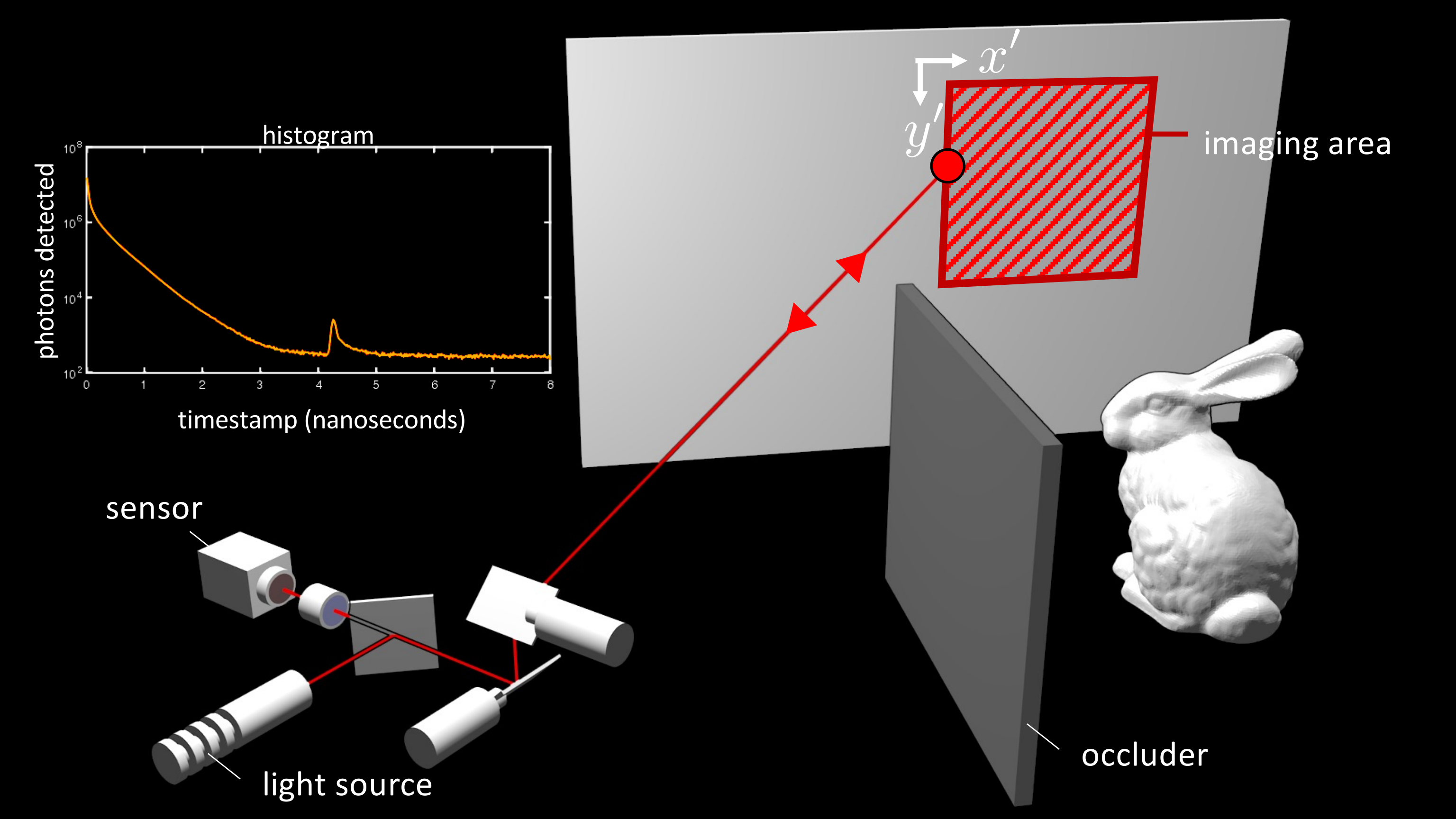
histogram
photons detected
timestamp (nanoseconds)
10^8
10^6
10^4
10^2
0
1
2
3
4
5
6
7
8
x'
y'
imaging area
sensor
light source
occluder

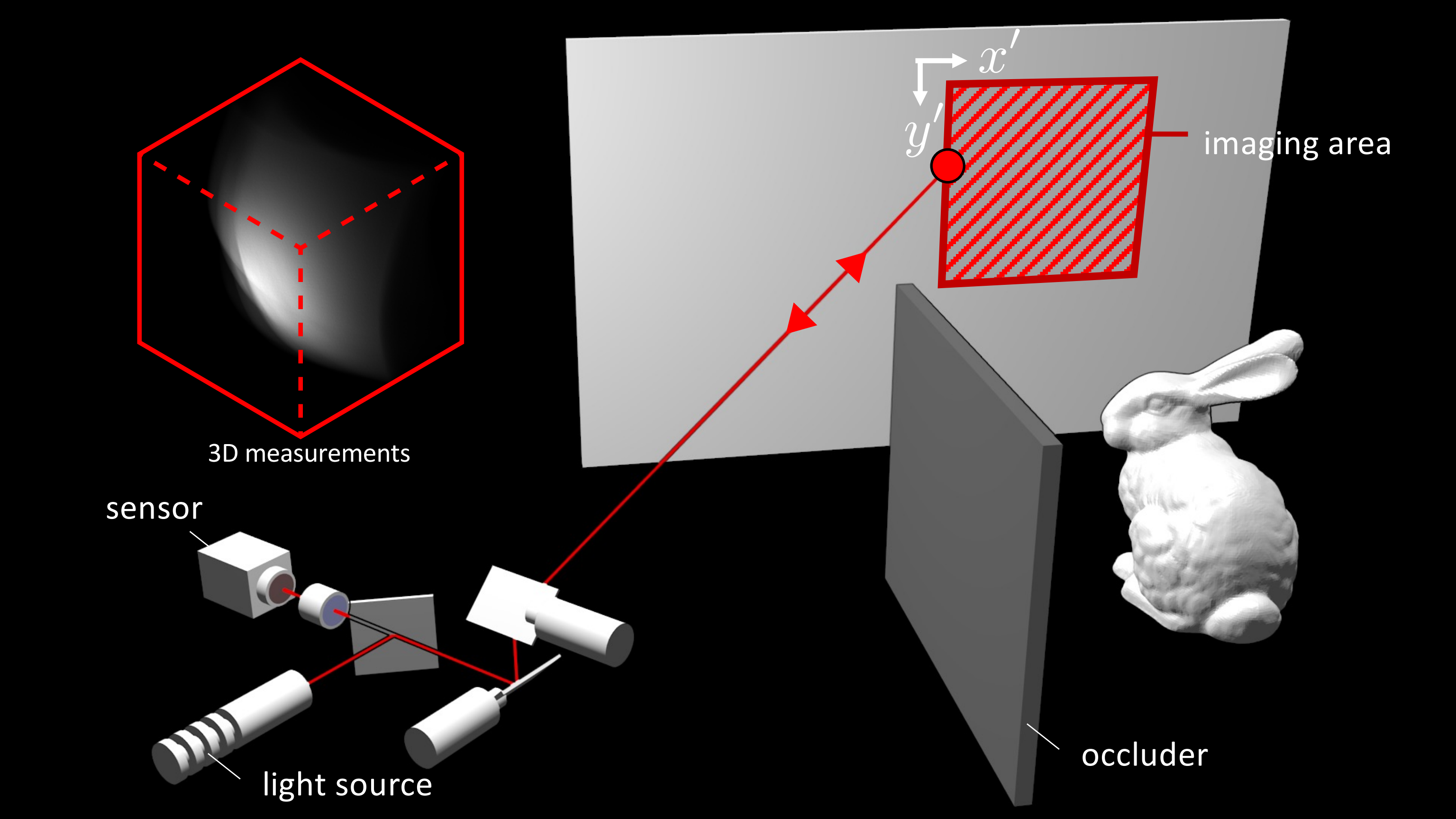

x'
y'
imaging area
3D measurements
sensor
occluder
light source

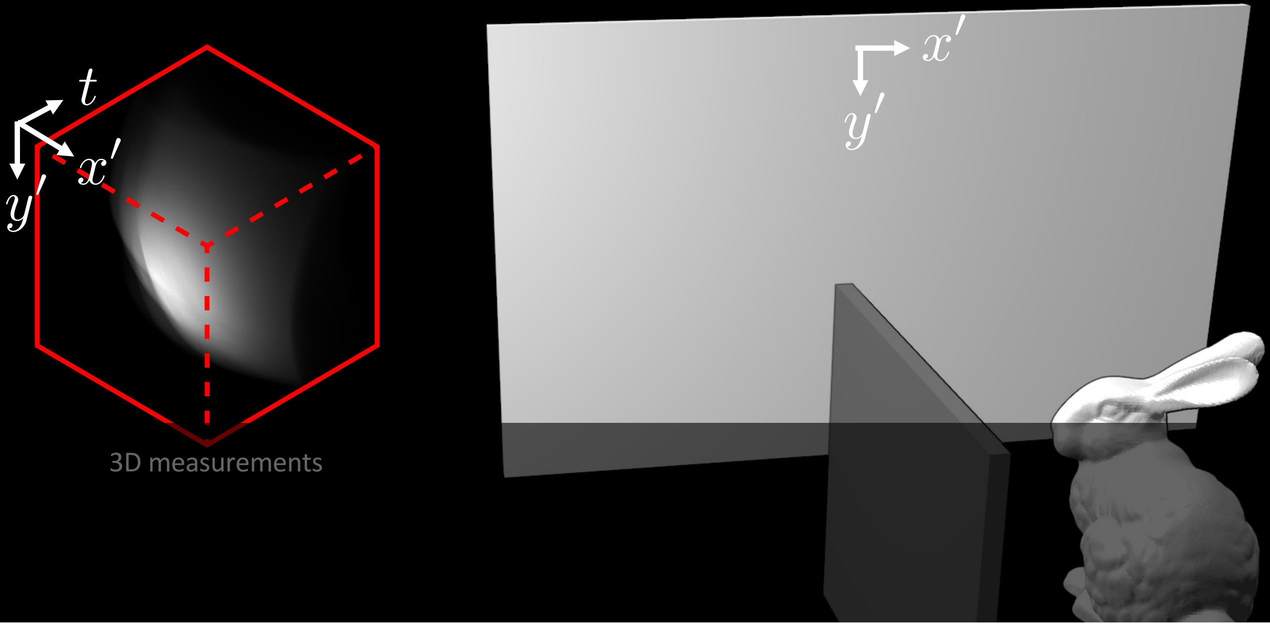

$$\underbrace{\tau(x',y',t)}_{\text{3D measurements}} = \iiint_{\Omega} \underbrace{\frac{1}{r_l^2 r^2}}_{\text{radiometric term}} \underbrace{\delta\left(r_l + r - tc\right)}_{\text{geometric term}} \cdot \underbrace{\rho(x,y,z)}_{\text{hidden 3D volume}} \; dx \; dy \; dz$$

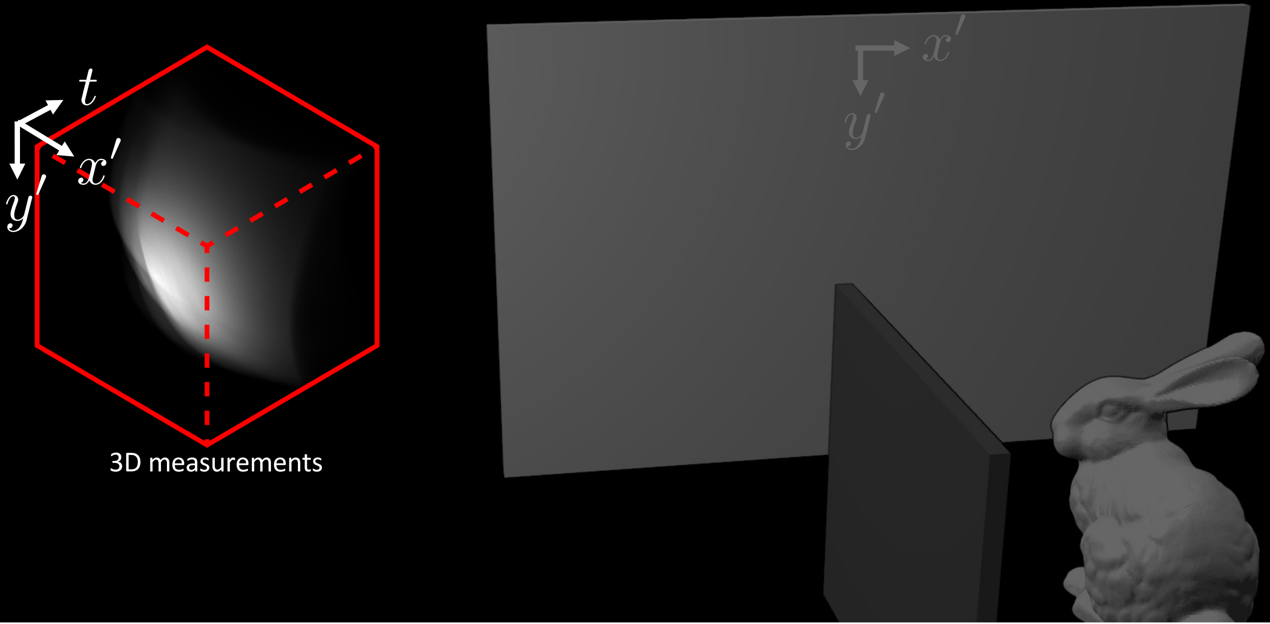

$$\underbrace{\tau(x',y',t)}_{\text{3D measurements}} = \iiint_\Omega \underbrace{\frac{1}{r_l^2 r^2}}_{\text{radiometric term}} \underbrace{\delta\left(r_l + r - tc\right)}_{\text{geometric term}} \cdot \underbrace{\rho(x,y,z)}_{\text{hidden 3D volume}} \; dx \; dy \; dz$$

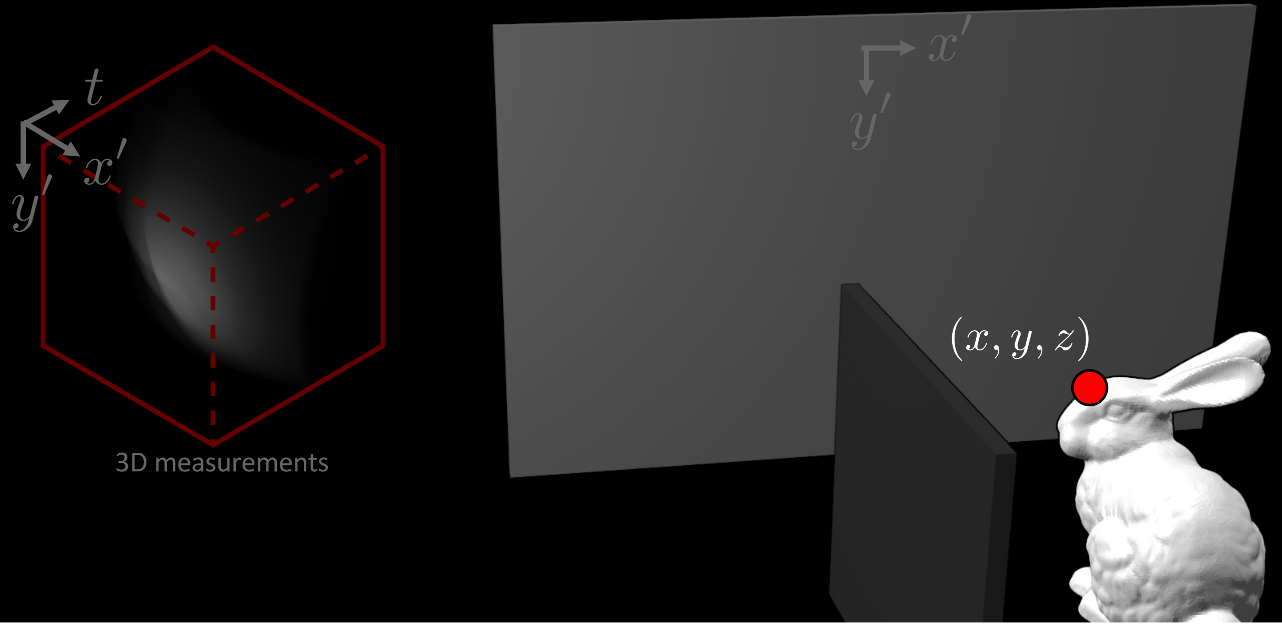

$$\underbrace{\tau(x', y', t)}_{\text{3D measurements}} = \iiint_{\Omega} \underbrace{\frac{1}{r_l^2 r^2}}_{\text{radiometric term}} \underbrace{\delta\left(r_l + r - tc\right)}_{\text{geometric term}} \cdot \underbrace{\rho(x, y, z)}_{\text{hidden 3D volume}} \; dx \; dy \; dz$$

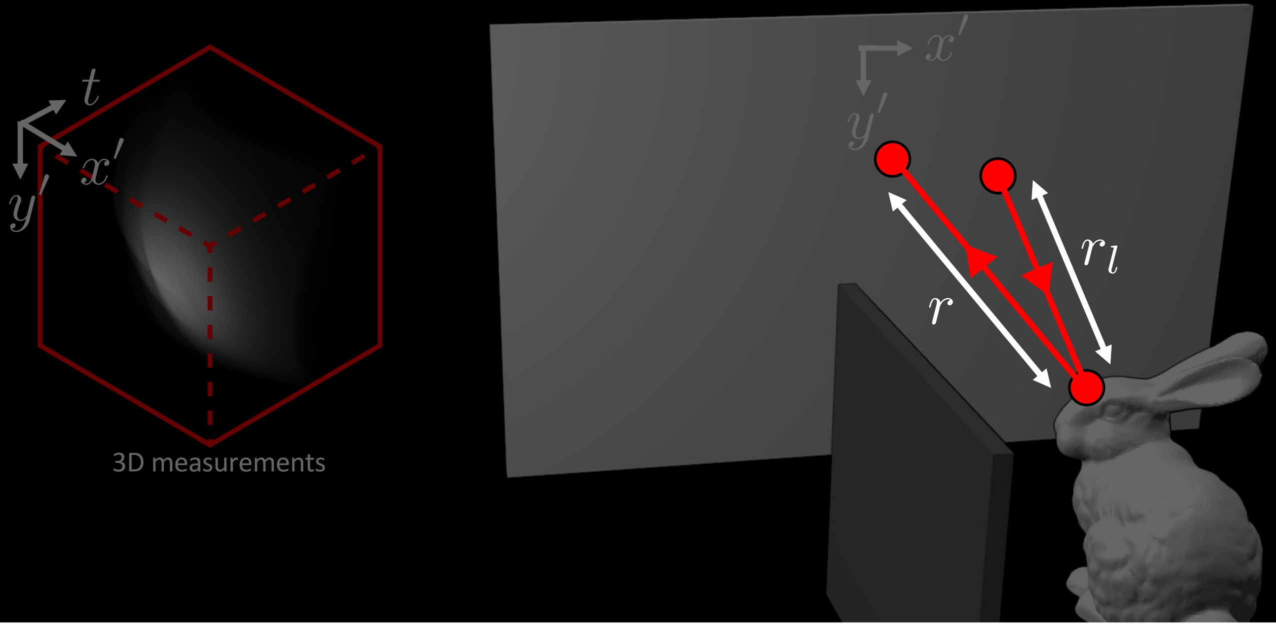

$$\underbrace{\tau(x', y', t)}_{\text{3D measurements}} = \iiint_{\Omega} \underbrace{\frac{1}{r_l^2 r^2}}_{\text{radiometric term}} \underbrace{\delta\left(r_l + r - tc\right)}_{\text{geometric term}} \cdot \underbrace{\rho(x, y, z)}_{\text{hidden 3D volume}} \, dx \, dy \, dz$$

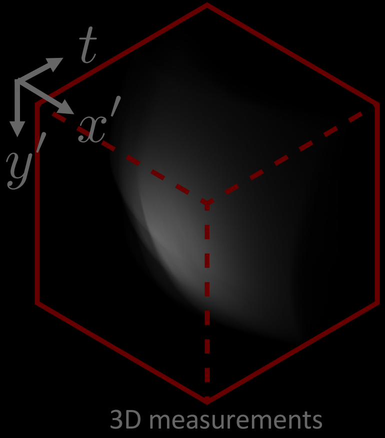

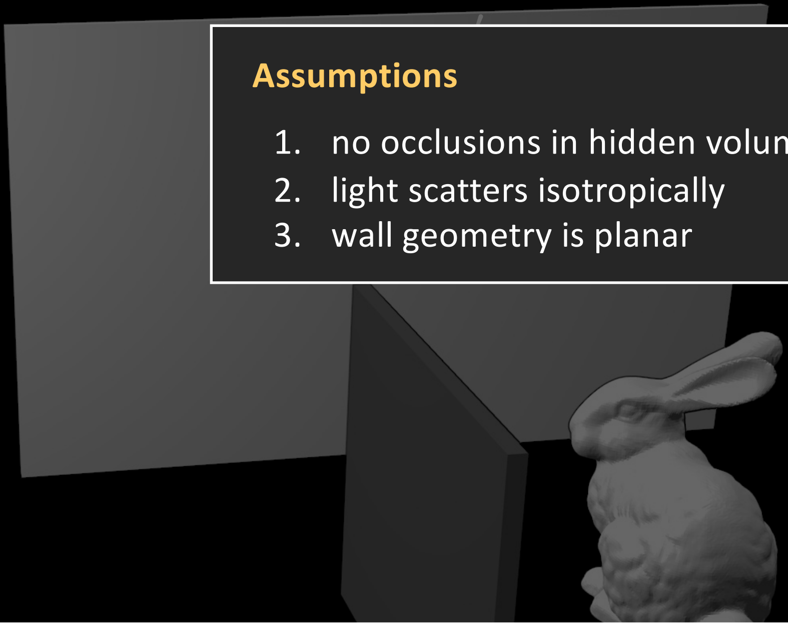

Assumptions

1. no occlusions in hidden volume
2. light scatters isotropically
3. wall geometry is planar

$$\underbrace{\tau(x',y',t)}_{\text{3D measurements}} = \iiint_\Omega \underbrace{\frac{1}{r_l^2 r^2}}_{\text{radiometric term}} \underbrace{\delta\left(r_l + r - tc\right)}_{\text{geometric term}} \cdot \underbrace{\rho(x,y,z)}_{\text{hidden 3D volume}} \, dx \; dy \; dz$$

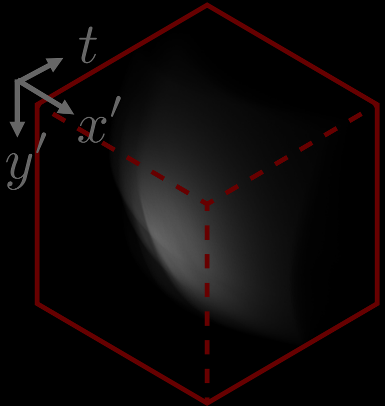

3D measurements

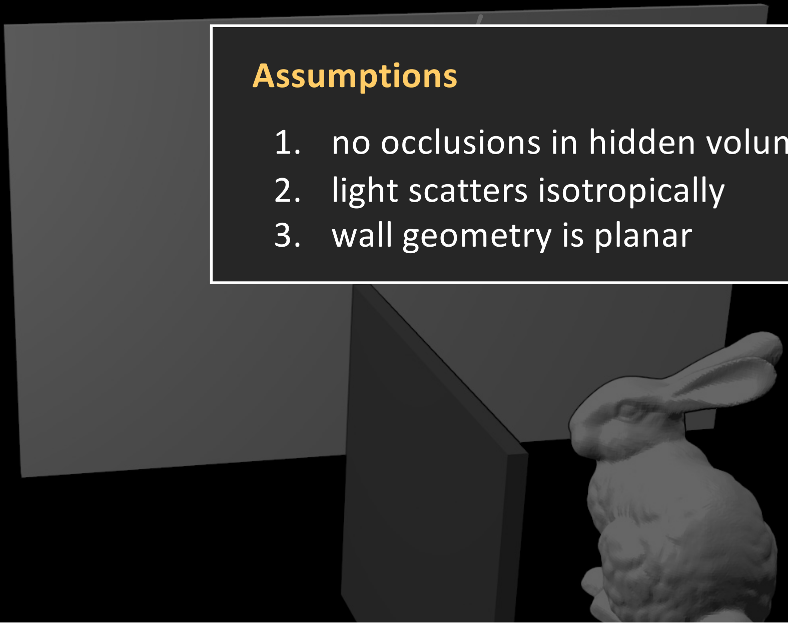

Assumptions

1. no occlusions in hidden volume
2. light scatters isotropically
3. wall geometry is planar

$$\tau(x',y',t) = \iiint_\Omega \frac{1}{r_l^2 r^2}\,\delta\left(r_l + r - tc\right)\cdot\rho(x,y,z)\;dx\;dy\;dz$$

$$\tau = \mathbf{A} \times \rho$$

NLOS image formation mode:

$$\tau = \mathbf{A}\rho$$

measurements $n^3 \times 1$

transport matrix $n^3 \times n^3$

unknown volume $n^3 \times 1$

PROBLEM: $\mathbf{A}$ extremely large in practice (e.g., for n = 100, $\mathbf{A}$ has 1 trillion elements)

Backpropagation [Velten 12, Buttafava 15]

Flops: $O(n^5)$

Memory: $O(n^3)$

Runtime: Approx. 10 min.

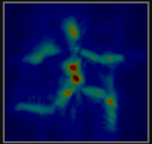

Iterative Inversion [Gupta 12, Heide 13]

Flops: $O(n^5)$ per iter.

Memory: $O(n^5)$

Runtime: > 1 hour

Our approach

express image formation model as a 3D convolution, by:

1. confocalizing measurements
2. performing a change of variables (set $z = \sqrt{u}$, $t = 2\sqrt{v}/c$)

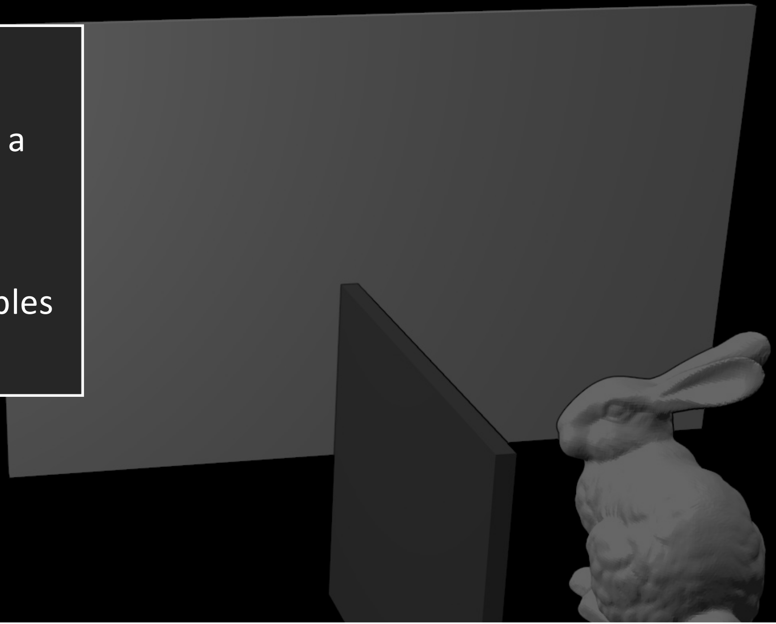

$$\tau(x', y', t) = \iiint_\Omega \frac{1}{r_l^2 r^2} \delta\left(r_l + r - tc\right) \cdot \rho(x, y, z)\ dx\ dy\ dz$$

Our approach

express image formation model as a 3D convolution, by:

1. confocalizing measurements
2. performing a change of variables (set $z = \sqrt{u}$, $t = 2\sqrt{v}/c$)

3D measurements

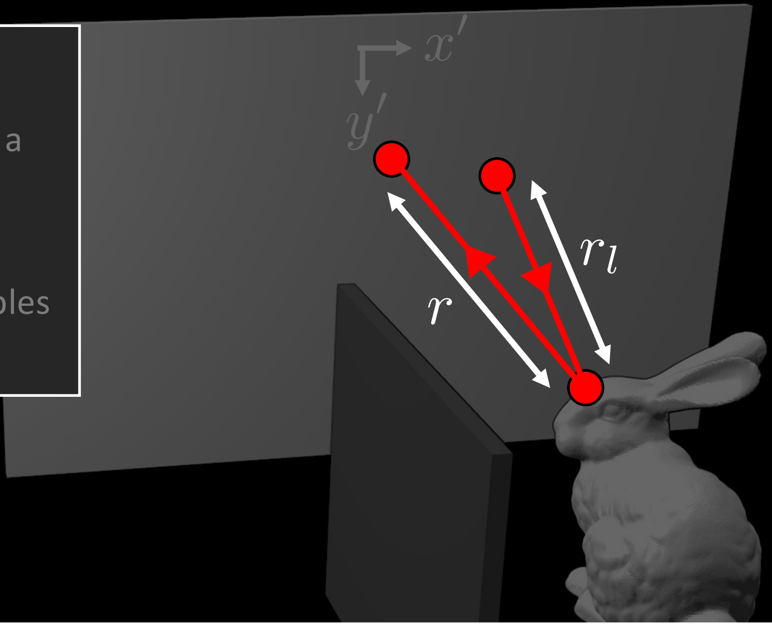

$$\tau(x', y', t) = \iiint_\Omega \frac{1}{r_l^2 r^2} \delta\left(r_l + r - tc\right) \cdot \rho(x, y, z)\ dx\ dy\ dz$$

Our approach

express image formation model as a 3D convolution, by:

1. confocalizing measurements
2. performing a change of variables (set $z = \sqrt{u}$, $t = 2\sqrt{v}/c$)

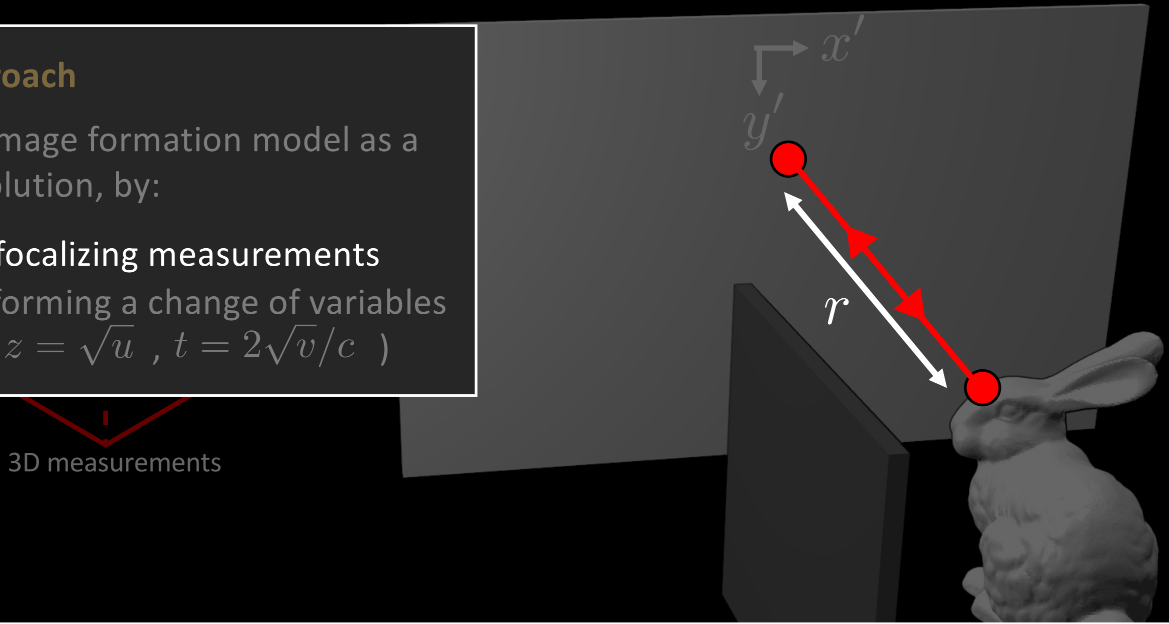

$$\tau(x', y', t) = \iiint_\Omega \frac{1}{r^4} \delta\left(2r - tc\right) \cdot \rho(x, y, z)\; dx\; dy\; dz$$

Our approach

express image formation model as a 3D convolution, by:

1. confocalizing measurements
2. performing a change of variables (set $z = \sqrt{u}$, $t = 2\sqrt{v}/c$)

3D measurements

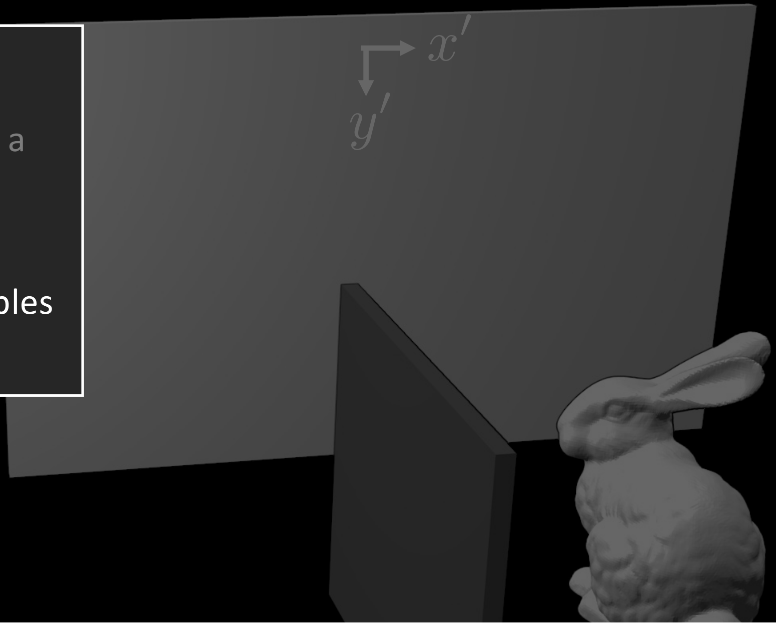

$$\tau(x', y', t) = \iiint_{\Omega} \frac{1}{r^4} \delta\left(2r - tc\right) \cdot \rho(x, y, z)\ dx\ dy\ dz$$

Our approach

express image formation model as a 3D convolution, by:

1. confocalizing measurements
2. performing a change of variables (set $z = \sqrt{u}$, $t = 2\sqrt{v}/c$)

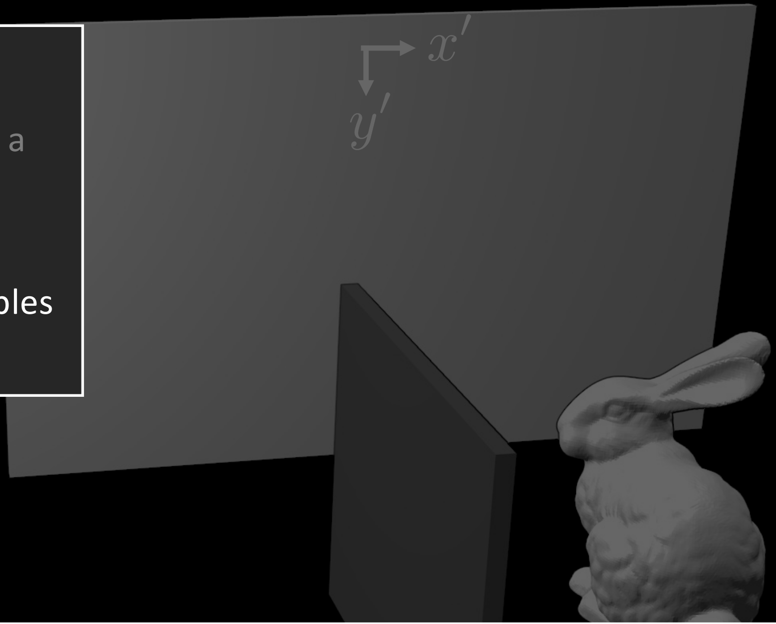

3D measurements

$$v^{3/2}\tau(x', y', \frac{2}{c}\sqrt{v}) = \iiint_\Omega \frac{1}{2\sqrt{u}} \delta\left((x'-x)^2 + (y'-y)^2 + u - v\right) \cdot \rho(x, y, \sqrt{u}) dx dy du$$

Our approach

express image formation model as a 3D convolution, by:

1. confocalizing measurements
2. performing a change of variables (set $z = \sqrt{u}$, $t = 2\sqrt{v}/c$)

3D measurements

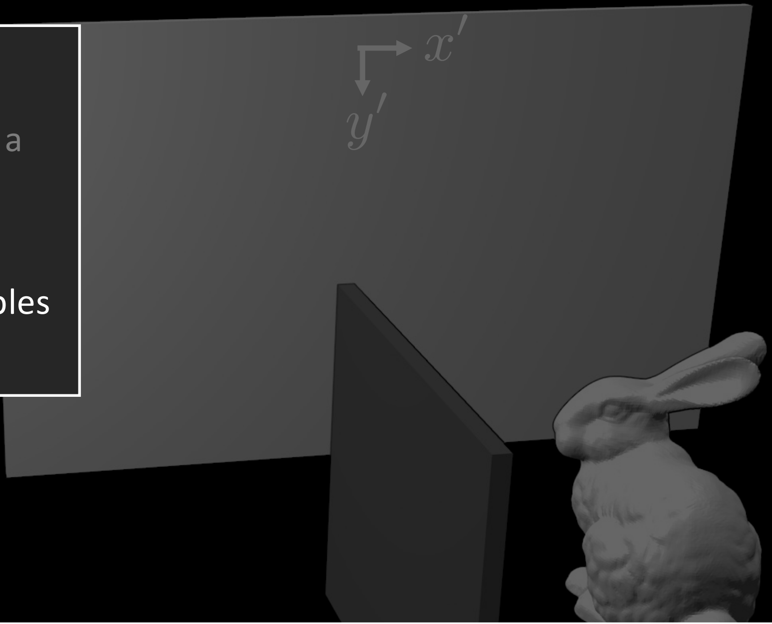

$$\underbrace{v^{3/2}\tau(x',y',\frac{2}{c}\sqrt{v})}_{\tau} \underset{=}{=} \iiint_\Omega \underbrace{\frac{1}{2\sqrt{u}}\delta\left((x'-x)^2+(y'-y)^2+u-v\right)}_{\mathbf{a}} \underset{*}{\cdot} \underbrace{\rho(x,y,\sqrt{u})}_{\rho}dxdydu$$

NLOS image formation mode:

$$\tau = \mathbf{A}\rho$$

measurements $n^3 \times 1$

transport matrix $n^3 \times n^3$

unknown volume $n^3 \times 1$

Backpropagation [Velten 12, Buttafava 15]

Flops: $O(n^5)$

Memory: $O(n^3)$

Runtime: Approx. 10 min.

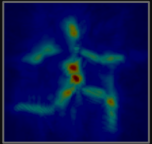

Iterative Inversion [Gupta 12, Heide 13]

Flops: $O(n^5)$ per iter.

Memory: $O(n^5)$

Runtime: > 1 hour

Confocal NLOS image formation mode:

$$\tau = \mathbf{a} * \rho$$

measurements $n \times n \times n$

blur kernel $n \times n \times n$

unknown volume $n \times n \times n$

NLOS image formation mode:

$$\tau = \mathbf{A}\rho$$

measurements $n^3 \times 1$

transport matrix $n^3 \times n^3$

unknown volume $n^3 \times 1$

Backpropagation [Velten 12, Buttafava 15]

Flops: $O(n^5)$

Memory: $O(n^3)$

Runtime: Approx. 10 min.

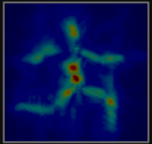

Iterative Inversion [Gupta 12, Heide 13]

Flops: $O(n^5)$ per iter.

Memory: $O(n^5)$

Runtime: > 1 hour

Confocal NLOS image formation mode:

$$\tau = \mathbf{a} * \rho$$

measurements $n \times n \times n$

blur kernel $n \times n \times n$

unknown volume $n \times n \times n$

3D Deconvolution (with Light Cone Transform)

[O'Toole et al. 2018]

Flops: $O(n^3 \log(n))$

Memory: $O(n^3)$

Runtime: < 1 second

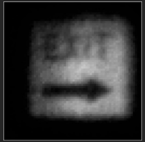

k c_qspck cl rq

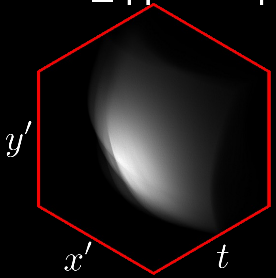

k c_qspck cl rq

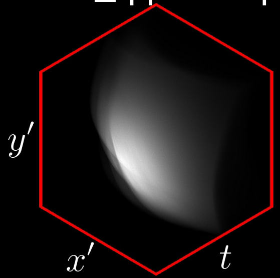

Step 1: resample and attenuate along t-axis

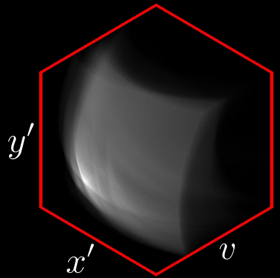

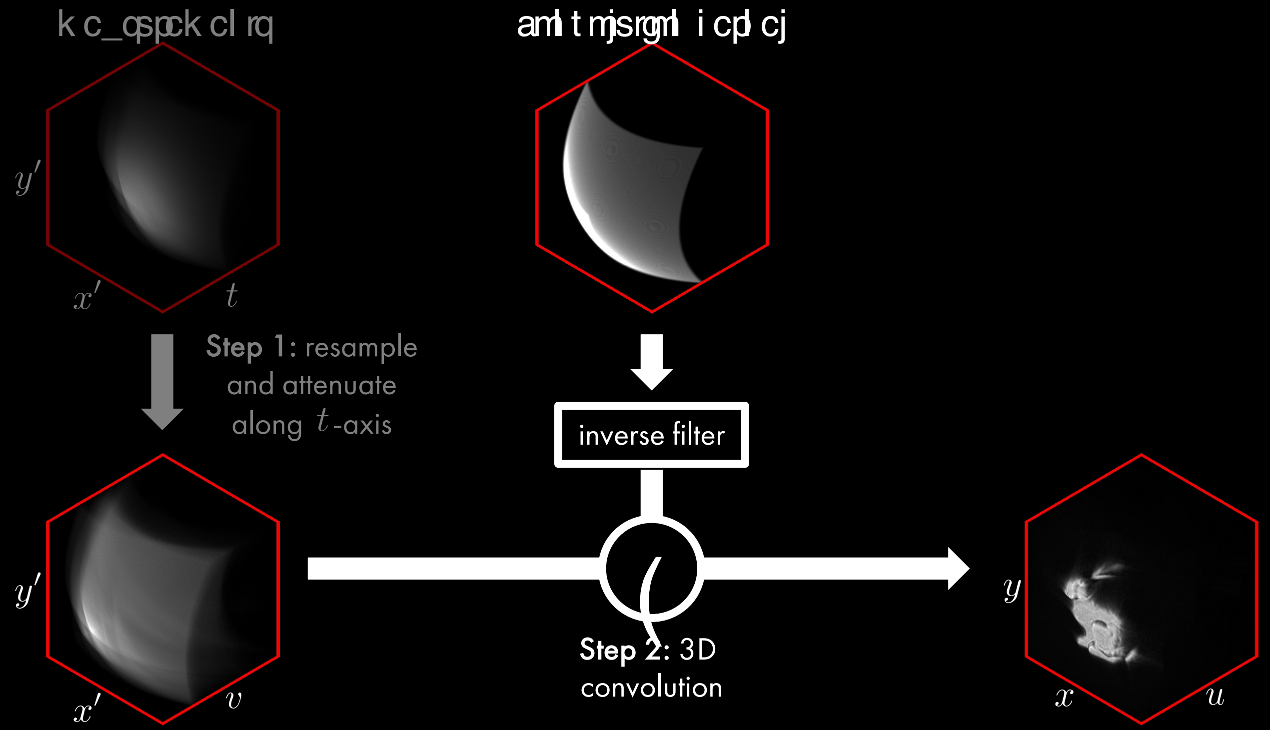

M̤ Rmmjc cr _j,* L _rspc 0. / 6

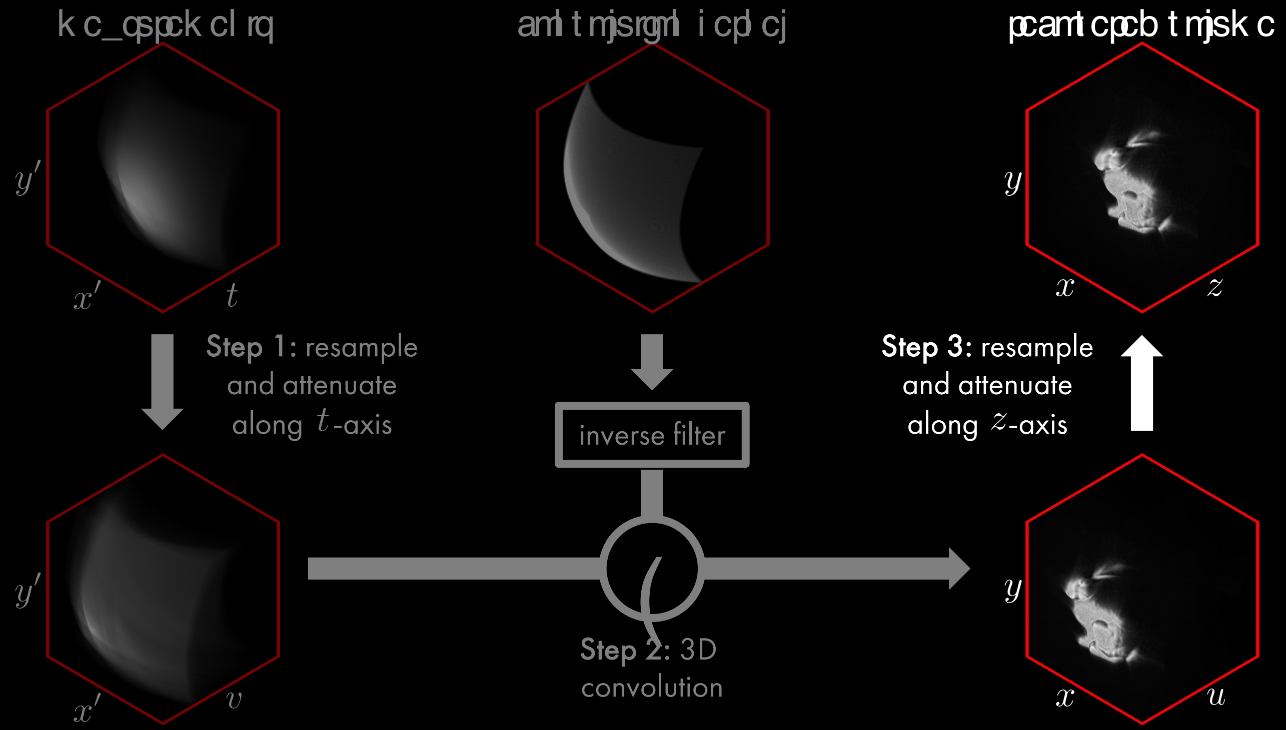

M. Rmmjc cr _j,* L _rspc 0. / 6

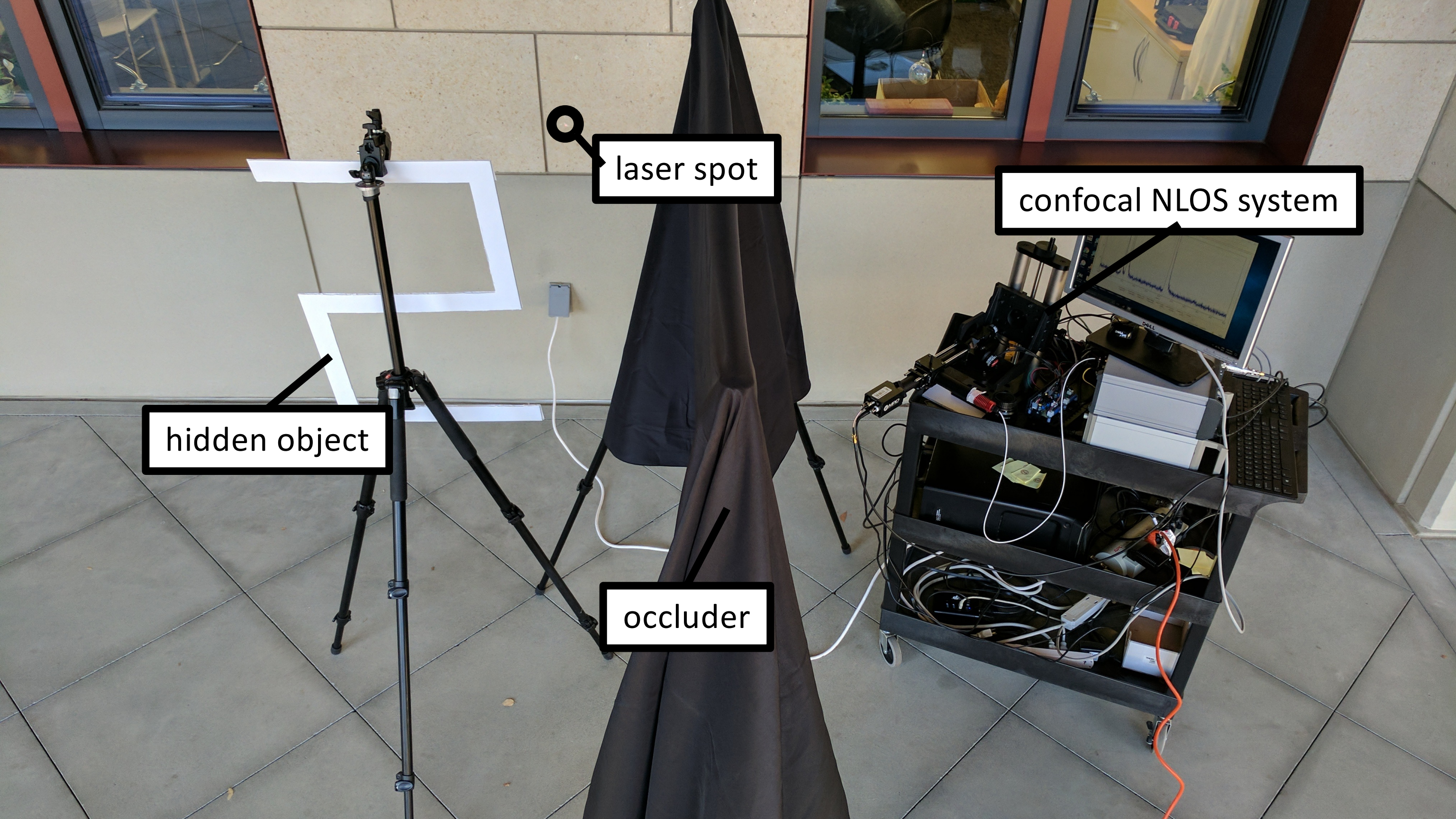
laser spot
confocal NLOS system
hidden object
occluder


1.25 meters

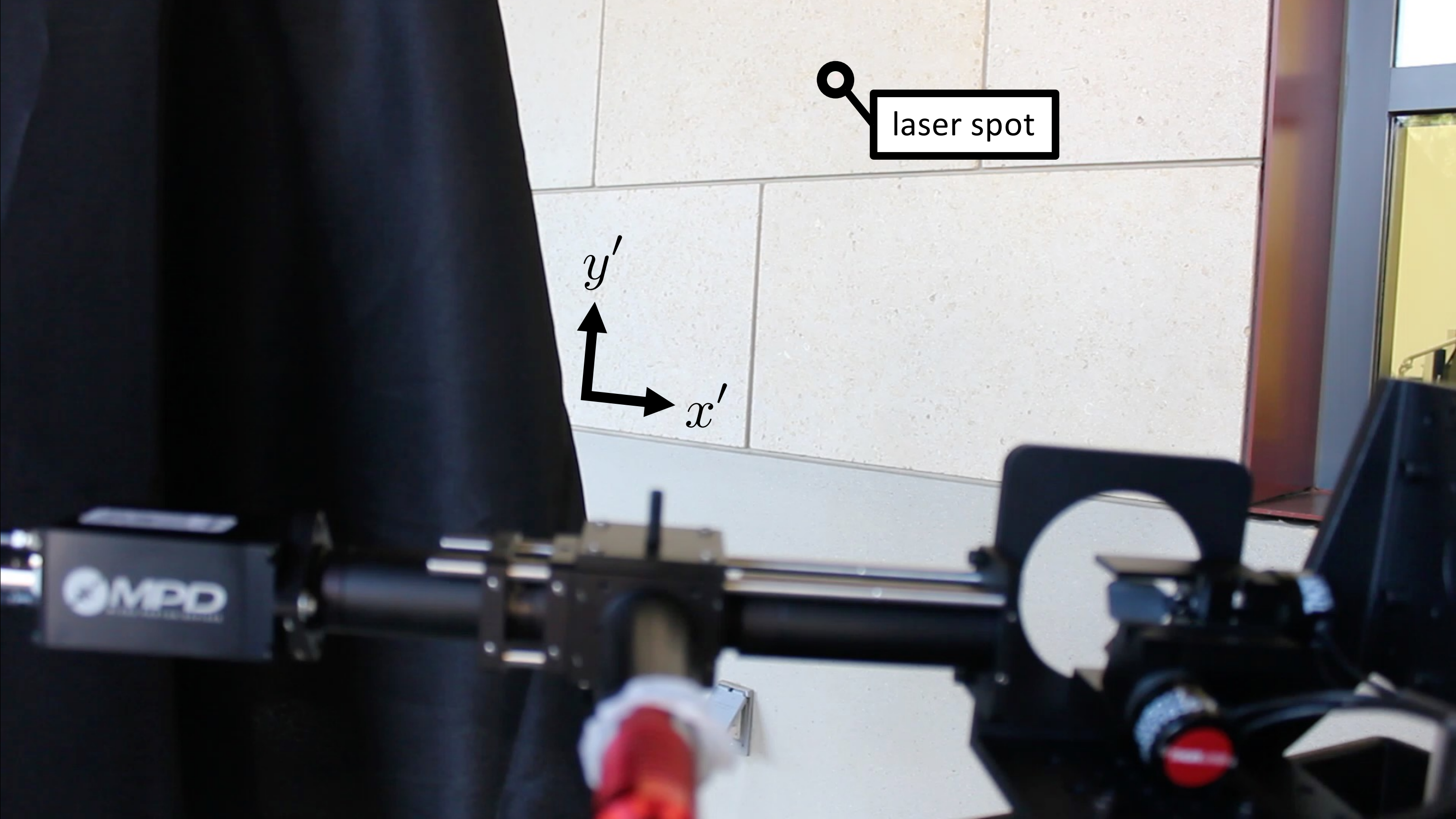

laser spot
y'
x'
MPD

measurements

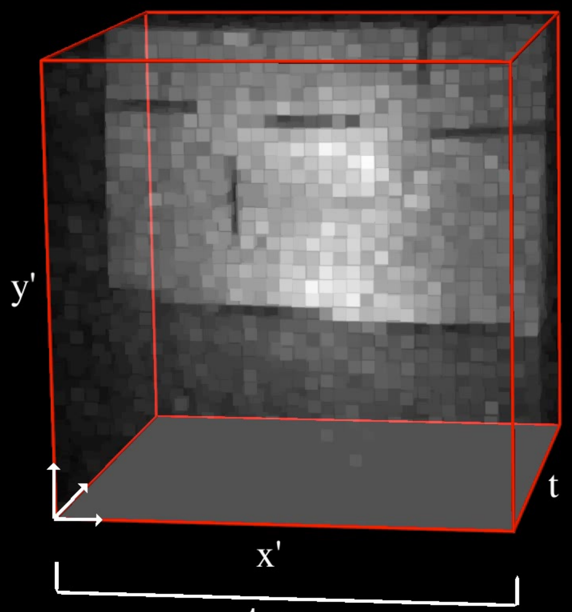

Maximum Intensity Projection

NLOS image formation model:

$$\tau = \mathbf{A}\rho$$

measurements $n^3 \times 1$

transport matrix $n^3 \times n^3$

unknown volume $n^3 \times 1$

Confocal scanning and Light-Cone Transfor

$$\tilde{\tau} = a * \tilde{\rho}$$

measurements $n \times n \times n$

blur kernel $n \times n \times n$

unknown volume $n \times n \times n$

Backprojection [Velten 12, Buttafava 15]

Flops: $O(n^5)$

Memory: $O(n^3)$

Runtime: Approx. 10 min.

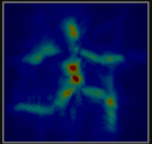

3D Deconvolution (with Light-Cone Transform)

[O'Toole et al. 2018]

Flops: $O(n^3 \log(n))$

Memory: $O(n^3)$

Runtime: < 1 second

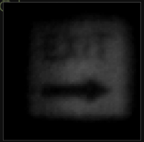

Iterative Inversion [Gupta 12, Wu 12, Heide 13]

Flops: $O(n^5)$ per iter.

Memory: $O(n^5)$

Runtime: > 1 hour

Assumption:

- Isotropic scattering (only diffuse or retroreflective objects)

overview

- Time-resolved imaging
- Single-photon avalanche diodes (SPADs)
- Single-photon lidar
- Non-line-of-sight imaging (part 2)
- passive ultra-wideband sensing

$$\nabla^2\Psi - \frac{1}{v^2}\frac{\partial^2\Psi}{\partial t^2} = 0$$

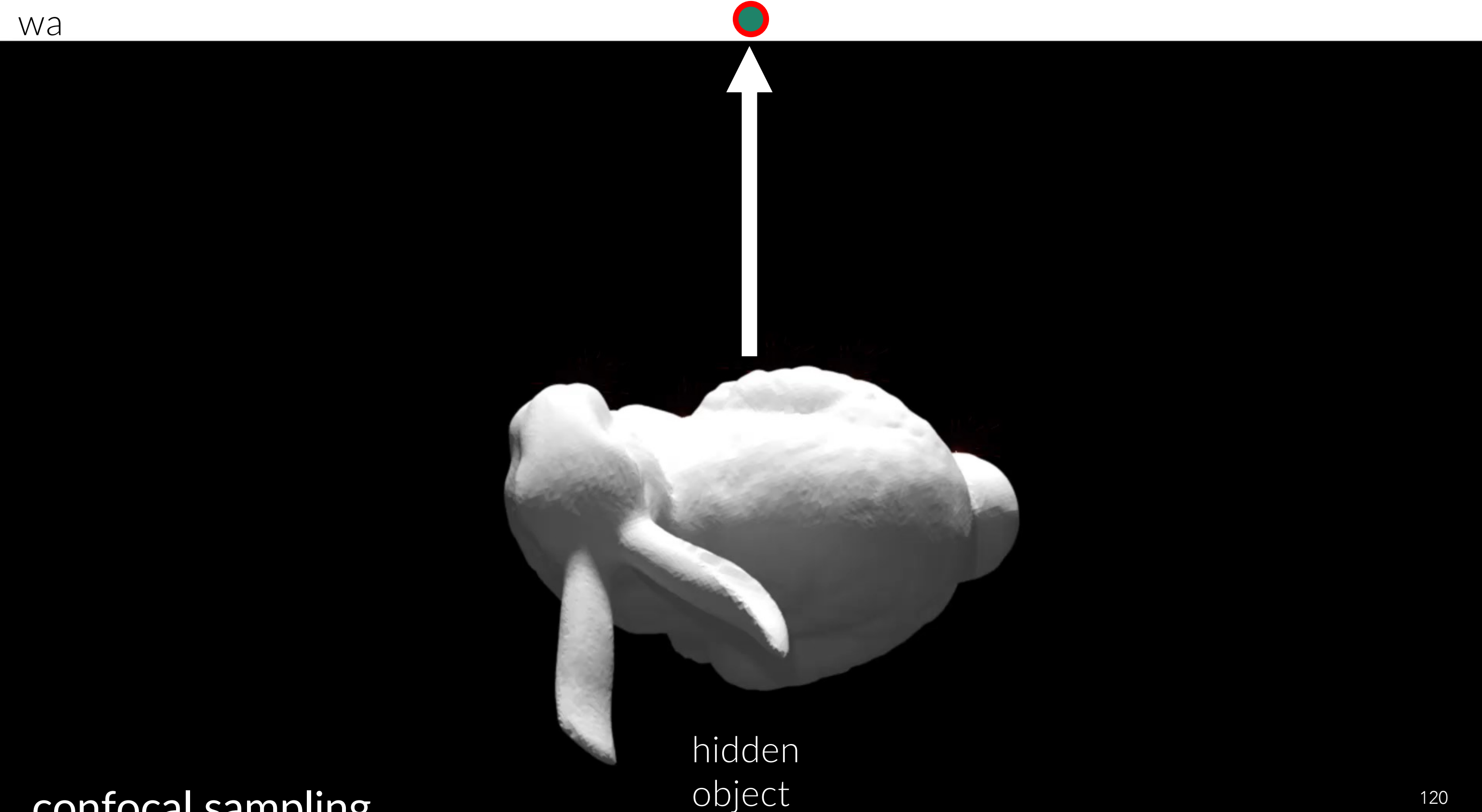

confocal sampling

image formation model

$$\Psi(x, z, t)$$

wavefield

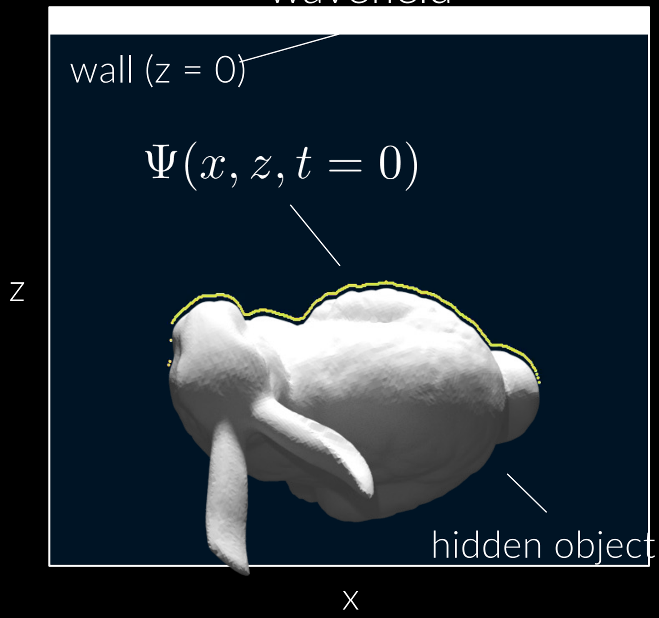

$$\Psi(x, z = 0, t)$$

confocal measurements

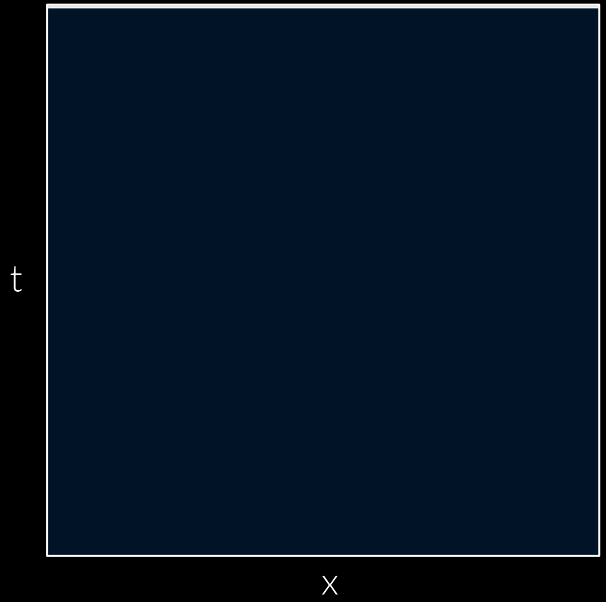

general solution (time reversal)

$\Psi(x, z, t = \textbf{03.000 ns})$

wavefield

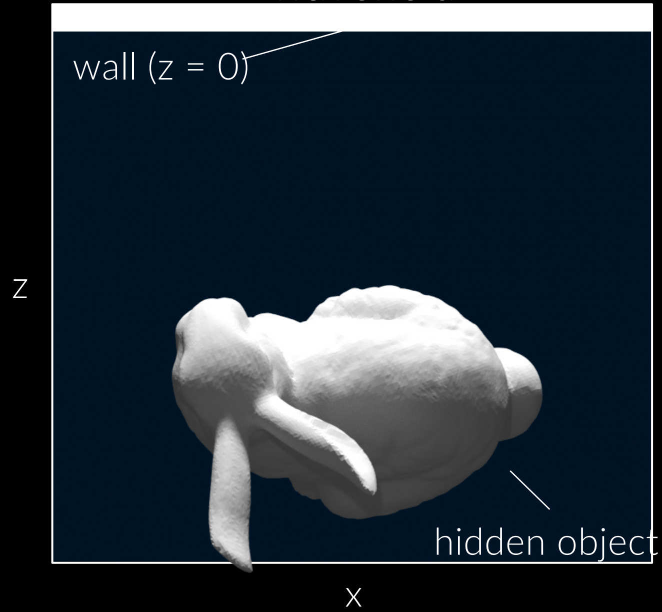

$\Psi(x, z = 0, t)$

confocal measurements

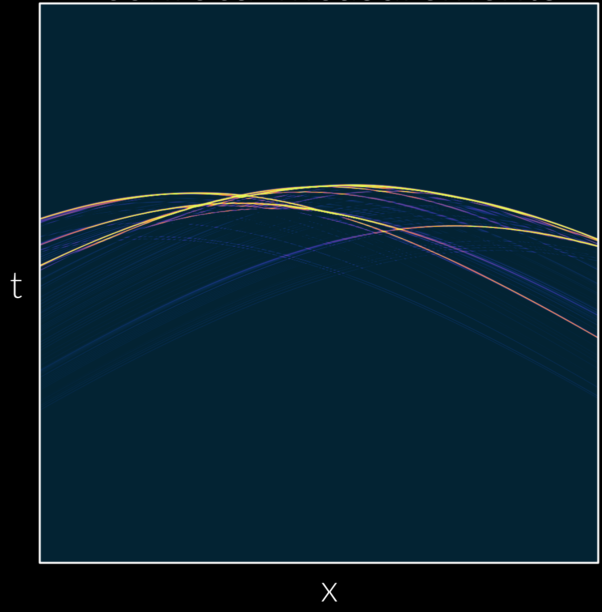

general solution (time reversal)

finite-difference time-domain method

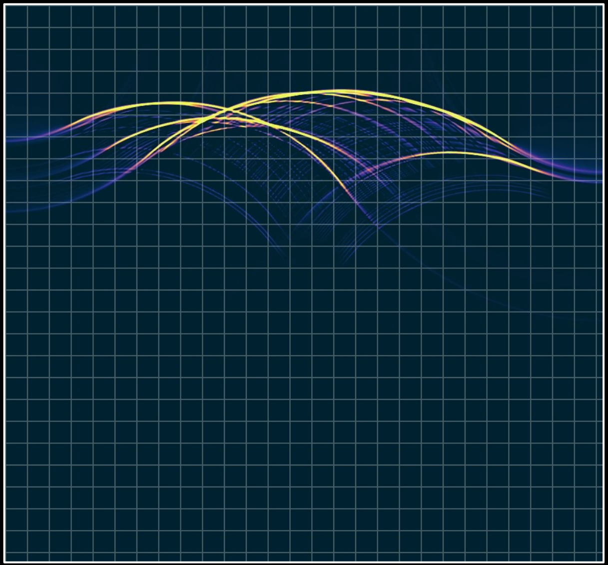

1. approximate wave equation with finite differences

$$\frac{\partial^2 \Psi}{\partial t^2} \approx \frac{\Psi_i^{n+1} - 2\Psi_i^n + \Psi_i^{n-1}}{(\Delta t)^2}$$

2. solve for previous timestep

$$\Psi_i^{n-1} = f\left(\Psi^n, \Psi^{n+1}\right)$$

3. repeatedly update Ψ at all grid cells

general solution (time reversal)

finite-difference time-domain method

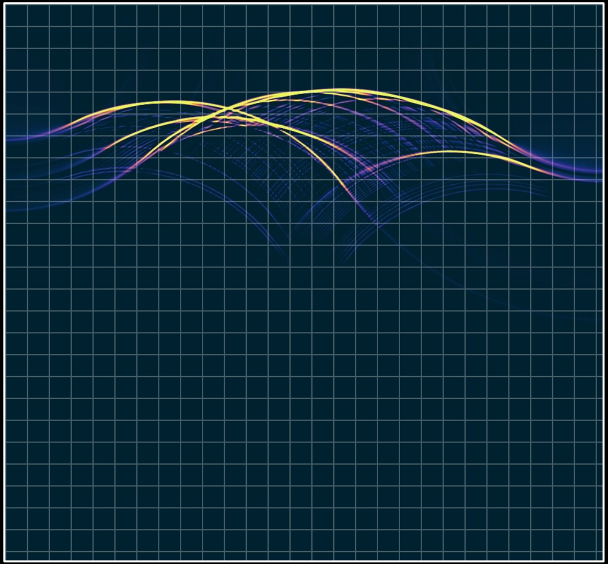

1. approximate wave equation with finite differences

$$\frac{\partial^2\Psi}{\partial t^2} \approx \frac{\Psi_i^{n+1} \ldots ^{n-1}}{\ldots}$$

2. solve … us timestep

$$\Psi_i^{n-1} = f\left(\Psi^n, \Psi^{n+1}\right)$$

3. repeatedly update Ψ at all grid cells

Slow to get t=0 at high-resolution!

frequency–wavenumber (*f*–*k*) Migration

$\Psi(x, z, t = 0)$

wavefield

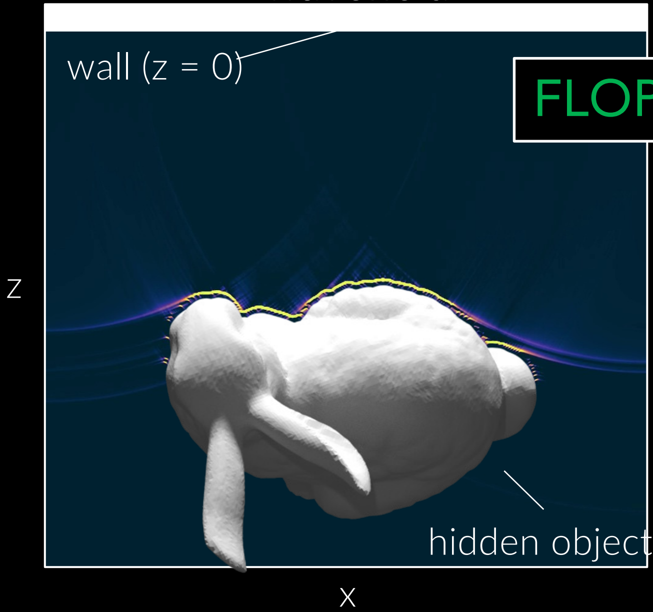

$\Psi(x, z = 0, t)$

confocal measurements

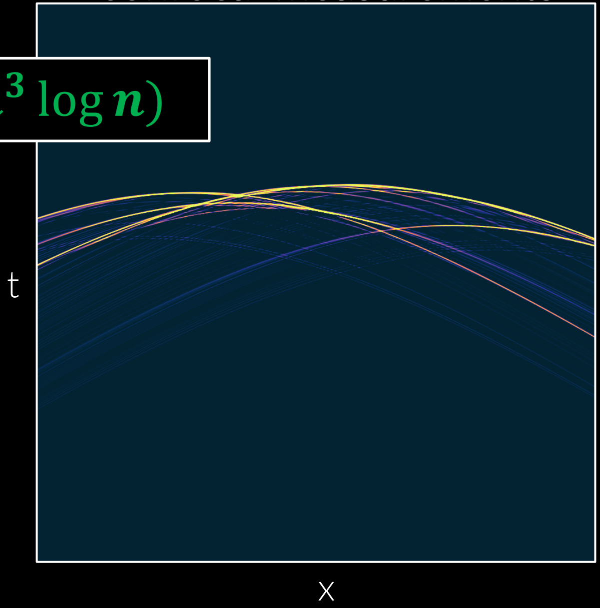

FLOPS: $O(n^3 \log n)$

hardware prototype

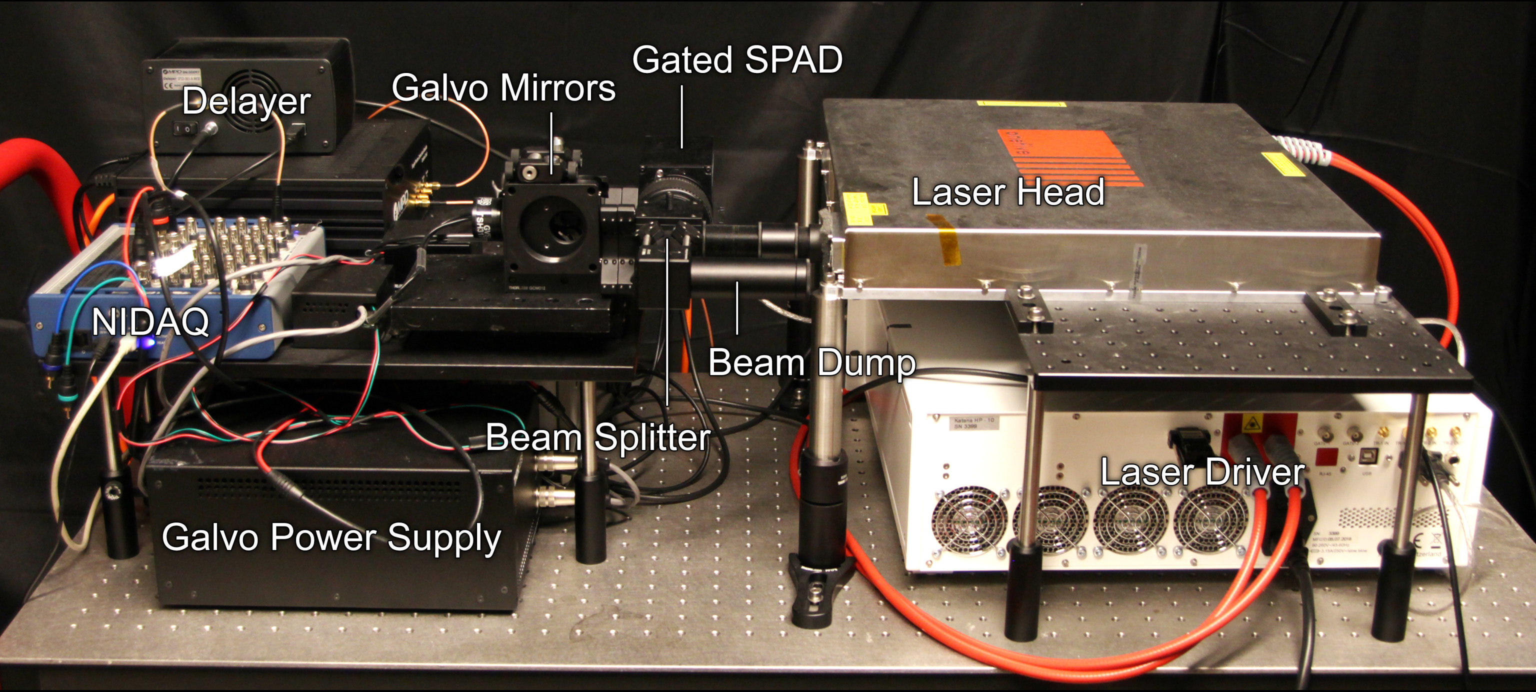

hardware prototype

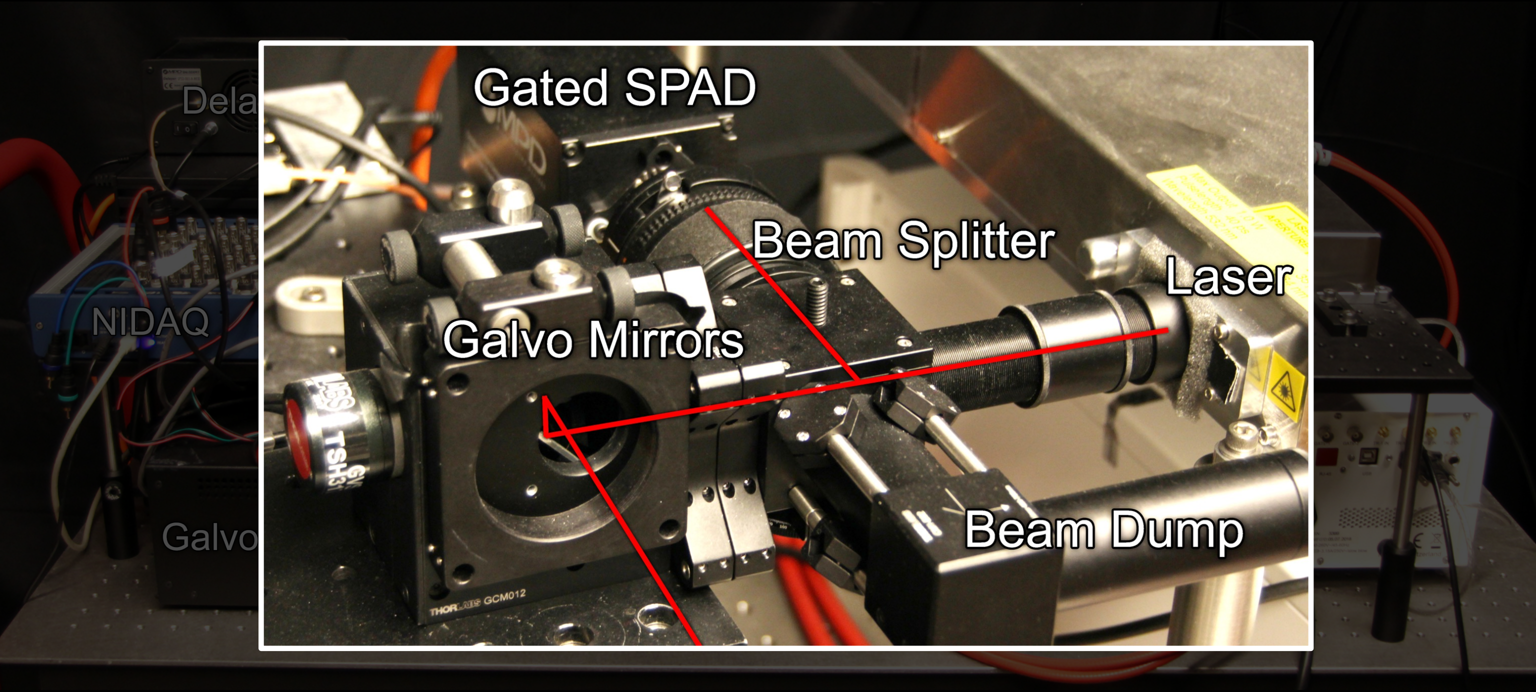

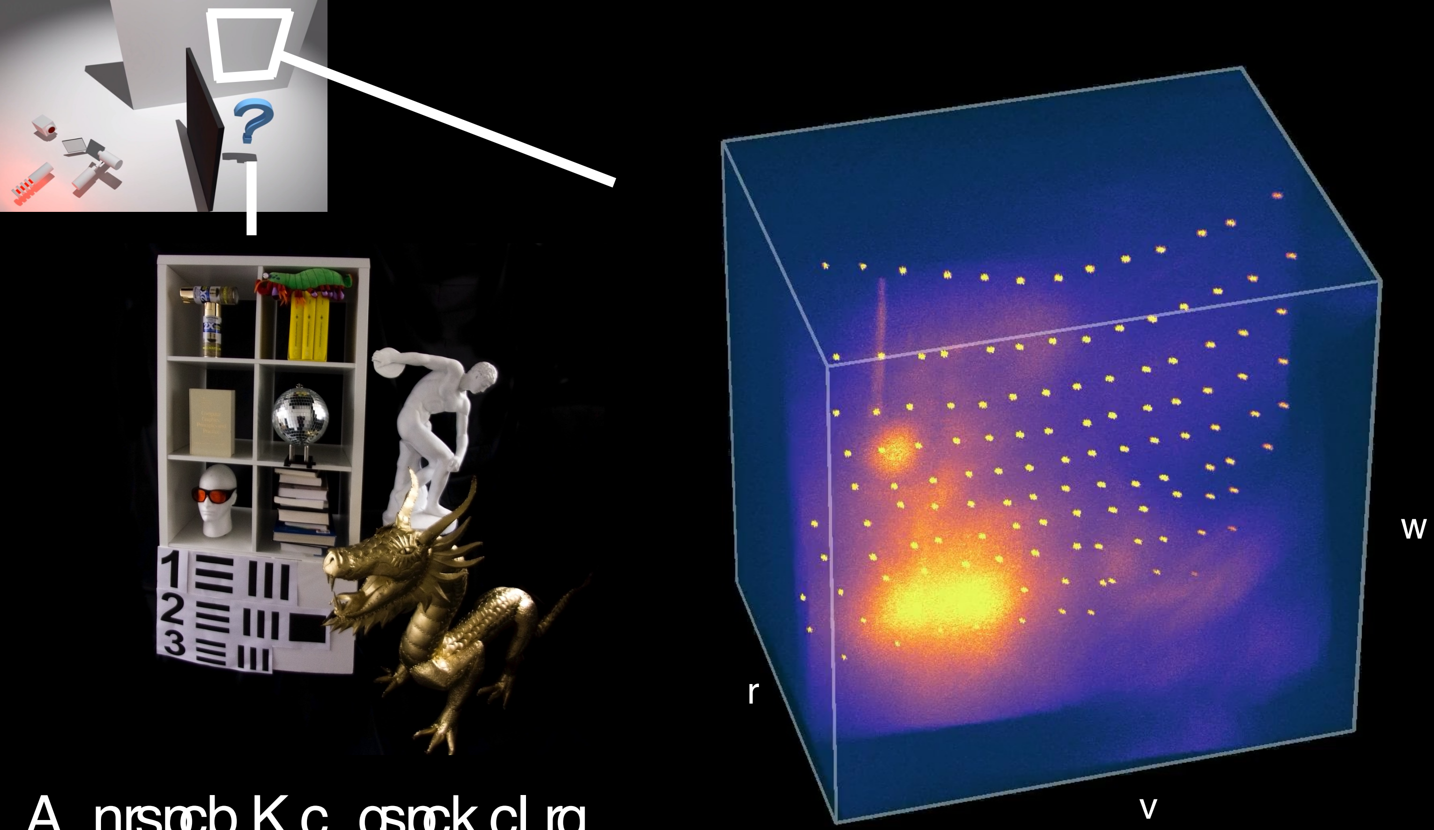

A_nrspcb Kc_qspckclrq

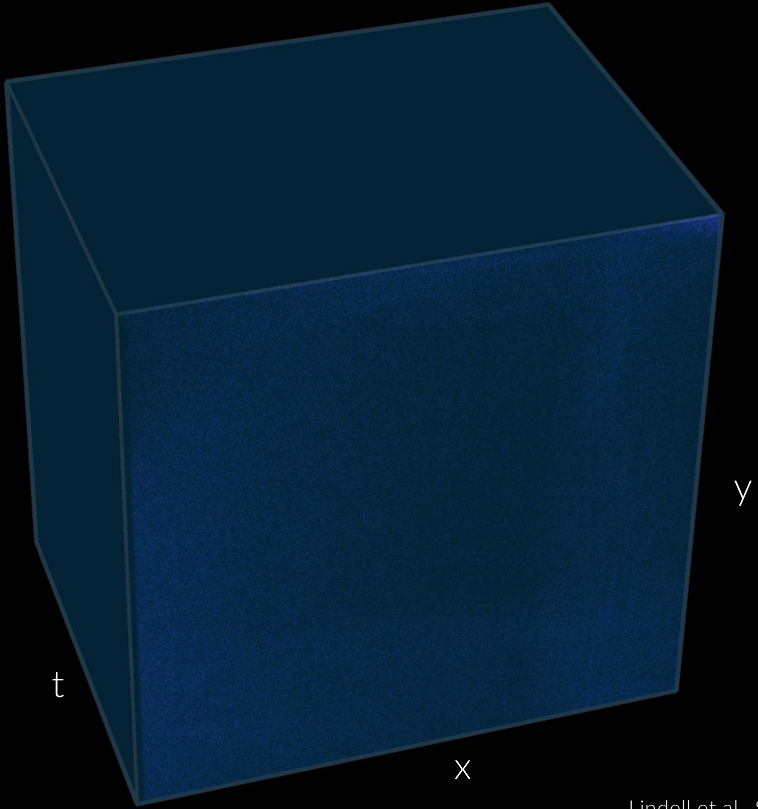

Lindell et al., SIGGRAPH 2019

f-k Migration

$\Psi(x, y, t)$

Measurements (z=0)

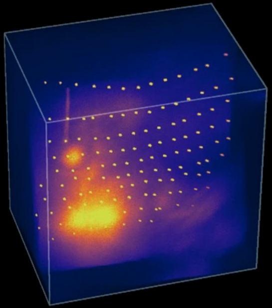

$\xrightarrow{}$ $\mathcal{F}$

$\bar{\Phi}(k_x, k_y, f)$

Spectrum

$\xrightarrow{}$ Resamp

$\Phi(k_x, k_y, k_z)$

Interpolated Spectrum

$\xrightarrow{}$ $\mathcal{F}^{-1}$

$\Psi(x, y, z)$

Hidden Volume (t=0)

f-*k* Migration

Express wavefield as function of measurement spectrum (plane wave decomposition)

$$\Psi(x,y,z,t) = \iiint \bar{\Phi}(k_x,k_y,f)e^{2\pi i(k_x x + k_y y + k_z z - ft)}dk_x dk_y df$$

wavefield

Fourier transform of measurements

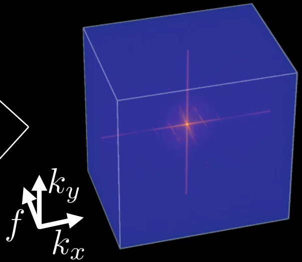

Set t=0 to get migrated solution

$$\Psi(x,y,z,t=0) = \iiint \bar{\Phi}(k_x,k_y,f)e^{2\pi i(k_x x + k_y y + \underbrace{k_z z}) }dk_x dk_y \underbrace{df}$$

Almost an inverse Fourier Transform!

f-*k* Migration

Set t=0 to get migrated solution

$$\Psi(x,y,z,t=0) = \iiint \bar{\Phi}(k_x,k_y,f)e^{2\pi i(k_x x+k_y y+\underbrace{k_z z})}dk_x dk_y \underbrace{df}$$

Almost an inverse Fourier Transform!

Use dispersion relation[1] to perform substitution of variables

$$f = v\sqrt{k_x^2+k_y^2+k_z^2}$$

$$\boxed{f \Rightarrow k_z}$$

[1] Georgi, Howard. *The physics of waves*. Englewood Cliffs, NJ: Prentice Hall, 1993.

Use dispersion relation[1] to perform substitution of variables

$$f = v\sqrt{k_x^2 + k_y^2 + k_z^2}$$

$$\boxed{f \Rightarrow k_z}$$

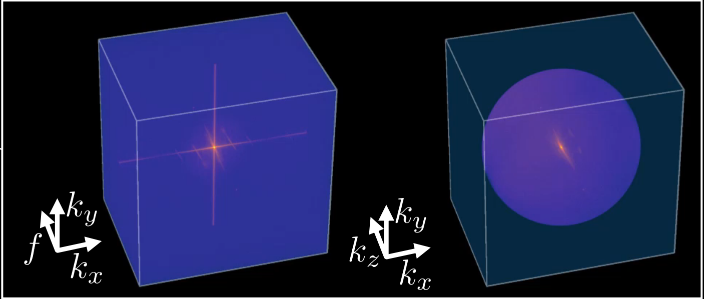

Use dispersion relation[1] to perform substitution of variables

$$f = v\sqrt{k_x^2 + k_y^2 + k_z^2}$$

$$\boxed{f \Rightarrow k_z}$$

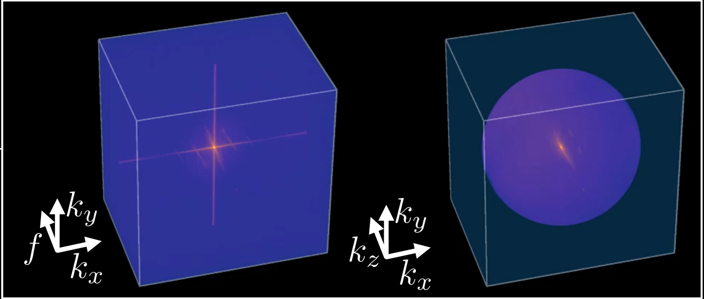

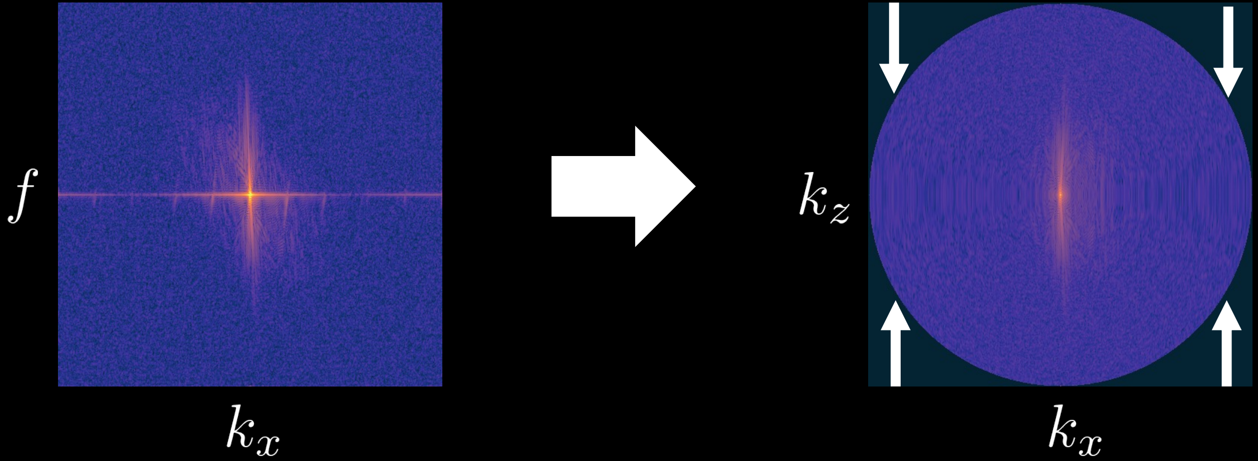

Use dispersion relation[1] to perform substitution of variables

$$f = v\sqrt{k_x^2 + k_y^2 + k_z^2}$$

$$\boxed{f \Rightarrow k_z}$$

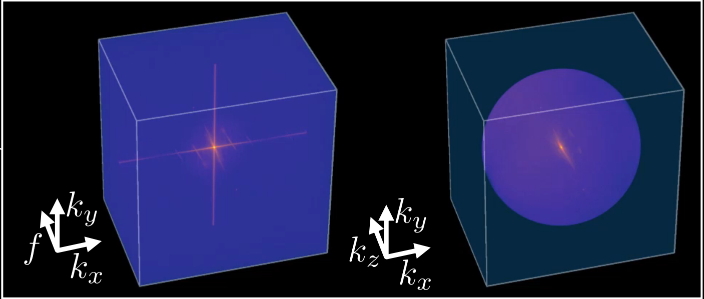

The migrated solution is an inverse Fourier Transform!

$$\boxed{\Psi(x,y,z,t=0) = \iiint \Phi(k_x,k_y,k_z)e^{2\pi i(k_x x + k_y y + k_z z)}dk_x dk_y dk_z}$$

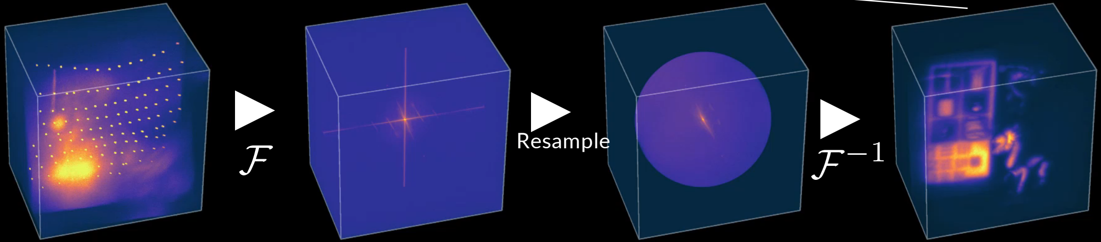

d i K gep_rgml

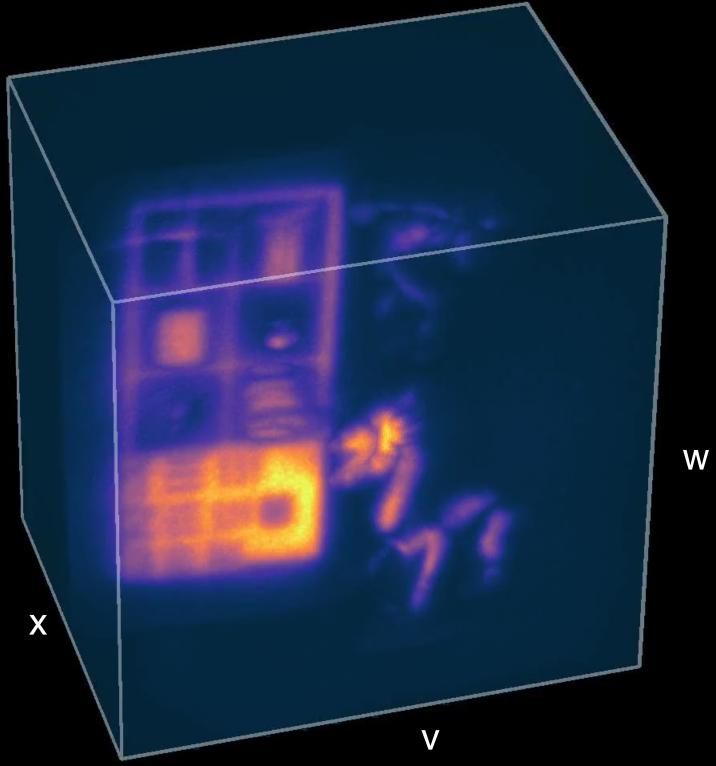

Bgk cl qgml q80 v0 k

Ovnmqspc8/ 6. k gl

Pcaml qrpsargml rgk c8l 7. qpca 8ANS'

Reconstruction Comparison

dimensions: 2 m x 2 m x 1.5 m

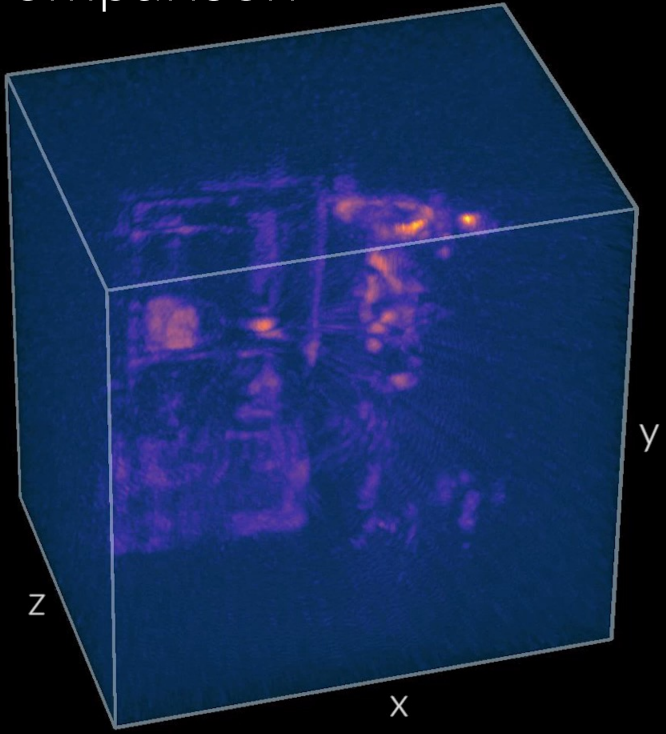

Filtered Backprojection

hardware prototype

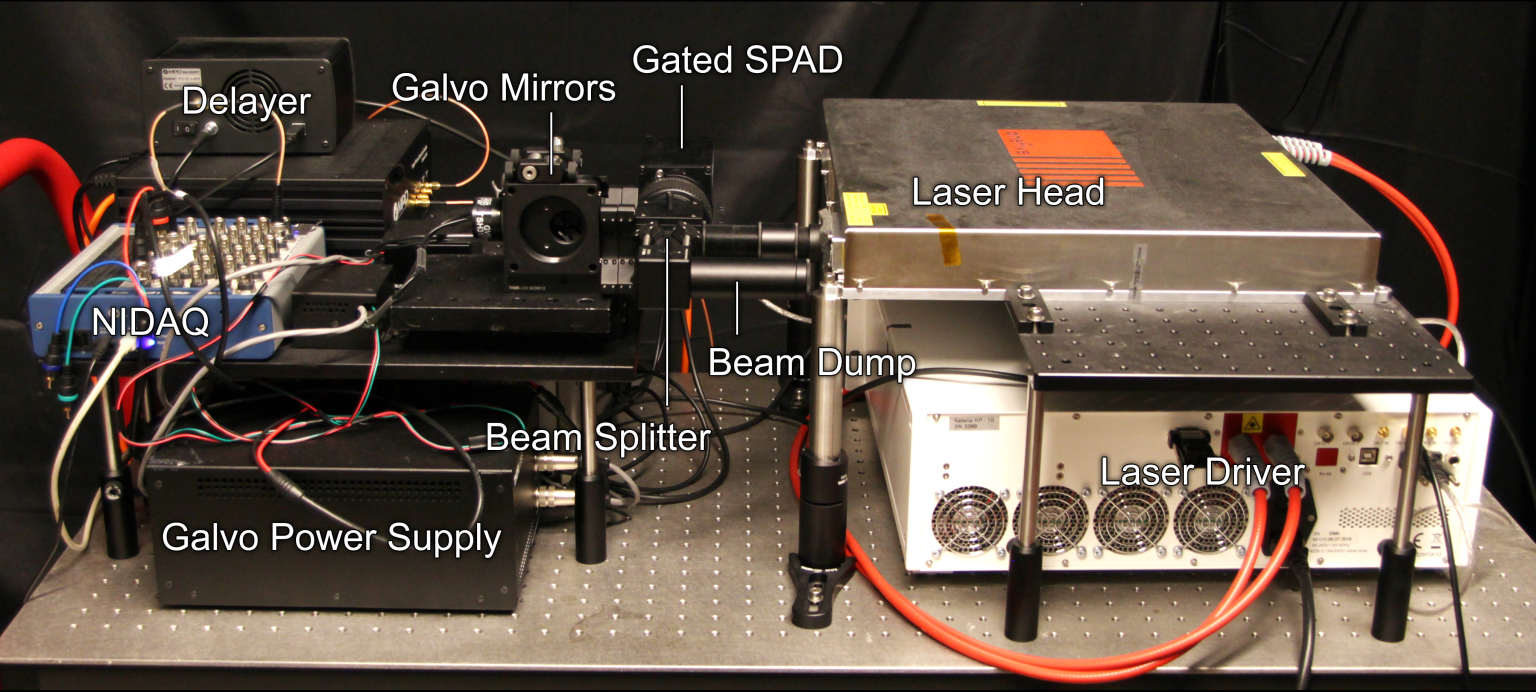

hardware prototype

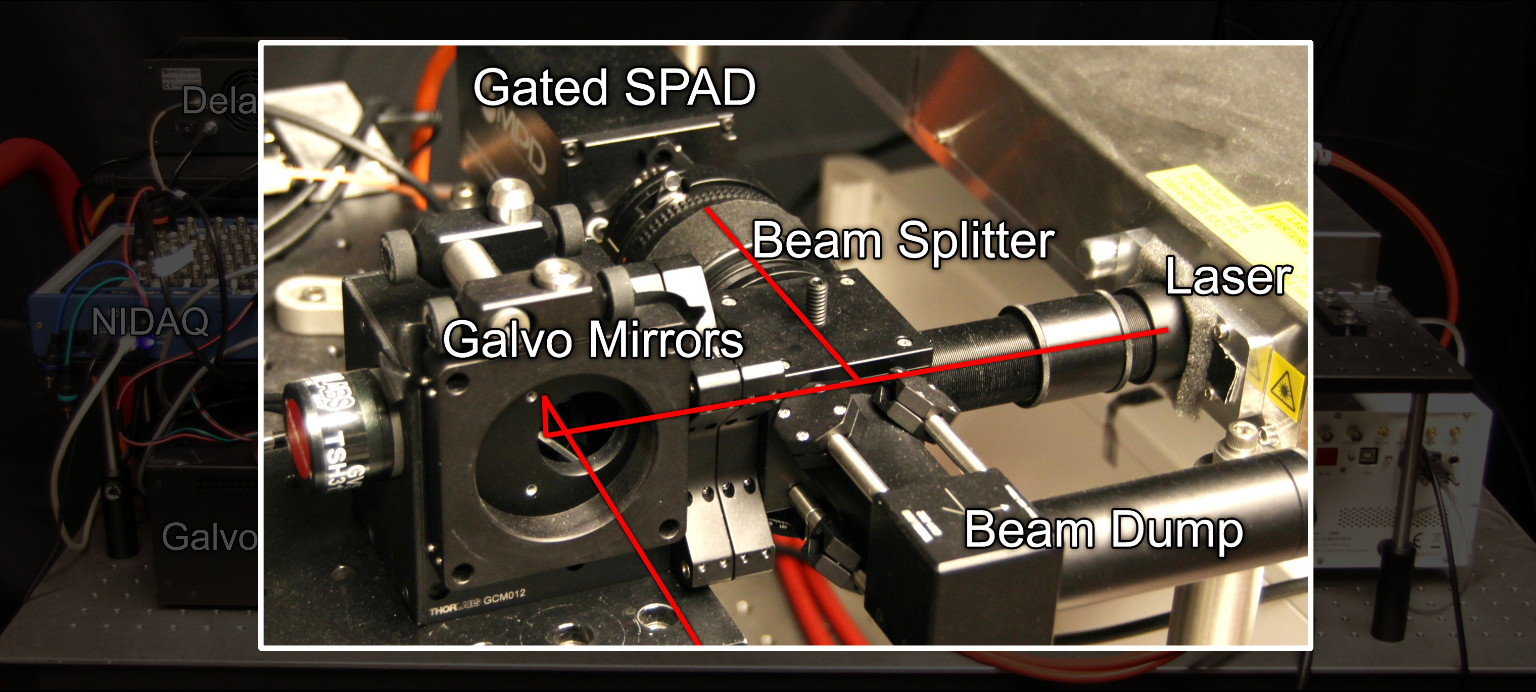

real-time scanning

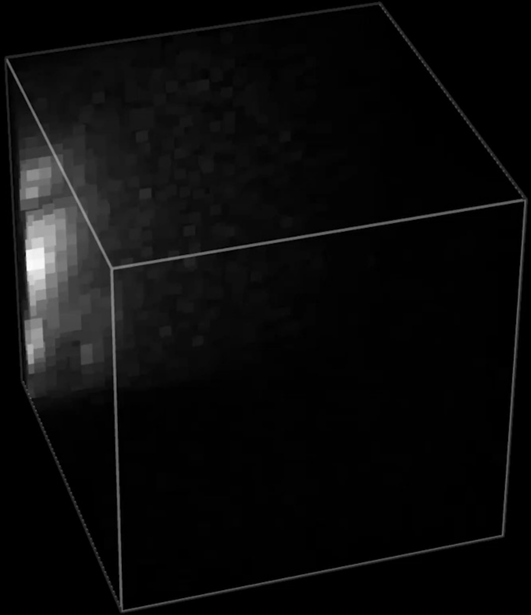

Framerate: 4 Hz
Resolution: 32 x 32
Dimensions: 2 m x 2 m x 2 m
Reconstruction time: ~1 s per frame

Lindell et al., SIGGRAPH 2019

Outlook

Directional Light-Cone Transform

hidden scene

Recovered surface

[Young et al., CVPR 2020]

Outlook

Keyhole NLOS Imaging

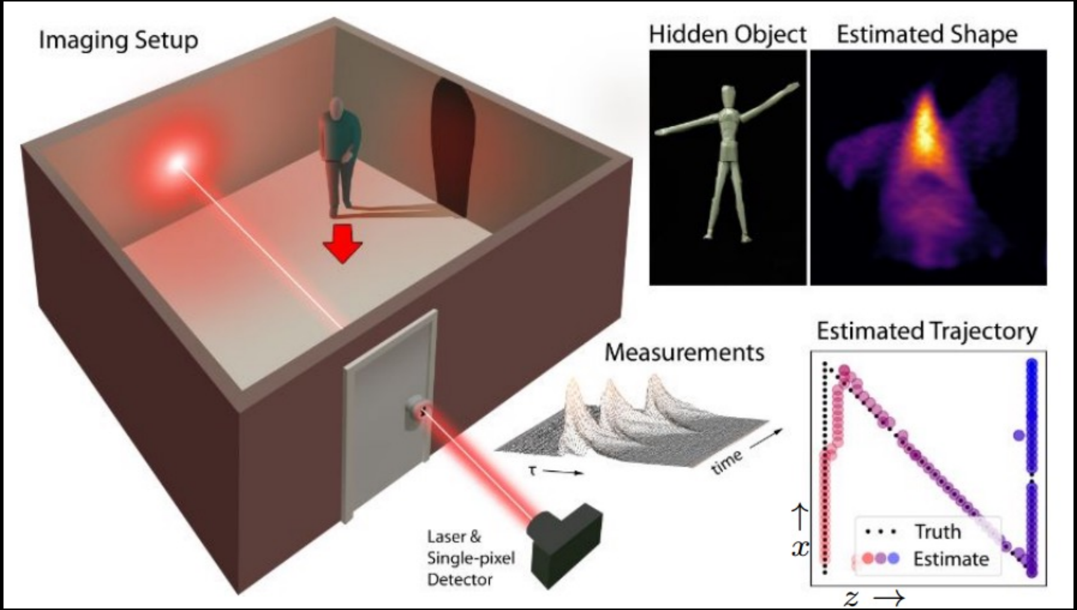

[Metzler et al., IEEE TCI 2021]

overview

- Time-resolved imaging
- Single-photon avalanche diodes (SPADs)
- Single-photon lidar
- Non-line-of-sight imaging
- passive ultra-wideband sensing

Nmu cpoqmdRcl

sjrp_+u gbc` _l b gk _egl e

240 FPS


Frame rate: 10.0Hz
Intensity tone mapped
Elapsed time: 24s + 500ms

f gef +qnccb gk _egje mnb_w


THE SLOW MO GUYS
@GAVINFREE
@DANIELGRUCHY

qb_k c p_rc83. . . Fx

ф_k c p_rc8/ . 1*. . . Fx

ф_k c p_rc8/ *. . . *. . . Fx

ϕb_k c bsp_rgml

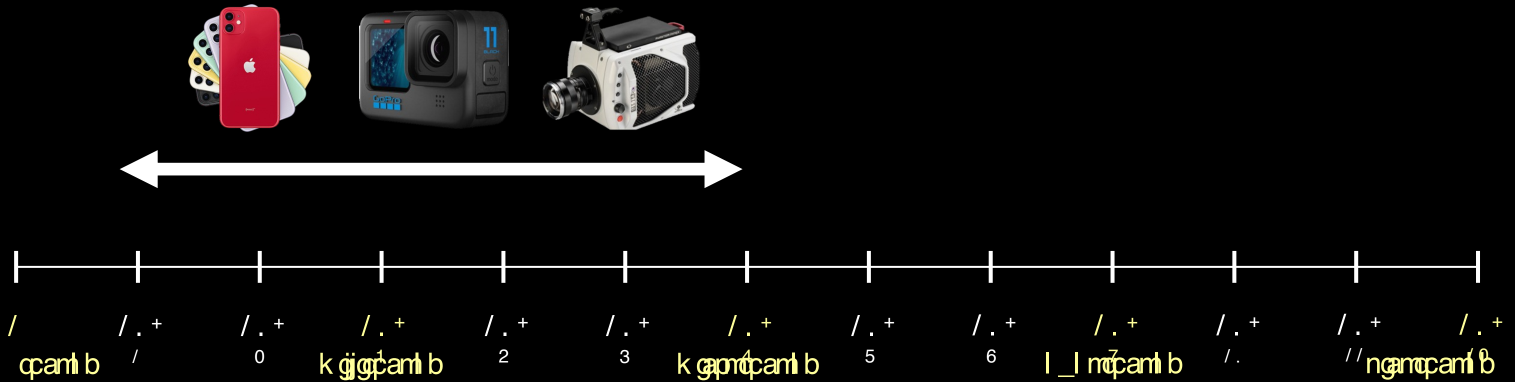

qb_kc $ ctcl r bsp_rgml

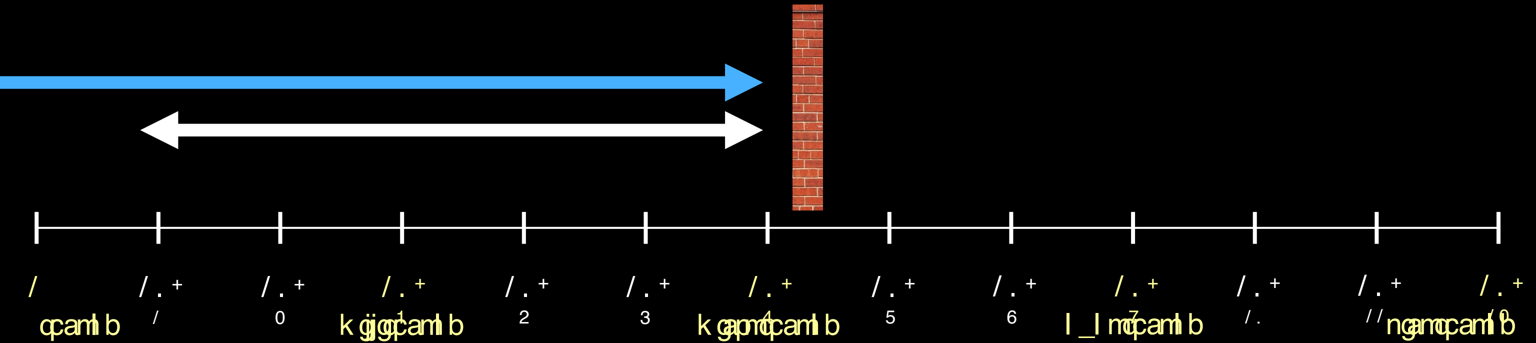

qb_kc $ ctclr bsp_rgml

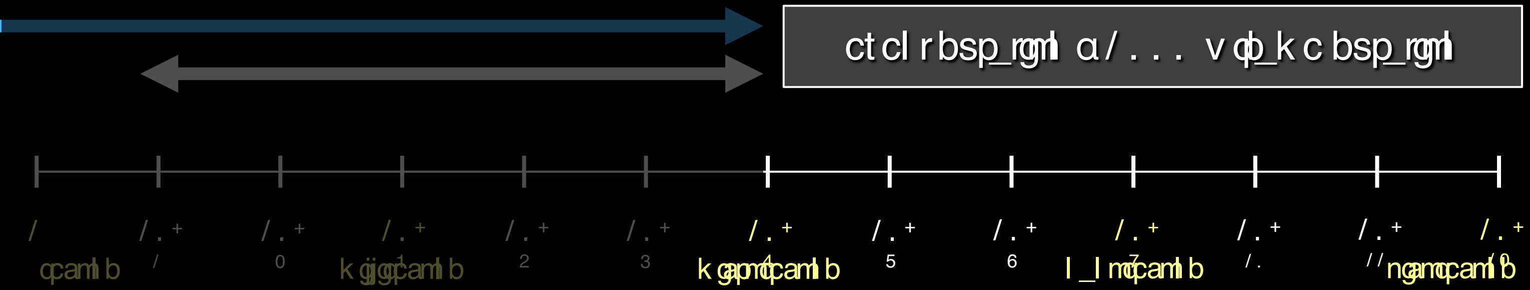

qb_kc $ ctclr bsp_rgml

/ /. + /. + /. + /. + /. + /. + /. + /. + /. + /. + /. + /. +

qcaml b / 0 kgijgcaml b 1 2 3 kgaprqcaml b 4 5 6 l_lmqcaml b 7 /. // ngamcaml b /0

rcafl mjmew

&n_cpgl c- _argl c'

high-speed cameras

quanta sensors

Ymrpsk. / 4* Kmpk mm 0. *
K_. 0. * [

qb_kc $ ctcl r bsp_rgml

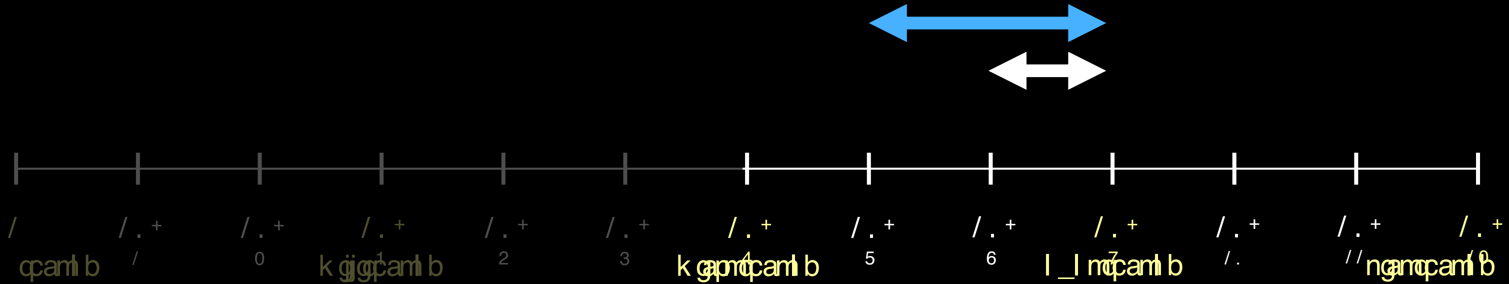

rcaf l mjmew

&n_qpgj c- _argj c'

time-of-flight cameras

YFcgbc. / 1* M. Rmmjc. / 2_ [

SPADs

YM Rmmjc. / 5* Jg bcjj*. / 6_ [

qb_kc $ ctcl r bsp_rgml

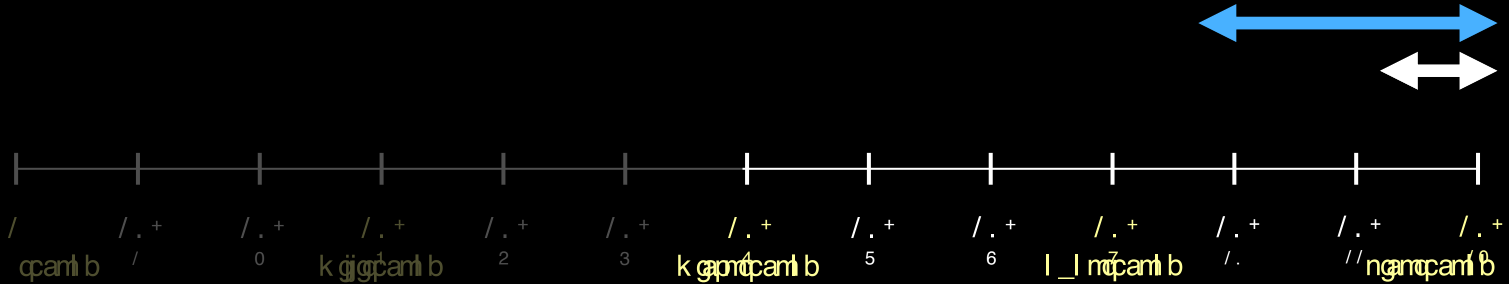

rcaf l mjmew

&n_qpgj c- _argj c'

streak cameras

YTcjrcl_ / 1* E_m / 2*_ [

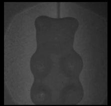

interferometry

YEi gmsjci _q / 3*_ [

qb_k c $ ct cl r bsp_rgml

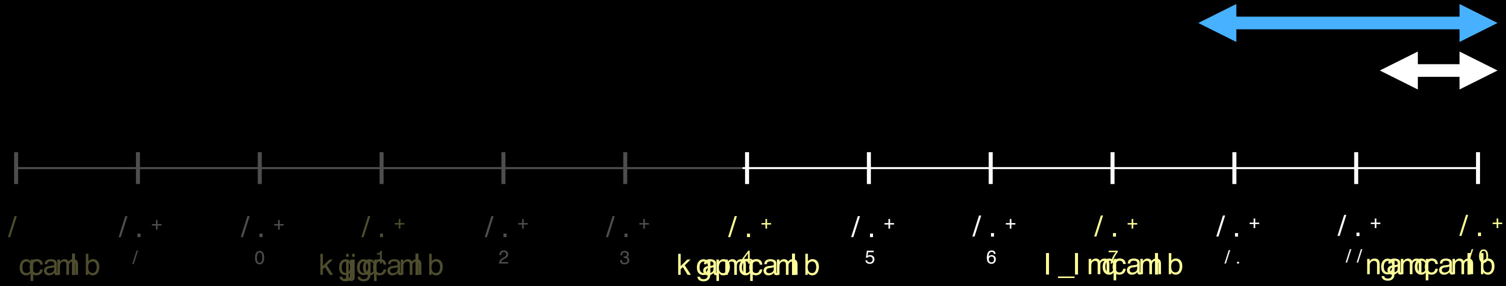

- L mrcaf l gosc a_l qgk sjr_l cmsqjwa_nrspc qjmu _l b sjrp_d_qr ct cl rq

qb_kc $ ctcl r bsp_rgml

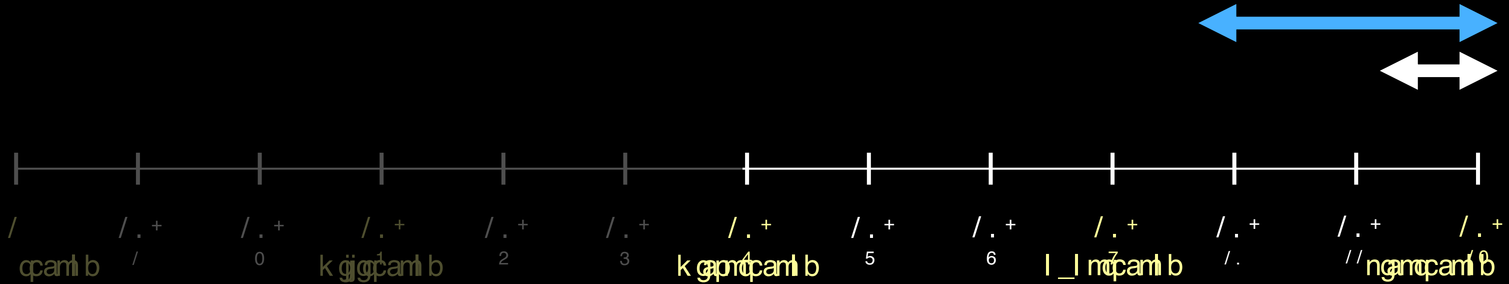

- L mrcafl gosc a_l ogk sjr_l cmsojwa_nrspc ojmu _l b sjrp_d_or ct cl rq (n_oog cjw(

qb_kc $ ctclr bsp_rgml

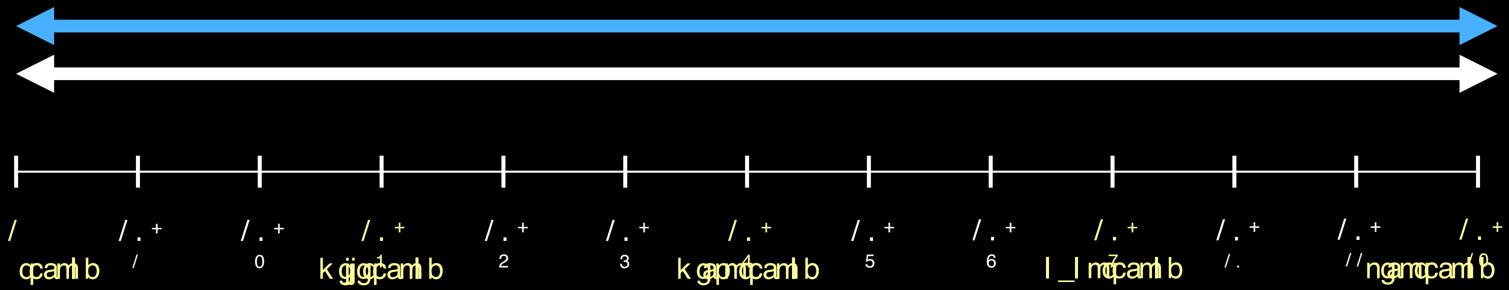

- a_nrspc ctclrq_apmqq rgk coq_jcq qn_llgle l/. mpbcpq mdk _elgrsbc
- n_qqgl c* l mqwl af pmlgx_rgml
- jmu gjsv

sjrp_+d_qr gk _egj e mnb_w

npcagqc qwl af pml gx_rgml

u gf _ qgj ejc bcbga_rcb f gef +qnccb jgef r sjrp_+d_qr gk _egj e mnb_w

npcagc qwl af pml gk_rgml

ugf _ qgejc bcbga_rcb fgef+qnccb jgef r


SmallHD

mpoeg mdrf c cjcarpml ga gl_qf

conventional flash bulb (ca. 1940)

Edgerton’s high-speed flash

Osgai cpl. _ugi &72.'
KGRK sqcsk Amjjcargml q

d_q-ehmpu _pb 6. wc_pq80. 0. '

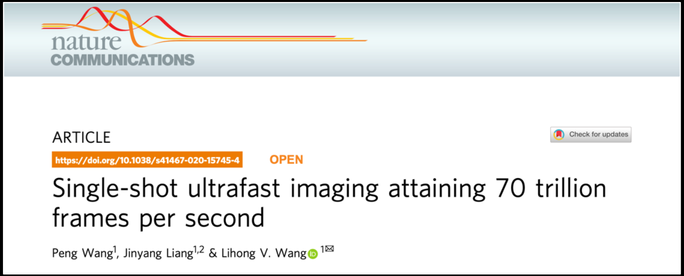

nature COMMUNICATIONS

ARTICLE

Check for updates

https://doi.org/10.1038/s41467-020-15745-4

OPEN

Single-shot ultrafast imaging attaining 70 trillion frames per second

Peng Wang[1], Jinyang Liang[1,2] & Lihong V. Wang[1]

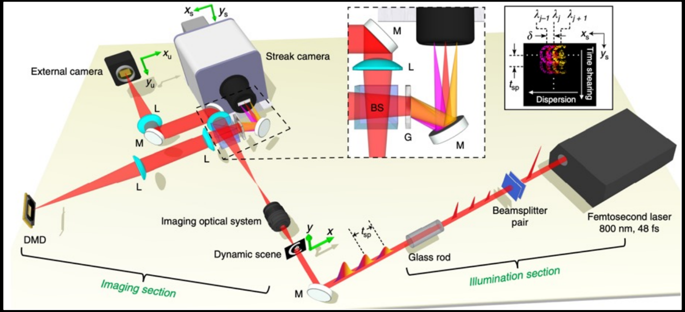

d_qr+dmpu _pb 6. wc_pq 80. 0. '

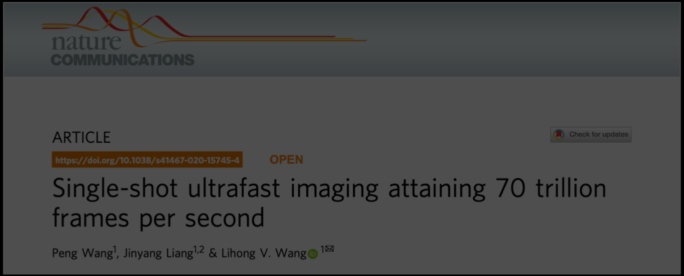
nature COMMUNICATIONS

ARTICLE

Check for updates

https://doi.org/10.1038/s41467-020-15745-4 OPEN

Single-shot ultrafast imaging attaining 70 trillion frames per second

Peng Wang[1], Jinyang Liang[1,2] & Lihong V. Wang[1]

(nc_i gp_bgl ac8 3,4 v/. [14] k U - ak [-2]

l / ` gjgml rgk cq` pgef rcprf _l _

amk k ml j_qcpnmgl rcp

((jcqqrf _l / . . . nsjqcq ncpqcaml b

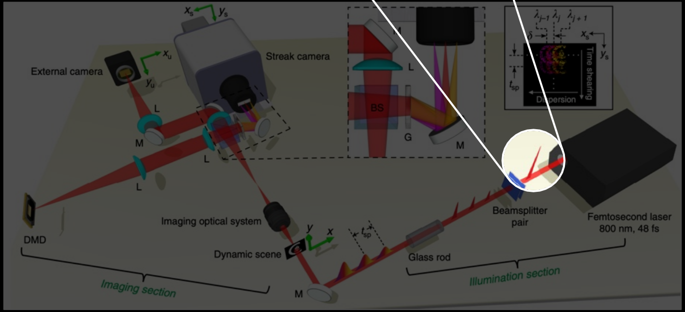

ql_kc $ ctclr bsp_rgml

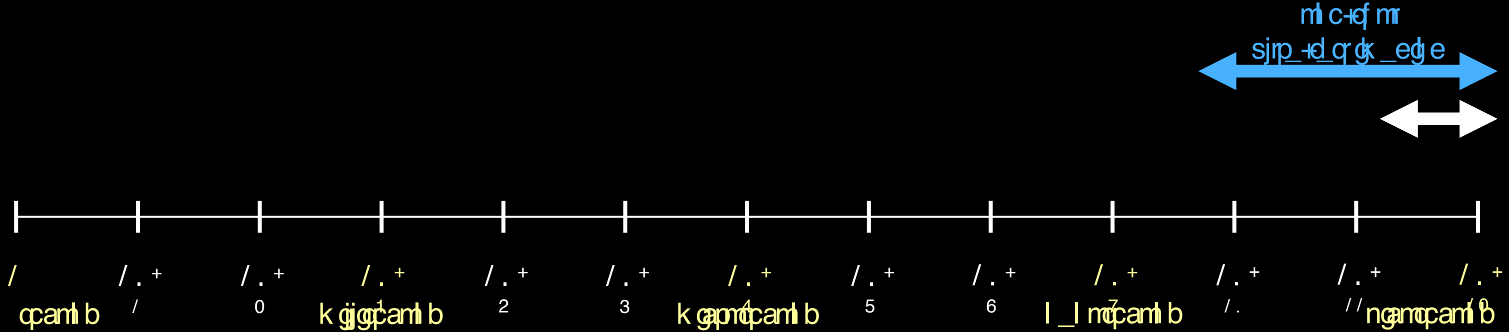

sjrp_+d_qr gk _egje mmb_w

npcagqc qwl af pml gx_rgml

u gf _ qgj ejc bcbga_rcb f gef +qnccb jgef r

F_pmjb Bmaǔ Obecpml
&7.1+/77.'

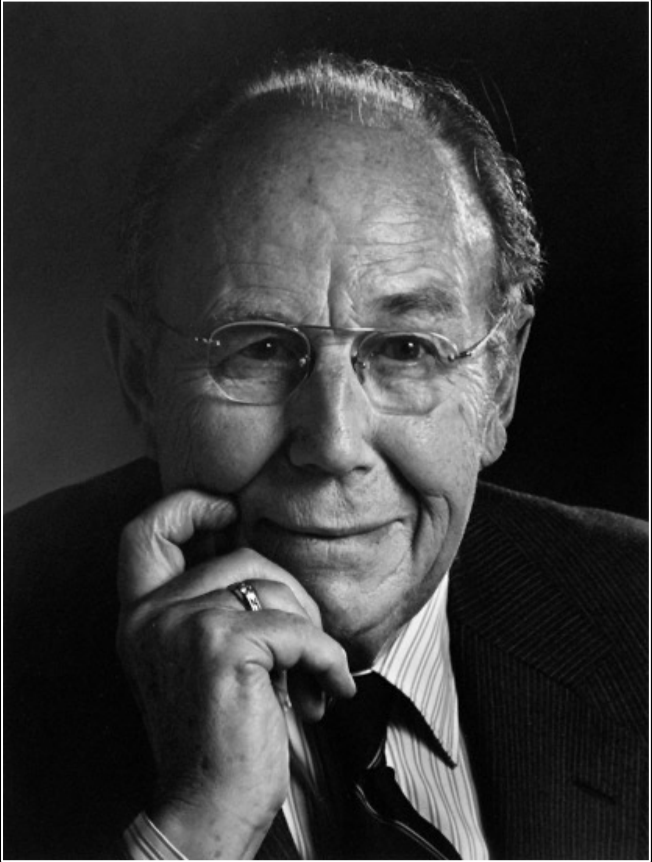

qpmì mcamnw8sjrp_+d_qrgk _edje ugf jcqpjgef r

Osgai cpl. _ugi &72. '
K GRK sqcsk Amjicagml q

rp_l oqgcl rgk _egj e &Tcjrcl cr _j* 0. / 1'

qb_kcp_rc83. . EFx

rp_lqgclr gk_egle &Tcjrcl cr_j* 0. / 1'

dp_kcp_rc83.. EFx

(qmsp`c dpcoscl aw853 KFx
l mctcl r qjmu cprf_l ..,/ 1 l_l mqcaml bq a_l `c gk_ecb

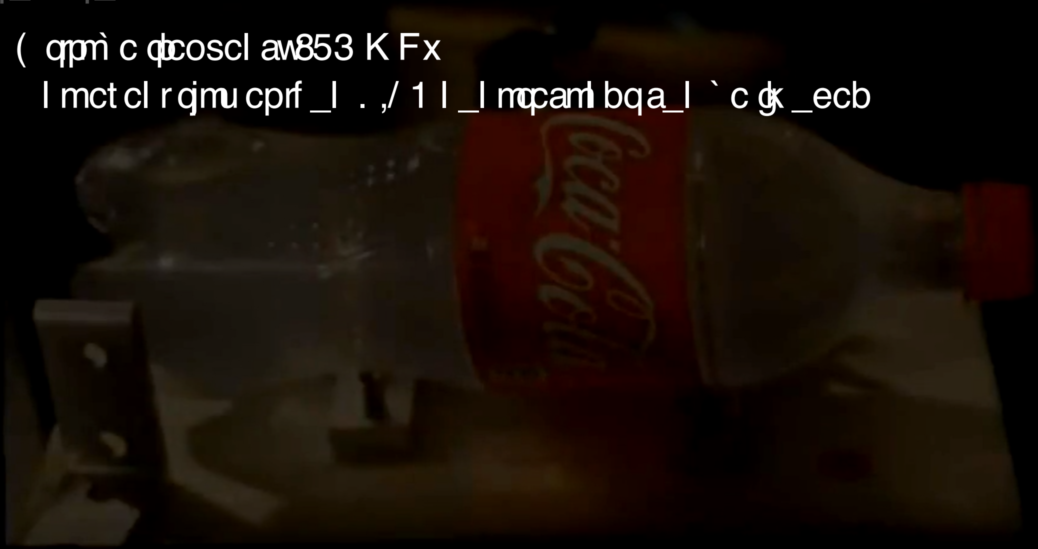


250 Billion FPS
Synchronized Result

Elapsed time: 26.1s + 15ms + 169us + 910ns + 848ps
Frame rate: 250.0GHz

nf mml q_l b qjsv csl argml q

qgl ejc-nf mml _t _j_l af c bgmbcq

qbcc-psl l gl e
rgk c-q_k ngl e QN?Bq

f rrnq8 - - u u u ,ngamos_l r,amk -

qgl ejc-nf mml _t_j_l af c bgmbcq

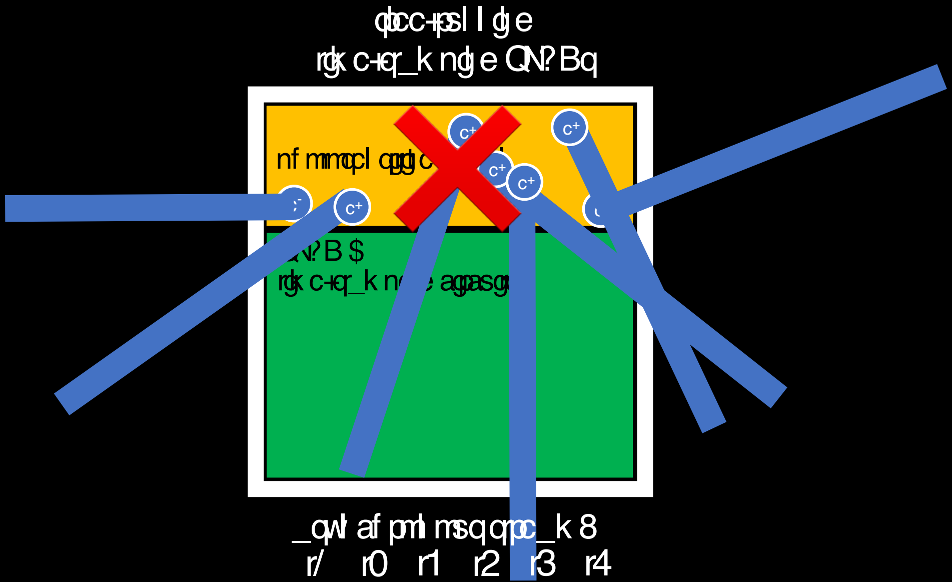

qgj ejc+nf mml _t_j_l af c bgmbcq

qbcc+psl l gje
rgk c+rq_k ngje QN?Bq

f rmq8 - u u u ,ngamos_l r,amk -

qgj ejc+ngycj qcl qmp
rf pmsef nsr8l 0K nf mml q+ qca
rgk c pcqmjsrgml 8l / 4 ngamqcaml bq
bc_b rgk c83. l _l mqcaml bq

Measurement Model

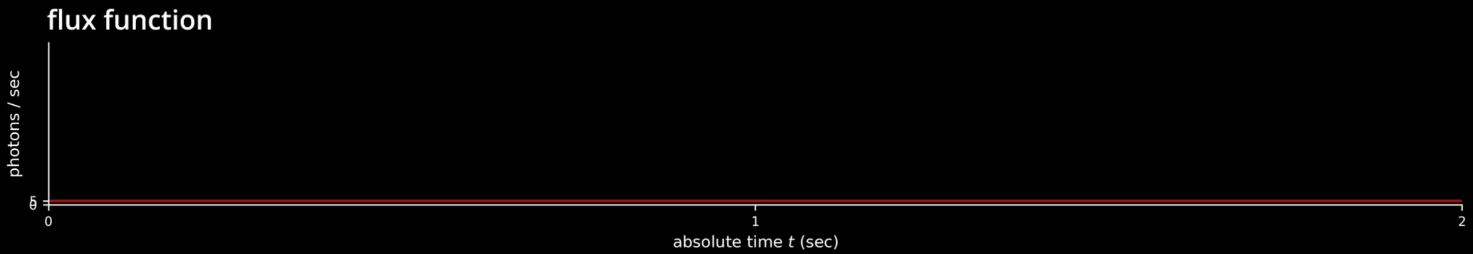

Active histogram-based imaging: Role of sync frequency

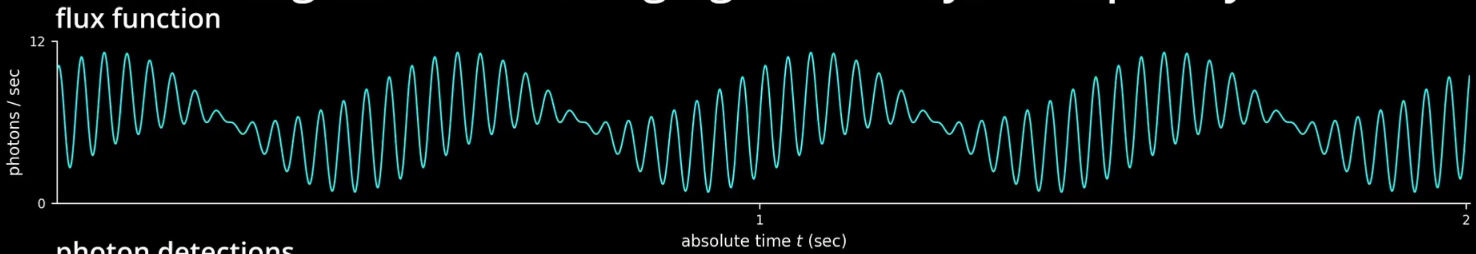

Active histogram-based imaging: Role of sync frequency

flux function

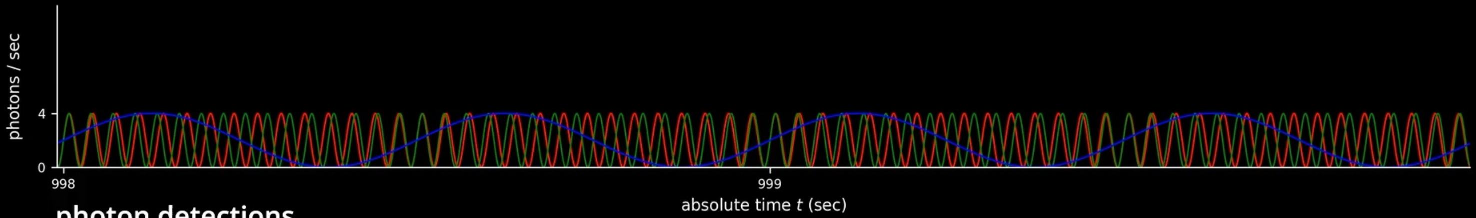

photon detections

histogram (sync freq = 02.00 Hz = freq of blue signal)

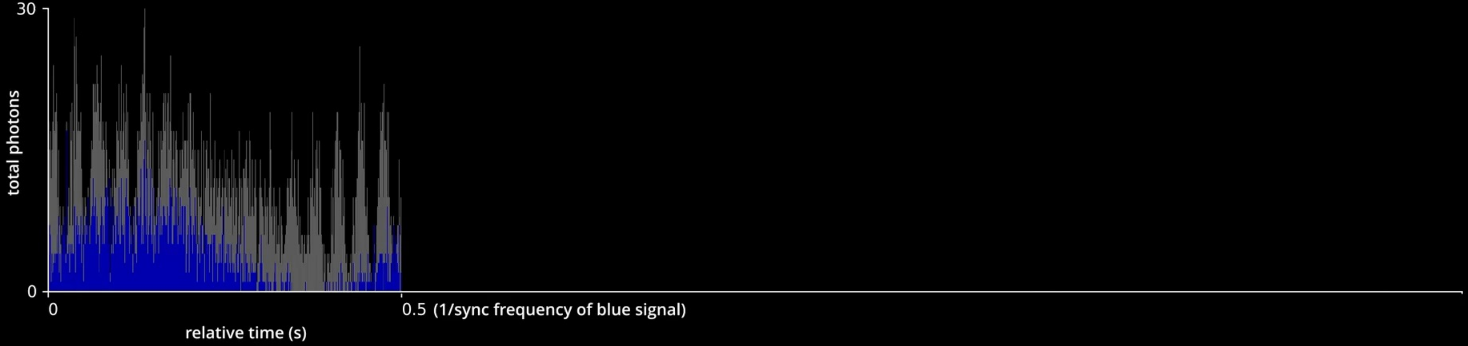

Active histogram-based imaging: Role of sync frequency

flux function

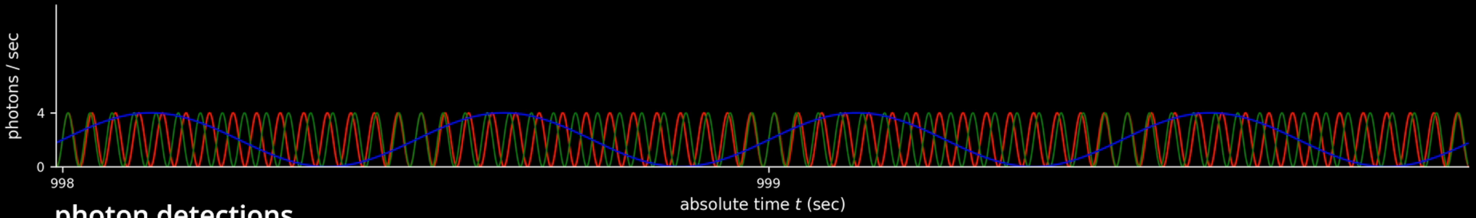

photon detections

histogram (sync freq = 32.00 Hz = freq of green signal)

Zoomed in view

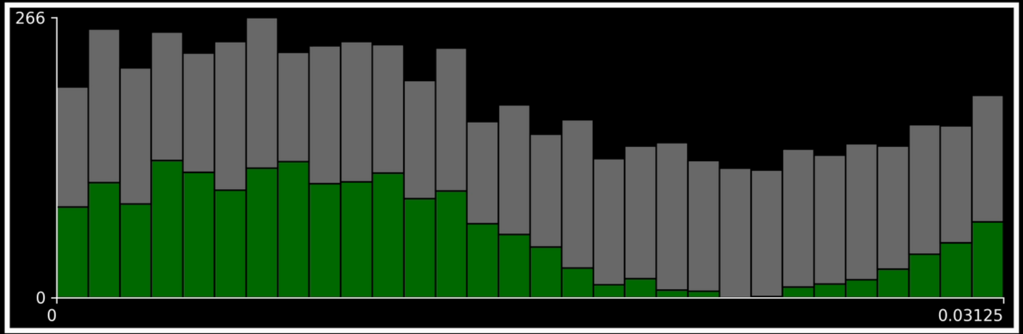

Active histogram-based imaging: Role of sync frequency

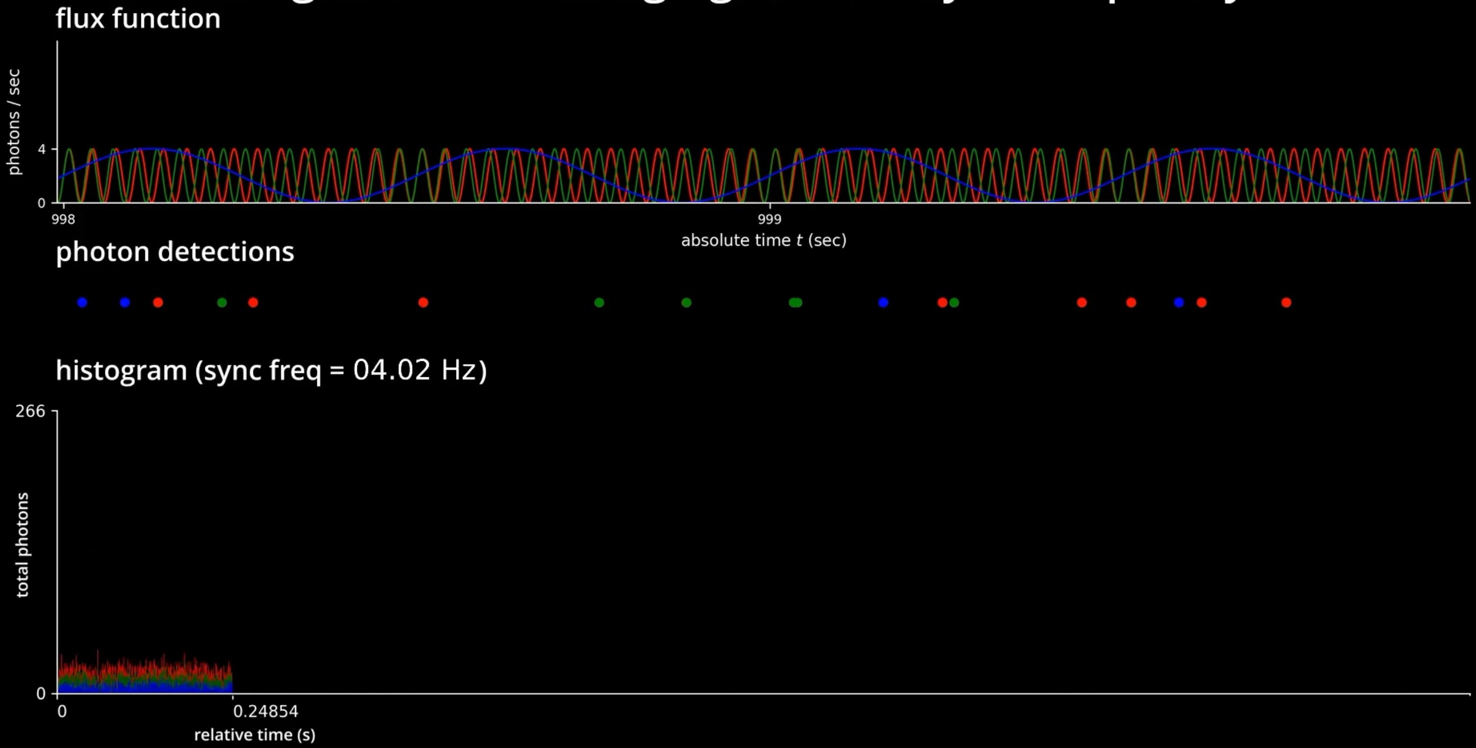

pcaml qppsargj e sjrp_+u gpc` _l b qjsv csl argml q

Flux Probing

$$\underbrace{N(t)}_{\text{counting process}} = \underbrace{\int_0^t \varphi(u)du}_{\text{flux integral up to time } t} + \underbrace{M(t)}_{\text{martingale noise}}$$

qjsv npmìgje cos_rgml

$$p(\mathcal{T}) = \langle p, \varphi \rangle + M_p(t)$$

npmìgje k c_qspck cl rq

gl cpnpmbsar
mdnpmìgje dsl a,
_l b qjsv dsl a,

k _prgje_jc

$$p(\mathcal{T}) \stackrel{\text{def}}{=} \sum_{\tau \in \mathcal{T}} p(\tau)$$

npmìgje k c_qspck cl rq

qpcoscl awnpmì gle

$$p(\mathcal{T}) = \langle p, \varphi \rangle + M_p(t)$$

$$\sum$$

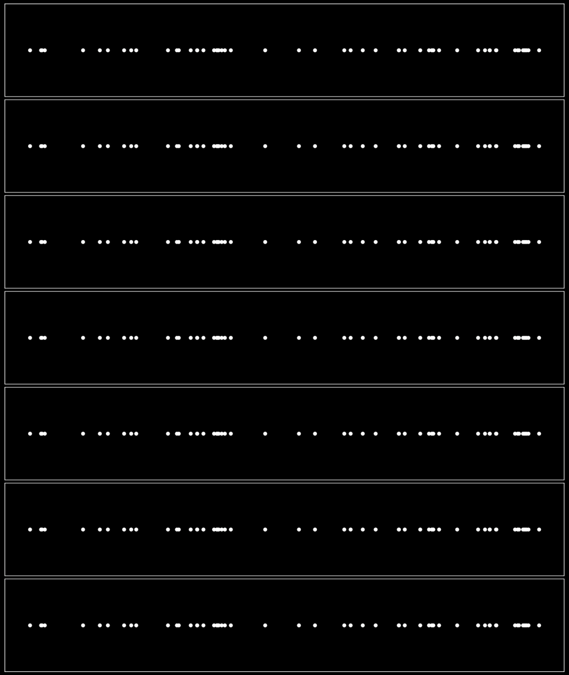

$$= p_f(\mathcal{T})$$

$$\vdots$$

l mgqw

Dmspgcp

amcdagcl rq

$$\approx \langle p_f, \varphi \rangle$$

qbcoscl awnpmì gje

qbcoscl awbcrcargml

$$\sum$$

$$= p_f(\mathcal{T})$$

$$\vdots$$

$$|p_f(\mathcal{T})|^2 \sim \chi^2$$

npmì gje k c_qspck cl r bgqpcì srgml

l mgow Dmspgcp amcddagcl rq

$$\approx \langle p_f , \varphi \rangle$$

$$\frac{P(p_f(\mathcal{T}) \mid H_1)}{P(p_f(\mathcal{T}) \mid H_0)} \underset{H_0}{\overset{H_1}{\gtrless}} \eta$$

jgi cjgf mmb p_rgmrcqr

Flux Probing

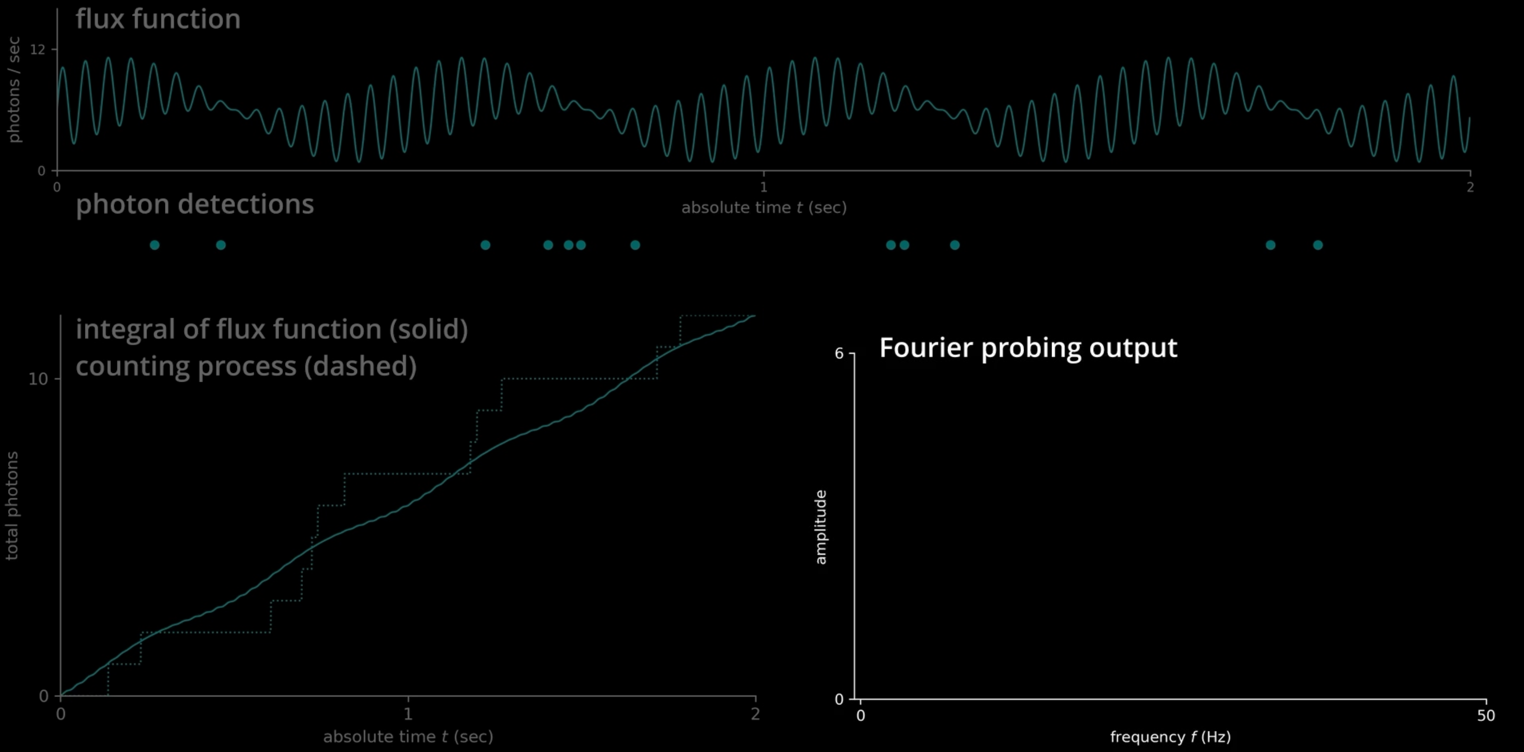

pcqsjrq

f wì pgb rdk coa_jc tgs_jcx_rgml
/ . l Fx- 03. EFx

l / . *. . . nf mml qncp

cvncpgk cl r_j qcrsn

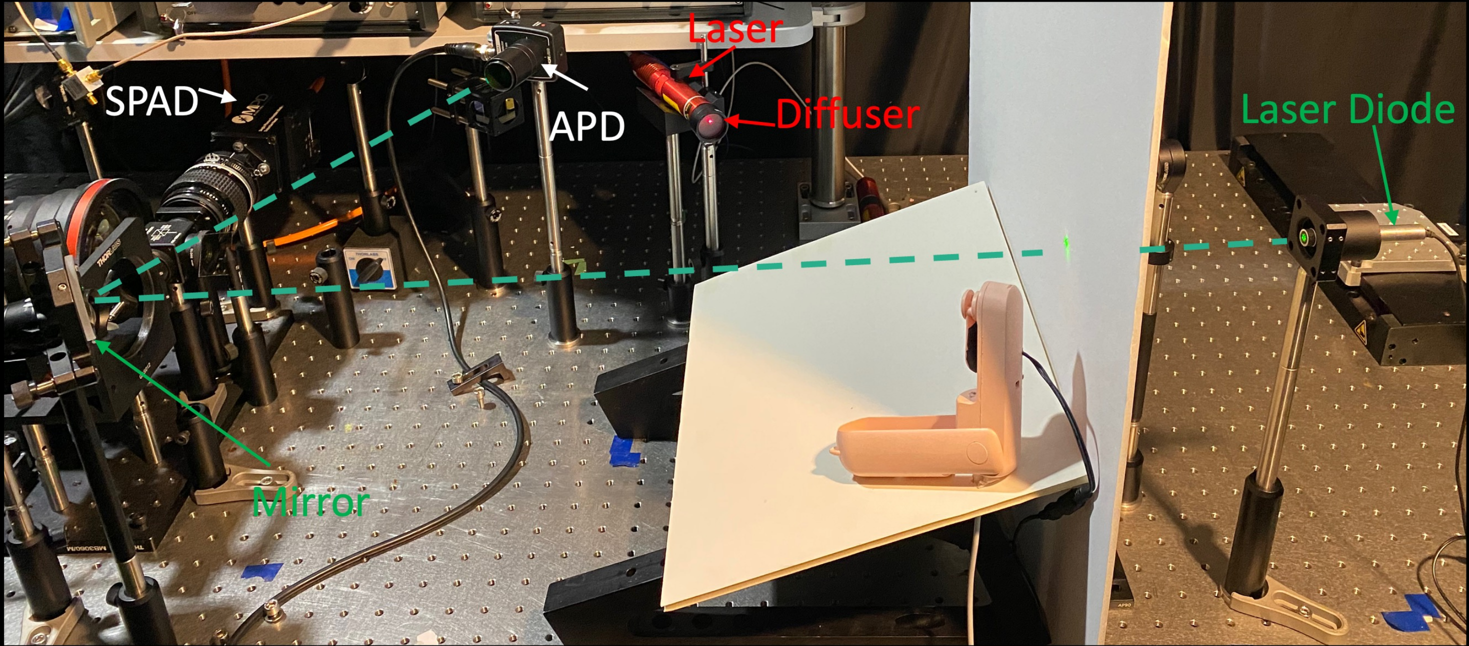

cvncpgk cl r_j qcrsn

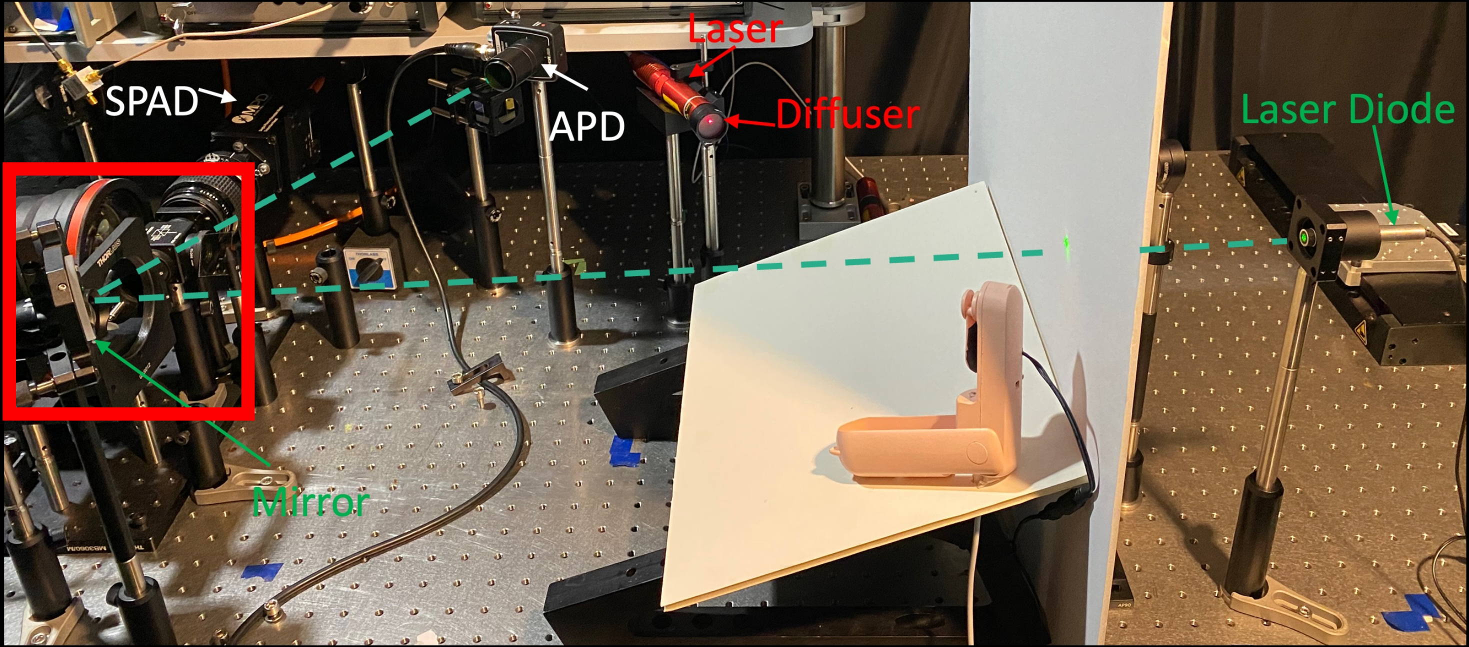

cvncpgk cl r_j qcrsn

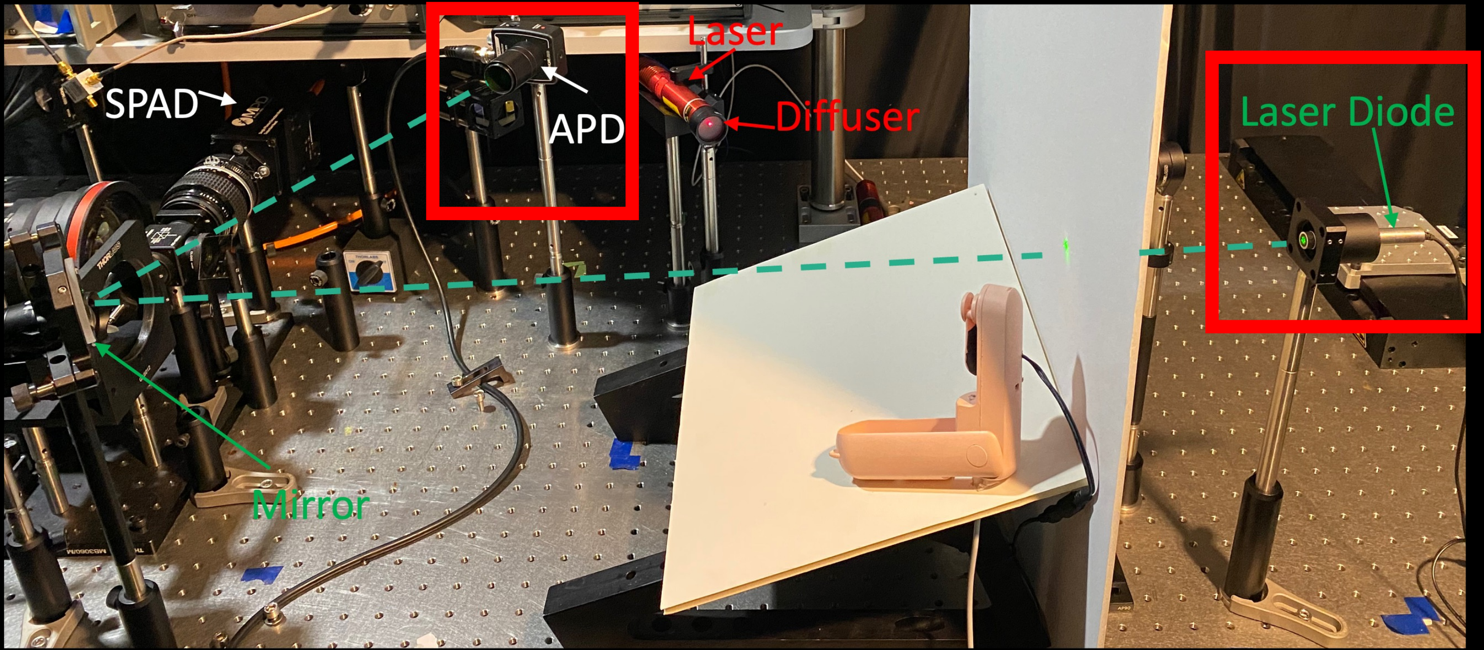

cvncpgk cl r_j qcrsn

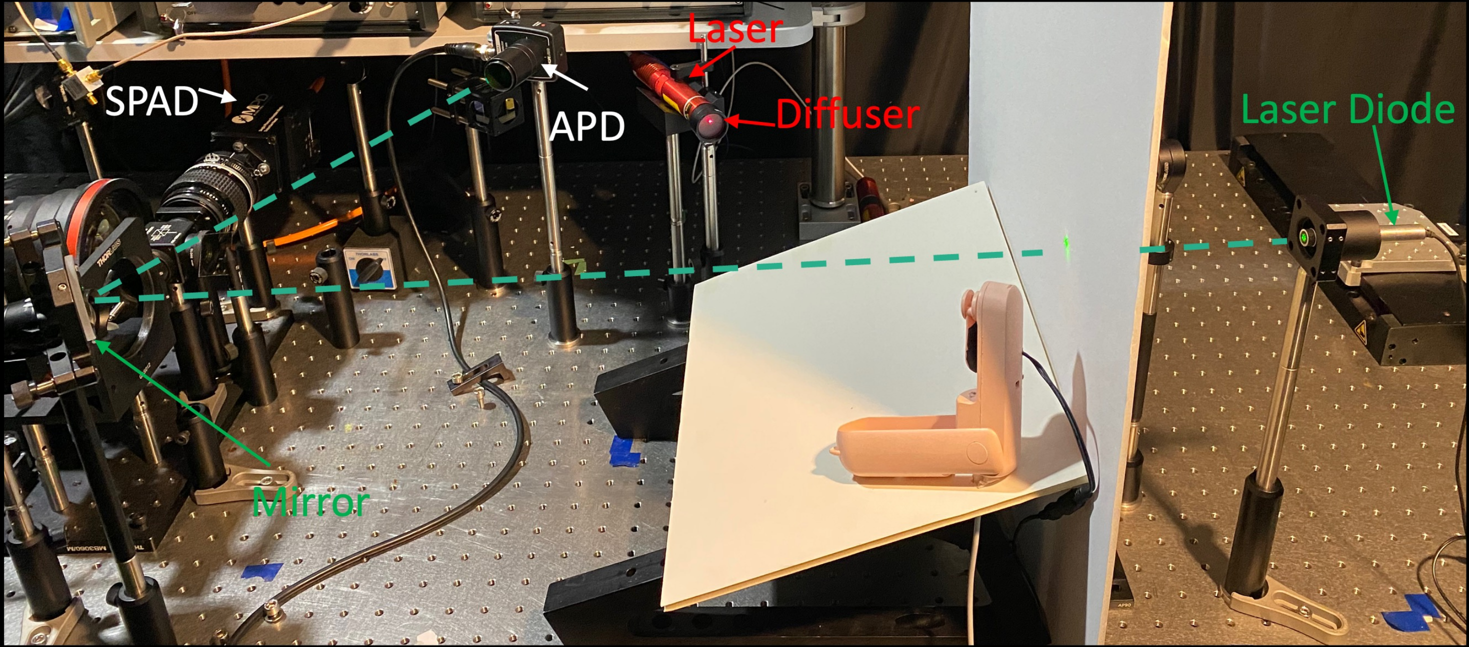

cvncpgkcl r_j
qcrsn

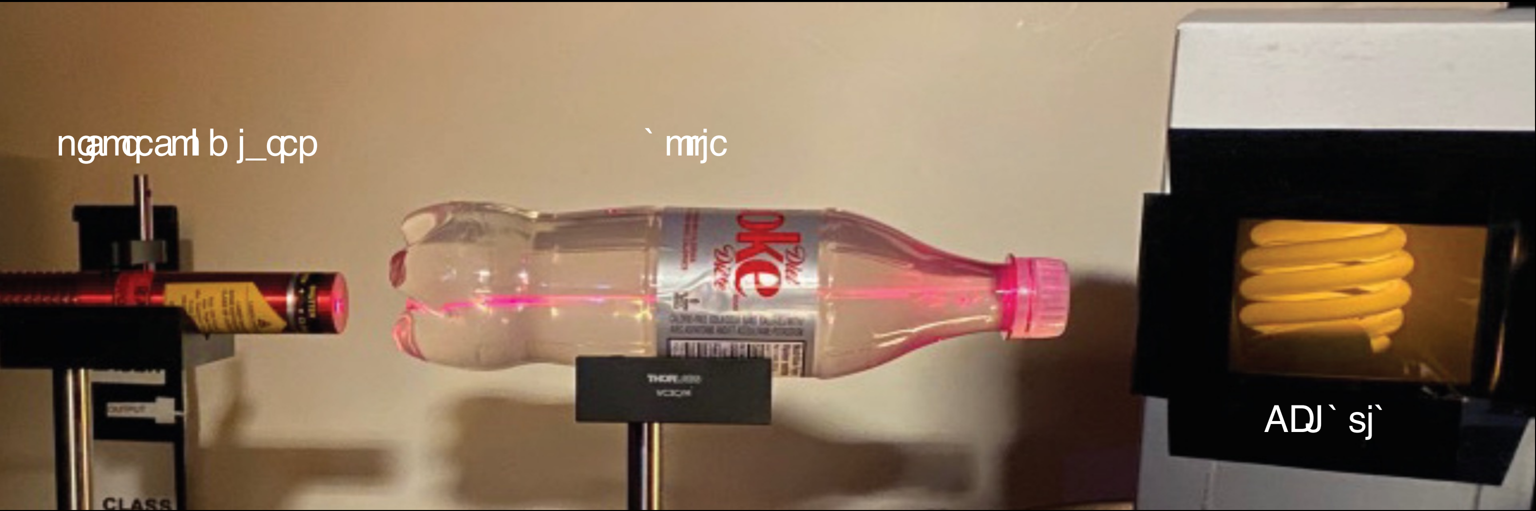

bulb flicker visible

Frame rate: 3 KHz

Elapsed: 000 ms

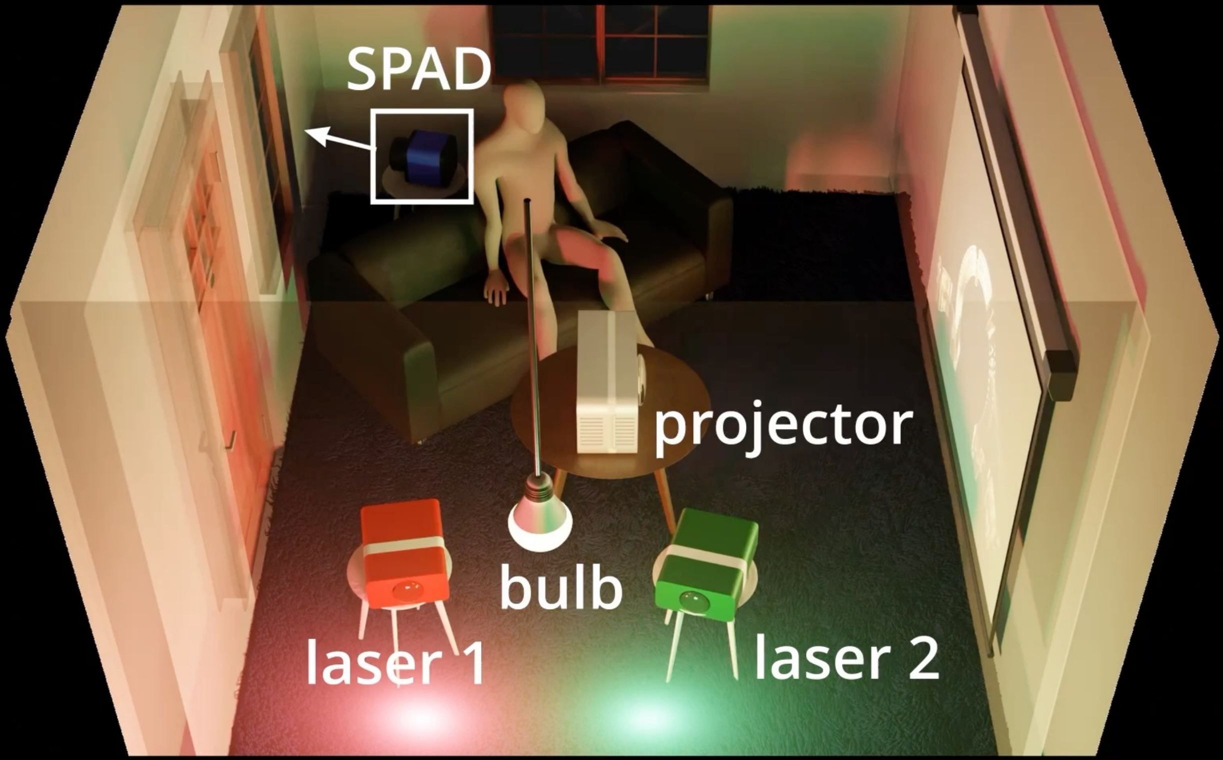
SPAD
projector
bulb
laser 1
laser 2

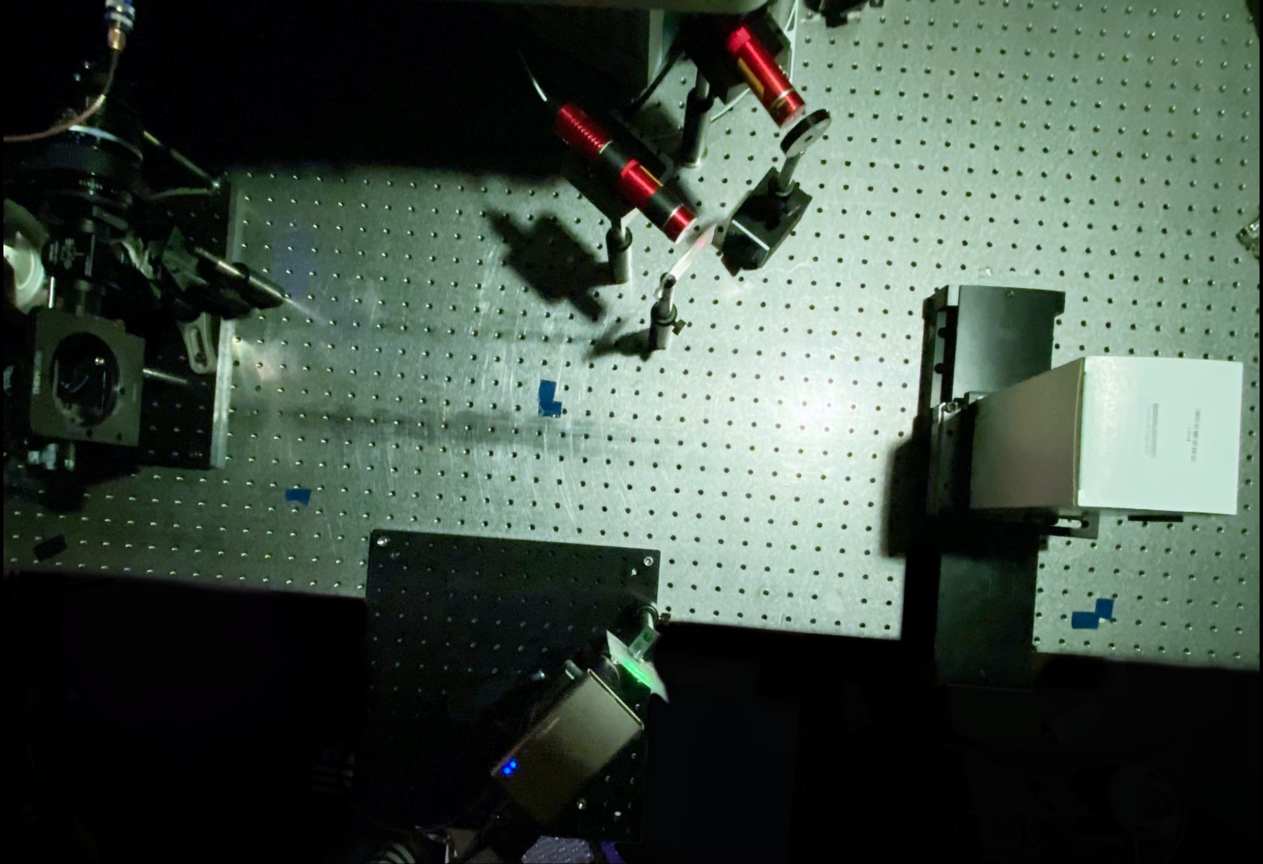

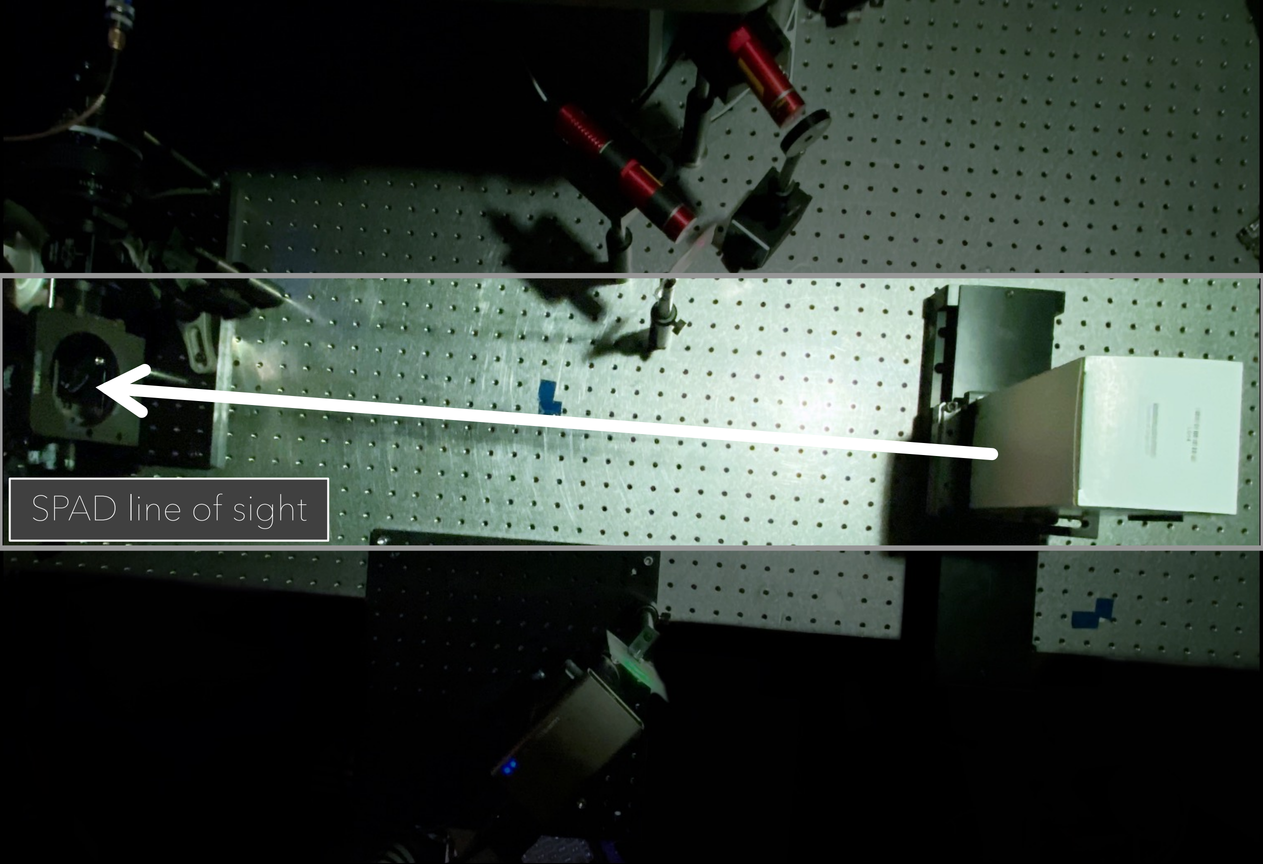
SPAD line of sight

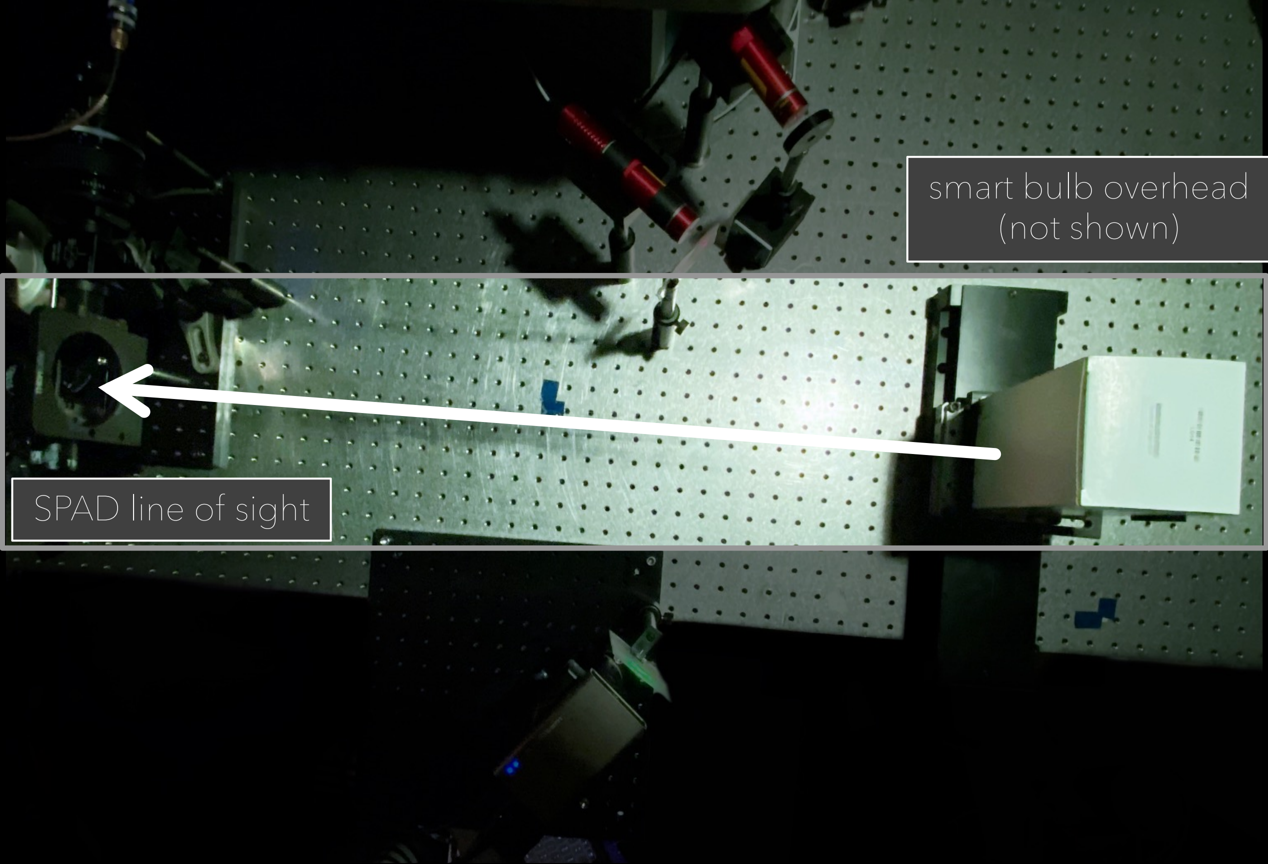
smart bulb overhead
(not shown)
SPAD line of sight

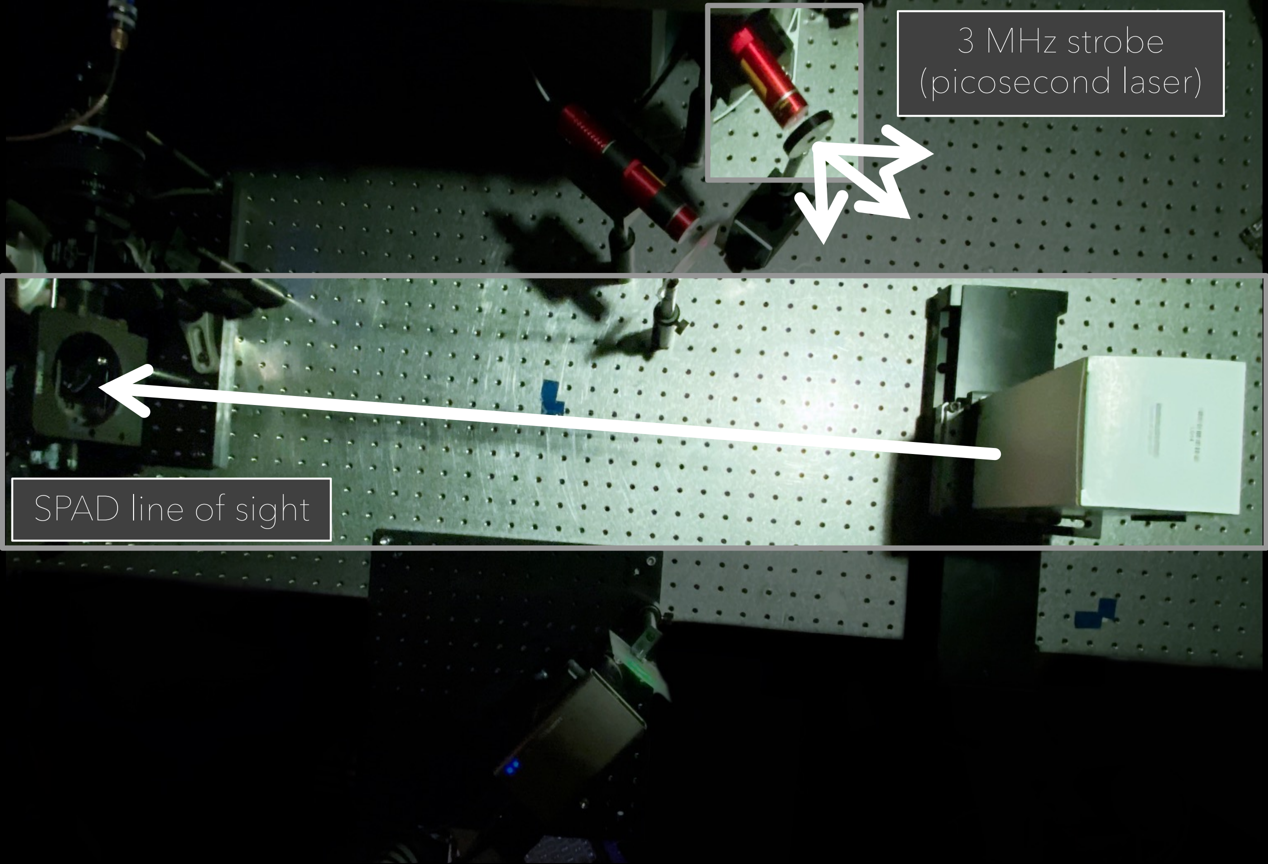
3 MHz strobe
(picosecond laser)
SPAD line of sight

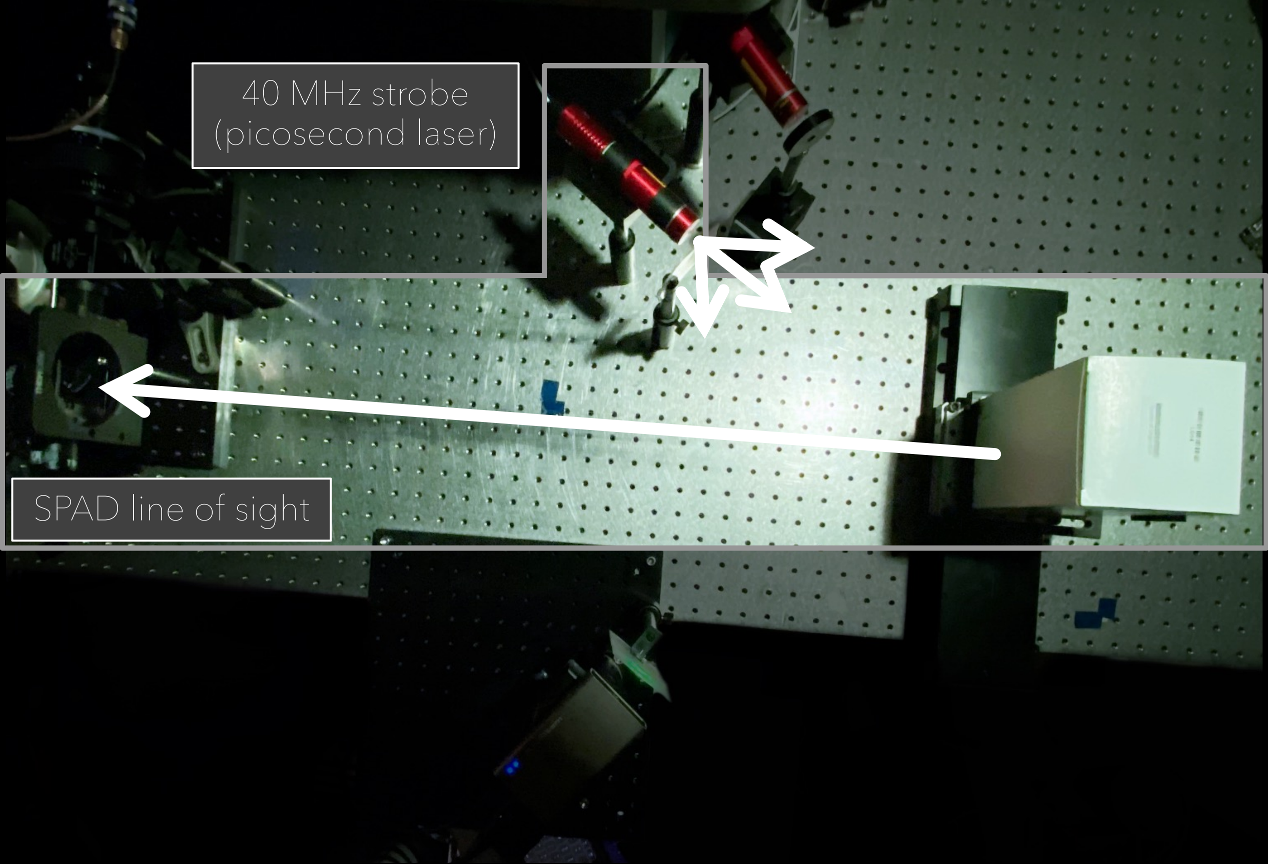

40 MHz strobe
(picosecond laser)
SPAD line of sight

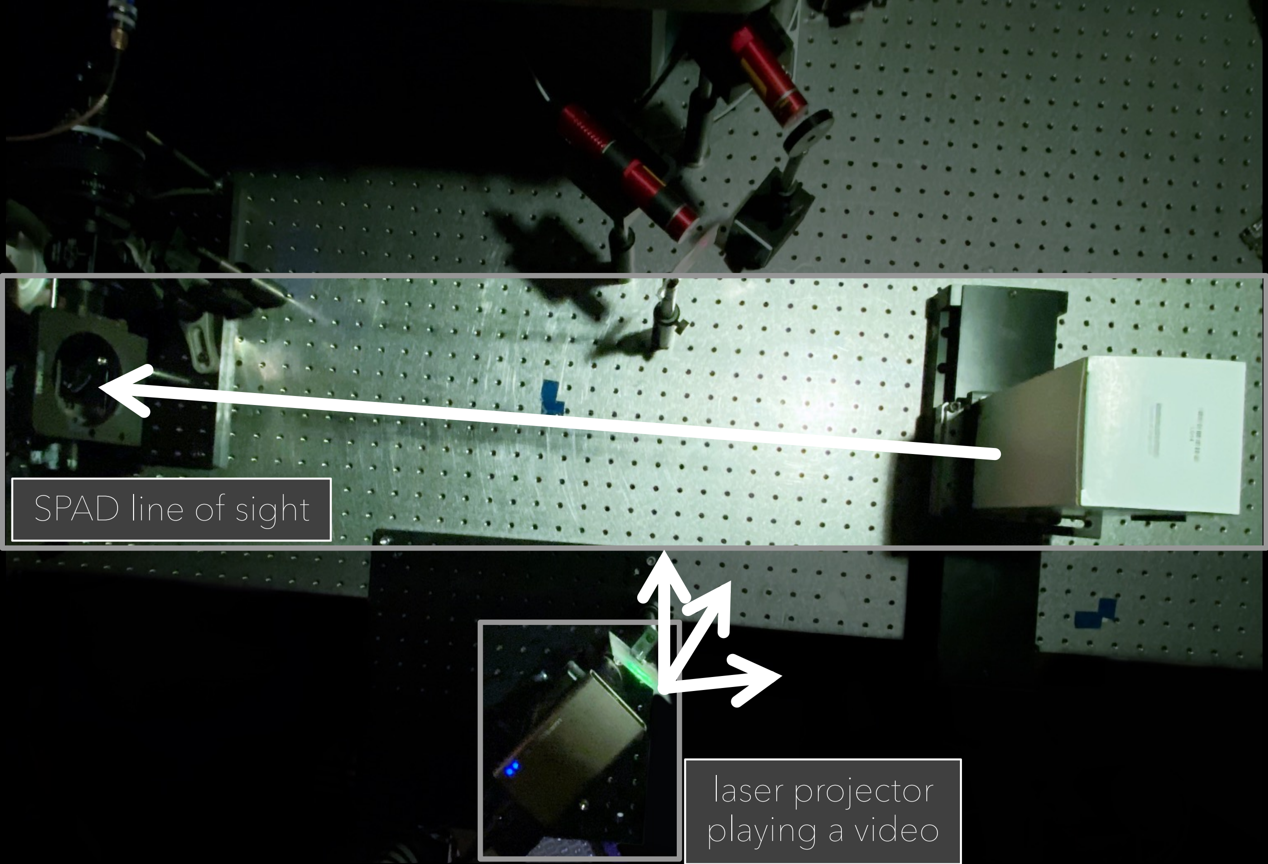
SPAD line of sight
laser projector
playing a video

Sampling Rate: 1.0 kHz

Timespan: 1.00 s

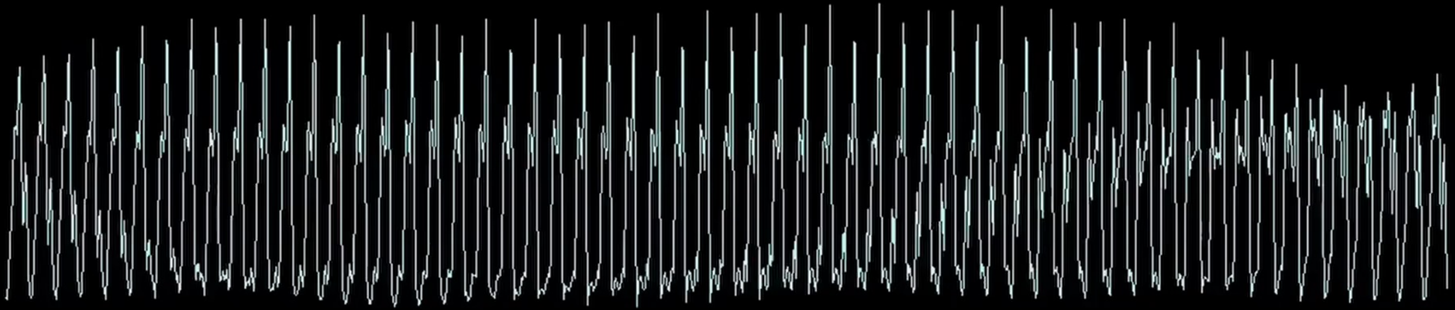

000 ps		000 ps
000 ns		000 ns
000 us	absolute time (s)	000 us
000 ms		000 ms
000 s		001 s

Sampling Rate: 1.0 kHz
Timespan: 1.00 s

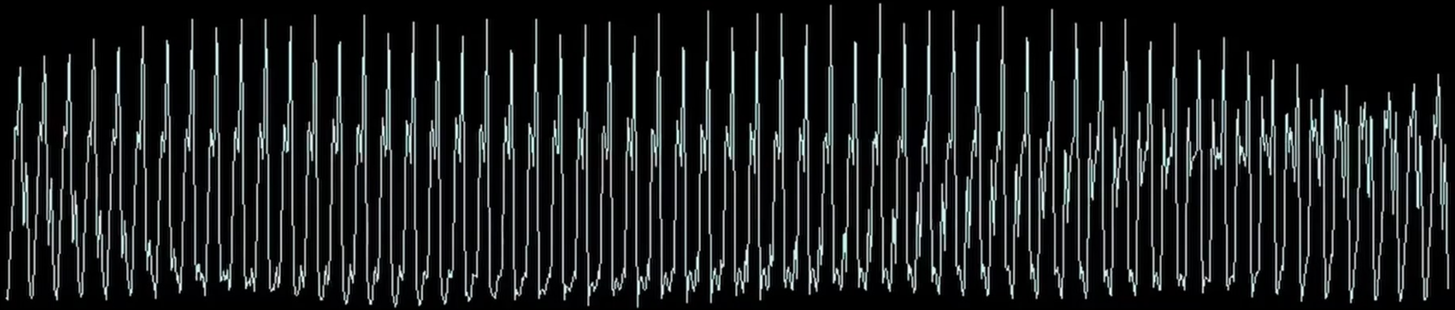

000 ps			000 ps
000 ns			000 ns
000 us	absolute time (s)		000 us
000 ms			000 ms
000 s			001 s

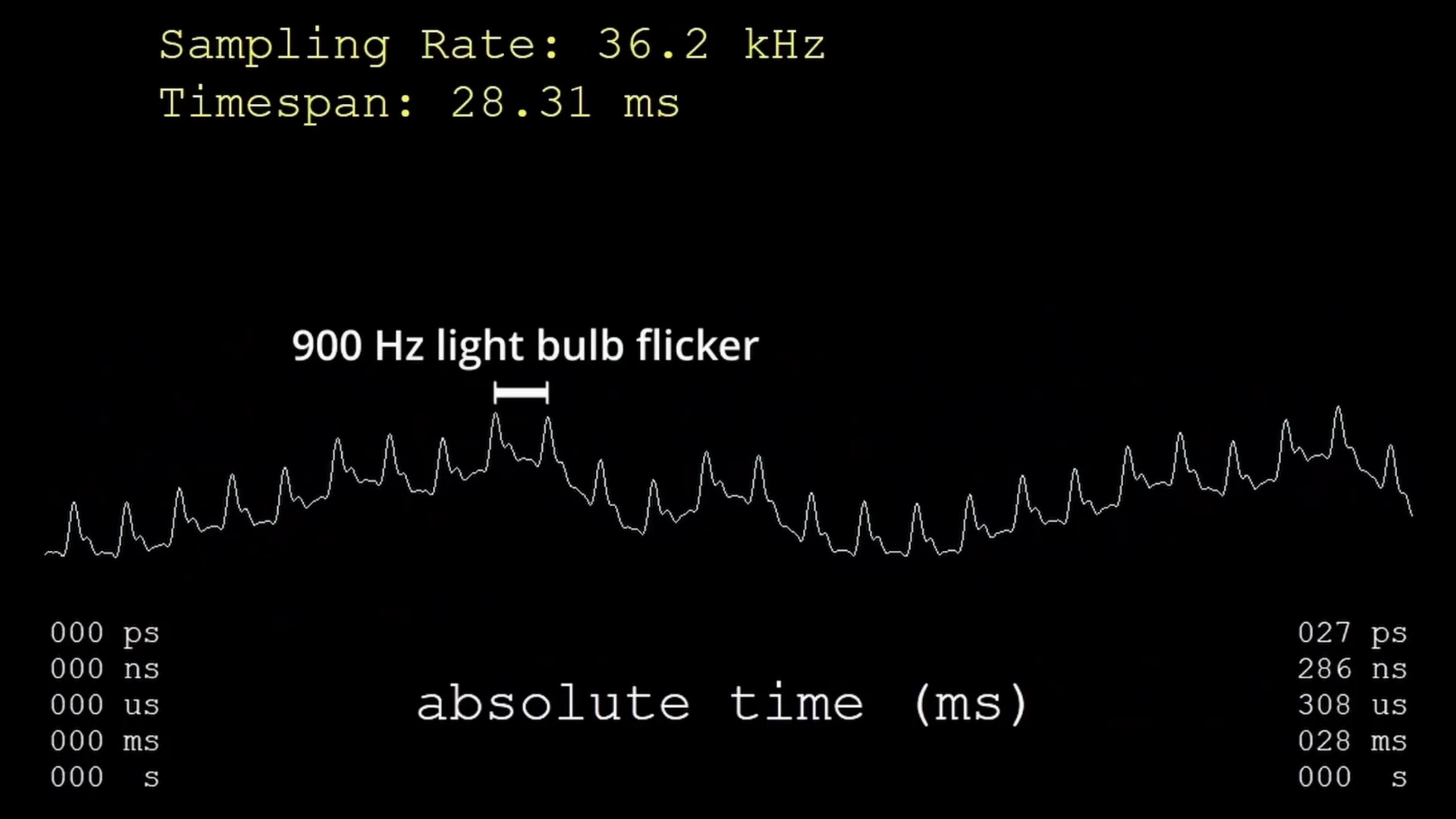
Sampling Rate: 36.2 kHz
Timespan: 28.31 ms
900 Hz light bulb flicker
000 ps
000 ns
000 us
000 ms
000 s
absolute time (ms)
027 ps
286 ns
308 us
028 ms
000 s

Sampling Rate: 137.4 kHz
Timespan: 7.45 ms

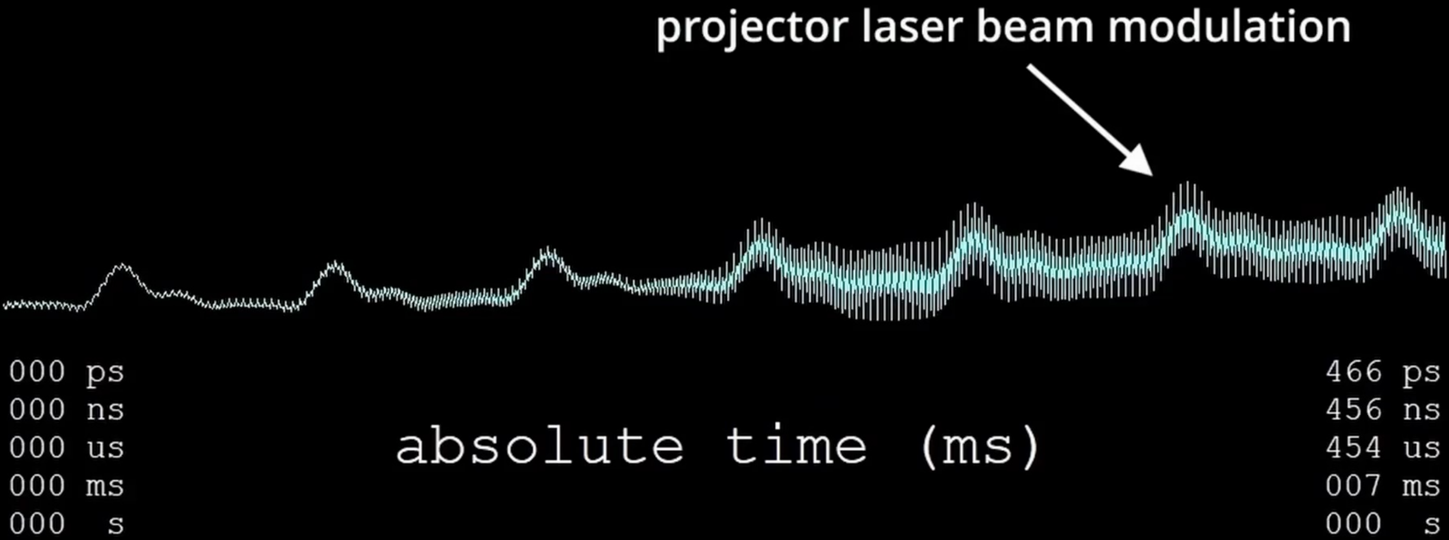

Sampling Rate: 39.1 MHz

Timespan: 26.17 µs

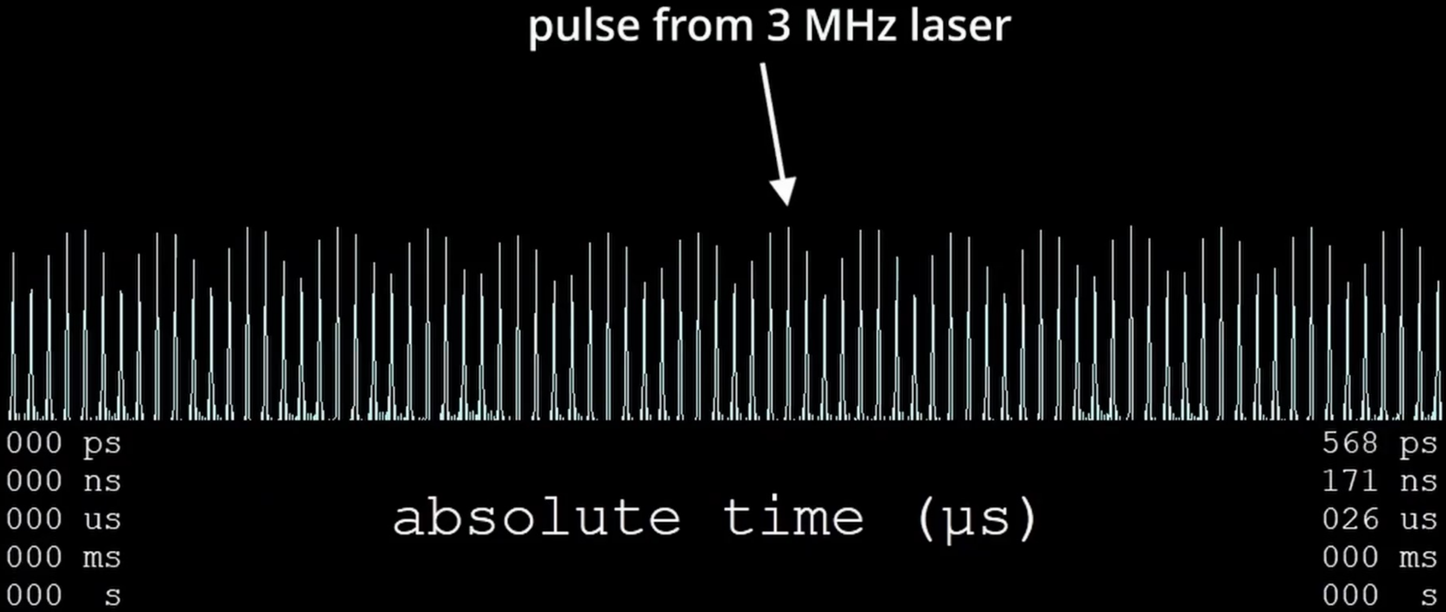

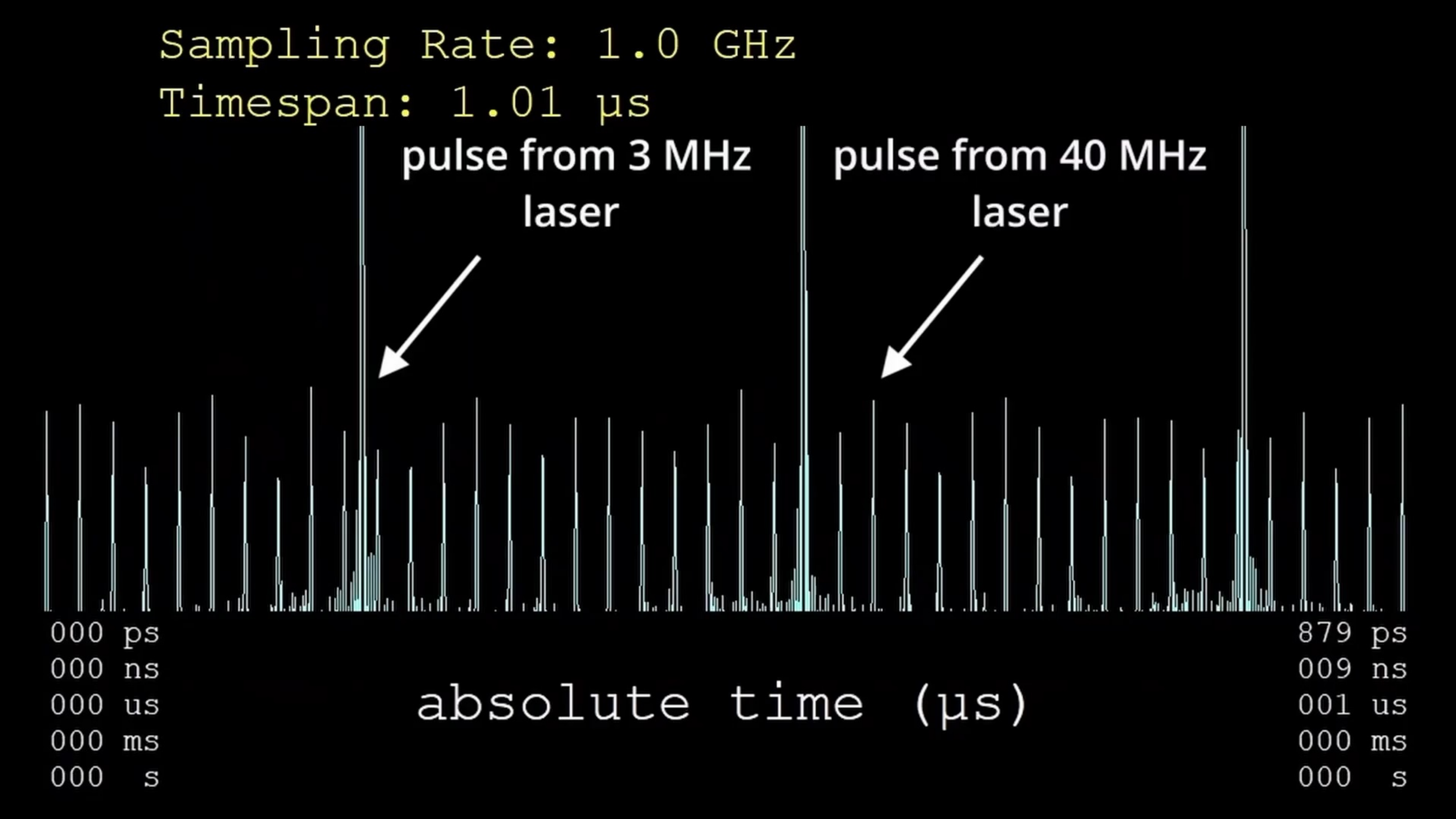
Sampling Rate: 1.0 GHz
Timespan: 1.01 μs
pulse from 3 MHz laser
pulse from 40 MHz laser
000 ps
000 ns
000 us
000 ms
000 s
absolute time (μs)
879 ps
009 ns
001 us
000 ms
000 s

uf_ru_qrfc npmlcampnj_wlge=

non-line-of-sight video reconstruction

reconstruction with lasers
and bulb turned off

(total of 4,000 photons
used in reconstruction
per frame)

(total of 3,000 photons
used in reconstruction
per frame)

[Seets et al. '21]

Proposed

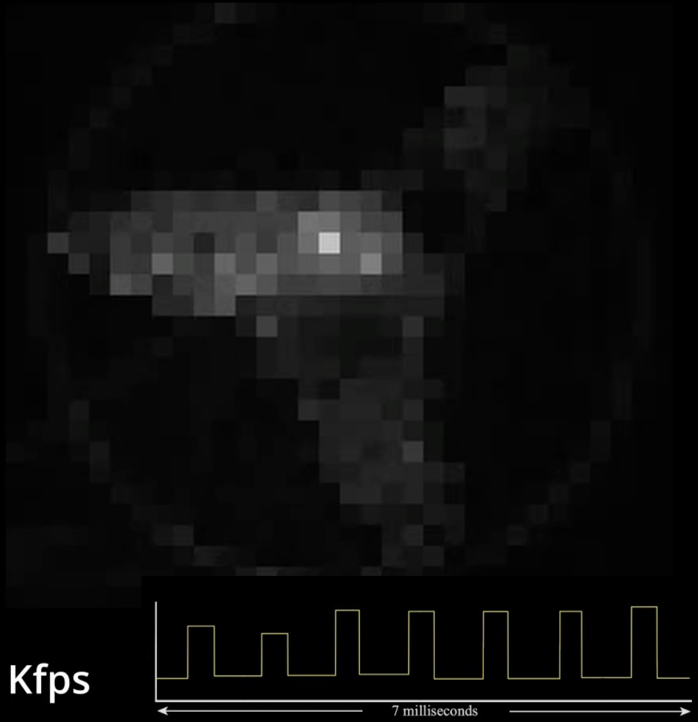

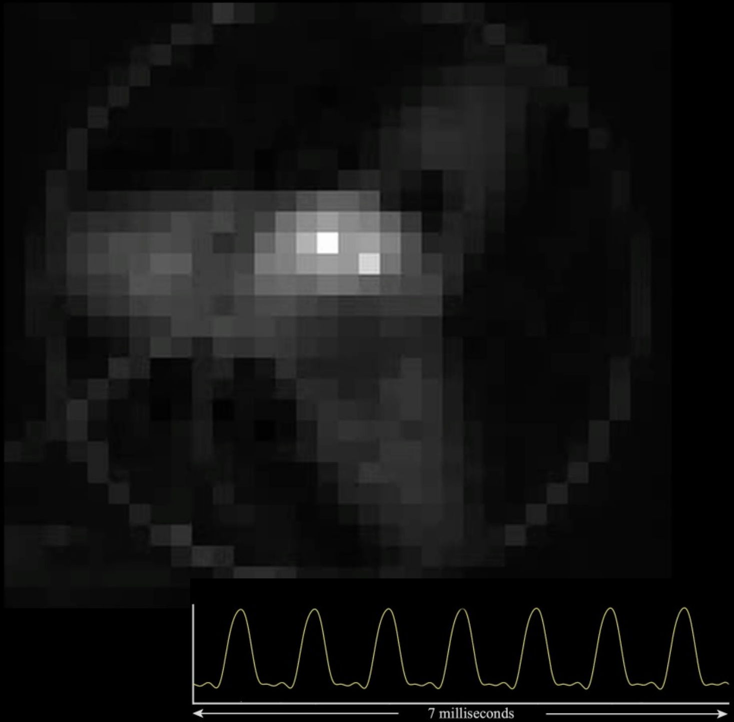

50 Kfps

bgpasopgml

bgqasqqgml

- dsl b_k cl r_j jgkgrq $f_{\max} \leq 1/(2Q)$
- coddgacl aw
- bcrcarmpbc_b rgkc

bgqasqqgml

- l cu _nnjga_rgmlq
  - mnrga_j k gapmqamnc; q * k ml gmpmnrga_j ` cf _tgmpqbmk ngamcami bqrmb_wq
  - sl amnncp_rgl c* qwl ajcoqjgb_p
  - sjrp_d_oq gk _egl e gl rfc b_pi
  - ` gmgk _egl e* k crpmjme w* _qpml mk w* pck mrc oql qgle

concluding remarks

- K_l w_nnjga_rgml qdmprgk c+ndgdgef rgk _egle
    - Jgb_p
    - Lml+jgl c+ndgef r
    - Rp_lqgcl rgk _egle
    - Gk_ege rf pmsef qa_rrcp
- Lcu a_n_`gjggcqrf pmsef amk`glge ck cpegle qcl qmpqu gf amk nsr_rgml

Co-Designing Optics and Algorithms for High-Dimensional Visual Computing

Vishwanath Saragadam
Incoming Assistant Professor,
UC Riverside

Monday Nov 27, 2-4 PM (lecture 10)

References

- D. B. Lindell and G. Wetzstein, “Three-dimensional imaging through scattering media based on confocal diffuse tomography,” Nature Communications, vol. 11, no. 4517, 2020. [J10] C. A. Metzler, D. B.
- C. A. Metzler, D. B. Lindell, G. Wetzstein, “Keyhole imaging: Non-line-of-sight imaging and tracking of moving objects along a single optical path at long standoff distances,” IEEE Trans. Comput. Imag., 2020, (Accepted).
- F. Heide, M. O’Toole, K. Zang, D. B. Lindell, S. Diamond, G. Wetzstein, “Non-line-of-sight imaging with partial occluders and surface normals,” ACM Trans. Graph., 2019
- D. B. Lindell, G. Wetzstein, M. O’Toole, “Wave-based non-line-of-sight imaging using fast f-k migration,” ACM Trans. Graph. (SIGGRAPH), vol. 38, no. 4, 2019.
- F. Heide, S. Diamond, D. B. Lindell, G. Wetzstein, “Sub-picosecond photonefficient 3D imaging using single-photon sensors,” Scientific Reports, vol. 8, no. 17726, 2018.
- D. B. Lindell, M. O’Toole, G. Wetzstein, “Single-photon 3D imaging with deep sensor fusion,” ACM Trans. Graph. (SIGGRAPH), vol. 37, no. 4, 2018.
- M. O’Toole, D. B. Lindell, G. Wetzstein, “Confocal non-line-of-sight imaging based on the light cone transform,” Nature, vol. 555, no. 7696, p. 338, 2018.
- S. I. Young, D. B. Lindell, B. Girod, D. Taubman, G. Wetzstein, “Non-line-ofsight surface reconstruction using the directional light-cone transform,” in IEEE Conference on Computer Vision and Pattern Recognition (CVPR), 2020, (Oral).
- D. B. Lindell, M. O’Toole, G. Wetzstein, “Towards transient imaging at interactive rates with single-photon detectors,” in IEEE International Conference on Computational Photography (ICCP), 2018.
- M. O’Toole, F. Heide, D. B. Lindell, K. Zang, S. Diamond, G. Wetzstein, “Reconstructing transient images from single-photon sensors,” in IEEE Conference on Computer Vision and Pattern Recognition (CVPR), 2017, (Spotlight).
- Wei, Mian, et al. "Passive Ultra-Wideband Single-Photon Imaging." Proceedings of the IEEE/CVF International Conference on Computer Vision. 2023.